2022-06-15

Quantum Decoherence in Time-Dependent Anharmonic Systems

Ty Beus
Brigham Young University

Quantum Decoherence in Time-Dependent Anharmonic Systems

Ty Beus

A dissertation submitted to the faculty of
Brigham Young University
in partial fulfillment of the requirements for the degree of

Doctor of Philosophy

Mark Transtrum, Chair
Manuel Berrondo
Jean-Francois Van Huele
John Colton
Michael Ware

Department of Physics and Astronomy

Brigham Young University

ABSTRACT

Quantum Decoherence in Time-Dependent Anharmonic Systems

Ty Beus
Department of Physics and Astronomy, BYU
Doctor of Philosophy

This dissertation studies quantum decoherence in anharmonic oscillator systems to monitor and understand the way the systems evolve. It also explores methods to control the systems' evolution, and the effects of decoherence when applicable. We primarily do this by finding the time evolution of the systems using their Lie algebraic structures.

We solve for a generalized Caldirola-Kanai Hamiltonian, and propose a general way to produce a desired evolution of the system. We apply the analysis to the effects of Dirac delta fluctuations in mass and frequency, both separately and simultaneously. We also numerically demonstrate control of the generalized Caldirola-Kanai system for the case of timed Gaussian fluctuations in the mass term. This is done in a way that can be applied to any system that is made up of a Lie algebra.

We also explore the evolution of an optomechanical coupled mirror-laser system while maintaining a second order coupling. This system creates anharmonic effects that can produce cat states which can be used for quantum computing. We find that the decoherence in this system causes a rotational smearing effect in the Husimi function which, with the second order term added, causes rotational smearing after a squeezing effect.

Finally, we also address the dynamic evolution and decoherence of an anharmonic oscillator with infinite coupling using the Born-Markov master equation. This is done by using the Lie algebraic structure of the Born-Markov master equation's superoperators when applying a strategic mean field approximation to maintain dynamic flexibility. The system is compared to the Born-Markov master equation for the harmonic oscillator, the regular anharmonic oscillator, and the dynamic double anharmonic oscillator. Throughout, Husimi plots are provided to visualize the dynamic decoherence of these systems.

Keywords: quantum dynamics, anharmonic, decoherence, Lie algebra, representation, mean field, unitarity conditions

ACKNOWLEDGMENTS

We thank Manuel Berrondo who was the advisor over most of this work. We also thank Michelle Beus who helped edit this dissertation.

Contents

List of Figures

Chapter 1

Introduction

1.1 Introduction and Background

This dissertation is on time-dependent anharmonic oscillator systems with decoherence. Anharmonic oscillators can create important quantum effects while decoherence degrades those effects. This topic can be challenging, rewarding, and relevant to quantum computing through this type of system's cat state creation.

In recent history, there has been considerable interest in quantum computers. Quantum computers are said to be essential for the future of physics simulation [1] as well as for the realization of computational feats such as Shor's algorithm (an efficient way to factor primes) [2] and Grover's algorithm (an efficient way to search through a list) [3]. Particularly, quantum computers show promise in cryptography and optimization problems [4, 5]. But to create quantum computers, we need qubits, which are a superposition between two quantum states. It has been shown that one path to creating these qubits can be "cat states" which are quantum states that can be created by nonlinear oscillator systems also known as anharmonic oscillator systems [6, 7]. Thus, studying the dynamics of anharmonic oscillator systems may be one way to develop quantum computers. Unfortunately,

studying the dynamics of anharmonic oscillator systems is insufficient by itself to effectively prepare the theoretical background for creating such quantum devices. When we actually attempt to build these anharmonic oscillators, there will be an environment of chaos that will inevitably tamper with, couple to, and adversely affect the dynamics of our anharmonic oscillator quantum device. Such outside tampering is called decoherence and must be limited, controlled, and understood, specifically for these time-dependent anharmonic oscillator systems. Thus, here I will propose to study quantum decoherence in time-dependent anharmonic oscillator systems.

To gain a little more understanding of what types of anharmonic oscillators can be studied, we must first look at linear or harmonic oscillators. Harmonic oscillators represent the quintessential physics problem since the times of Hooke and Newton. They are applicable to many situations and can approximate any system near a point of equilibrium up to first order in a Taylor series approximation [8]. Some such systems are molecular vibrations [9], photons, or field modes in a cavity [10]. Problems become more interesting when time dependence is added to such situations. Examples of these kinds of oscillators include the parametric oscillator in which the frequency is time-dependent and the Caldirola-Kanai system in which the mass is time-dependent. In the quantum version, both of these oscillators result in squeezing, which is the sacrifice of quantum precision of one variable for more precise knowledge of another [11]. Harmonic oscillators are well behaved in that they are linear and in terms of the potential energy have a clean parabolic well, whereas oscillators that are nonlinear and do not have a parabolic potential well are anharmonic oscillators. Some specific instances of anharmonic oscillators are cavities with Kerr media and Morse potentials for vibrating molecules [9]. We will also look at the previously mentioned harmonic systems, such as parametric oscillators and Caldirola-Kanai [12–14], with some anharmonic effects added.

Decoherence, model-wise, is the coupling of a quantum system to an outside, probabilistically ignored, environment. When decoherence occurs, the simple models that we make for quantum devices tend to break down. The concept of decoherence, although relatively new, has been well

studied for several situations. The dynamics of some systems containing decoherence have been analytically solved, such as a simple harmonic oscillator coupled to a single harmonic oscillator heat bath [15]. Another popular system which has been well studied is the Bateman model (a set of oscillators coupled and constantly leaking energy to a second single oscillator heat bath) [12]. A special case of the Bateman model leads to the dynamics of the Caldirola-Kanai Hamiltonian which have also been well studied [12, 13]. Decoherence for more complicated systems requires some simplifying assumptions such as the Born approximation (that the environment and the system are weakly coupled) and the Markov approximation (that the effect of the environment has no "memory") [16]. The Born-Markov Master equation is of particular note as it allows one to solve for the dynamics of the system after having already taken into account the effects of the environment [16]. Theorists have already analytically solved for the dynamics of the Born-Markov Master equation for a simple harmonic oscillator coupled to a continuous spectrum of coupled oscillators in the environment [17, 18]. Thus, much work has been done on decoherence for harmonic oscillators, but it turns out little work has been done for decoherence with anharmonic oscillators.

In conclusion, anharmonic oscillators create cat states that approximate qubits, which are important for quantum computing. However, the effects of decoherence on an anharmonic oscillator system have not been well studied theoretically. Thus, I propose to analyze the effects of decoherence in several anharmonic oscillator models, as well as further the general progress in the field of limiting and controlling decoherence.

1.2 Objectives

We will study quantum decoherence in anharmonic oscillator systems to monitor and understand the way the systems evolve, then try to find ways to control the decoherence and evolution of such

systems.

1.3 Methodology and Procedures

In order to get a broad understanding of anharmonic oscillator systems with decoherence, we will study the anharmonic oscillator with different models, as well as some simpler models without anharmonic terms and possibly without decoherence to gain practice, obtain insight, and compare to the anharmonic oscillators with decoherence. First we will look at the Caldirola-Kanai Hamiltonian, which is the classical time-dependent Hamiltonian for a harmonic oscillator with resistance made quantum. Here we may study the effects of squeezing from this leaky system. It has dissipation, yet no decoherence, and it does not have an anharmonic term. This case is a good practice problem to analyze before studying more complex problems. We will then move on to a double oscillator with one of the oscillators gauged and measured, and the other oscillator set as the environment and probabilistically ignored, thus simulating decoherence. We will then add an anharmonic term to the double oscillator, and solve for the new dynamics. We will also add anharmonic effects. After working on these systems, we will attempt to couple an anharmonic oscillator to an environment of a continuous spectrum of coupled oscillators. In a system as complex as this, we will take the Born-Markov approximation referred to in the introductory section.

As an overview and general rule, each of the above-mentioned systems will be analyzed in the following way. First, if the system has anharmonic effects, we will typically need to rearrange the problem and make a small approximation to make the rest of the steps manageable. Second, we will use the Wei-Norman method to solve for the time evolution operator. Third, we will find the conditions for unitarity of the time evolution operator to simplify results and analysis. Fourth, if there are decoherence effects, we will take the partial trace of the density matrix. Fifth, we will analyze the system by solving for expectation values of relevant variables, finding the von Neumann

entropy, and plotting the Husimi and Wigner distributions at different times. We will then attempt to find patterns, features, and ways to control the dynamics of each system we study.

We will now begin with the first step. Anharmonic effects tend to complicate the methods we will use to solve for and analyze the systems we want to study. Namely, this effect causes the Hamiltonian to be made up of a set of time-independent operators that have no closure under commutation which will make it impossible to apply the Wei-Norman method in the next step. Here we look at an example of how we may get around this problem. Observe the Hamiltonian $H = A(t)\,a + A(t)^*\,a^\dagger + \left(a^\dagger a\right)^2$, where a and $a^\dagger$ are the standard creation and annihilation operators with the commutation relation of a and $a^\dagger$ defined by $\left[a, a^\dagger\right] = 1$, then $\left(a^\dagger a\right)^2$ would be a term that adds anharmonic effects. The time-independent operators in this Hamiltonian are $\{a, a^\dagger, \left(a^\dagger a\right)^2\}$. The closure with respect to commutation of the set of time-independent operators in this is $\{a, a^\dagger, \left(a^\dagger a\right)^2, 1, a^\dagger a, {a^\dagger}^2, a^2, {a^\dagger}^2 a, a^\dagger a^2, \dots\}$, which is an infinite set. This type of system makes it impossible to apply step 2, so we need to somehow reformat or make an approximation that makes the operators in the Hamiltonian closed under commutation. One option is to replace the term $\left(a^\dagger a\right)^2$ with its expectation value, but such an approximation would remove all anharmonic effects from the dynamics, which is the very thing we want to study. Another method is to take the interaction picture with respect to the anharmonic term, and then apply the mean field approximation where necessary. Thus for this case, we assume the time evolution operator to be $U = U_0\,U_\mathrm{I}$, where $i\hbar\frac{dU_0}{dt} = \left(a^\dagger a\right)^2 U_0$. Doing so and plugging this into the Schrödinger equation, we obtain a second equation $i\hbar\frac{dU_\mathrm{I}}{dt} = H_\mathrm{I}\,U_\mathrm{I}$, where $H_\mathrm{I} = U_0^{-1}\left(A(t)\;a + A(t)^*\,a^\dagger\right)U_0$. U_0 is easily solved for and is $U_0\;e^{t\;\frac{\left(a^\dagger a\right)^2}{i\hbar}}$, and simplifying H_I we get $H_\mathrm{I} = A(t)\;a\;e^{4t\;\frac{a^\dagger a - 1}{i\hbar}} + A(t)^* e^{-4t\;\frac{a^\dagger a - 1}{i\hbar}} a^\dagger$. The term that is now problematic in H_I is $e^{4t\;\frac{a^\dagger a - 1}{i\hbar}}$, so we now take the mean field approximation by replacing that term with its expectation value. Thus after doing so, $H_\mathrm{I} = B(t)\,a + B(t)^* a^\dagger$ where $B(t)$ is a time-dependent scalar that is the expectation value of $A(t)\,e^{4t\;\frac{a^\dagger a - 1}{i\hbar}}$. Thus, now the interaction Hamiltonian is made up of time-independent operators closed under commutation, which is compat-

ible with step 2. Furthermore, we have preserved some anharmonic effects by allowing our time evolution operator to be $U = U_0\, U_{\mathrm{I}}$.

After having set up a Hamiltonian that is made up of time-independent operators that are closed under commutation, as our second step, we would apply the Wei-Norman method to solve for the time evolution operator for the system. The Wei-Norman method solves for the time evolution operators associated with Hamiltonians that are composed of time-independent operators that are closed under commutation with time-dependent coefficients. Basically if the Hamiltonian is of the form $H = \sum_{i=1}^{n} b_i(t)\, A_i$ where the set $\{A_1\}_{i=1}^{n}$are time-independent operators closed under commutation and the $b_i(t)$'s are time-dependent scalar coefficients, then we can make the ansatz $U = \prod_{i=1}^{n} e^{g_i(t)\, A_i}$, and substitute this expression into the Schrödinger equation. Using properties of Lie algebras, we can then match coefficients to obtain a set of coupled first order nonlinear differential equations to solve for the $g_i(t)$ given in the ansatz.

Whenever the Hamiltonian is Hermitian, the time evolution operator is unitary, which brings us to the step 3. As per the previous step, we can assume U, the time evolution operator, is of the form $U = \prod_{i=1}^{n} e^{g_i(t)\, A_i}$ and that it is unitary. We can set $U^{\dagger} = U^{-1}$ then find some relationships between the $g_i(t)$ coefficients in the exponentials by using some representation theory. As an example, suppose we were working with a time evolution operator $U = e^{g_1(t)\, a^{\dagger}} e^{g_2(t)\, a} e^{g_3(t)\, 1}$. Using some Lie algebra properties, we find a faithful representation of the basis $\left\{a^{\dagger}, a, 1\right\}$ that preserves the commutation relations. An appropriate representation is for this case given by $\left\{ \begin{pmatrix} 0 & 0 & -1 \\ 0 & 0 & 0 \\ 0 & 0 & 0 \end{pmatrix}, \begin{pmatrix} 0 & 0 & 0 \\ 0 & 0 & 0 \\ 0 & 1 & 0 \end{pmatrix}, \begin{pmatrix} 0 & 1 & 0 \\ 0 & 0 & 0 \\ 0 & 0 & 0 \end{pmatrix} \right\}$. Replacing the operators with this representation in the equation $U^{\dagger} = U^{-1}$ we match matrix indexes and algebraically eliminate redundant equations to obtain the unitarity conditions for this U which are $g_2(t) = -g_1(t)^*$ and $\Re[g_3(t)] = -\frac{1}{2} g_1(t)^* g_1(t)$, where $\Re$ means the real part. Thus, since $g_2(t)$ and $\Re[g_3(t)]$ are in terms of $g_1(t)$ our problem is reduced to finding $g_1(t)$ and the imaginary part of $g_3(t)$, significantly

reducing the complexity of this system. Note that the finding of a faithful representation that preserves commutation is not usually a trivial matter but an algorithm has been published to do this [19].

After having found the unitarity conditions, the time evolution operator and thus the density matrix become simpler and easier to work with, which brings us to step 4, taking a partial trace of the density matrix. The density matrix is an operator that describes the state of a quantum system. When you apply a bra and ket of a respective state here labeled s to the density matrix ρ, it gives the probability P that the system is in that state: $P[s] = \langle s \,|\rho|\, s\rangle$. In decoherence problems, usually the operators of the problem are a direct product of a system S that we care about and an environmental system E that we wish to ignore. To ignore the environment, we take the partial trace of the density matrix by applying all the possible states to the density matrix with respect to the environment: $\rho_S = \sum_{y\in E} \langle y \,|_E \rho|\, y\rangle_E$. Doing this type of partial averaging, we eliminate all operators and variables with respect to the environment, and leave only operators and variables with respect to the system that we care about. Such partial tracing usually makes the density matrix become non-idempotent due to information loss.

For step 5, we will analyze the evolutions of these systems using analytic methods and visualization through plots and animations [20]. Some analytic methods will be used to find the expectation value of relevant terms such as the position, momentum, and energy number operators, as well as find the von Neumann entropy of the system when applicable [21]. We will visualize the evolution of the system by plotting the evolution of the Wigner and Husimi distribution functions [22, 23]. By looking at how all these variables (and plots) act, we will then find ways to manipulate inputs so that we may be able to control interesting phenomena of the system as it evolves in time.

Note that steps 2 through 5 will be automated and assisted via a Mathematica program that I have developed over several years including a general program to find the nonlinear ordinary differential equations mentioned in step 2, the unitarity conditions in step 3, some methods of partial

tracing in step 4, a general method to find expectation values and some methods for finding the von Neumann entropy as well as the Wigner and Husimi distribution functions in step 5.

1.4 Scope and Limitations of Research

This research will be mainly limited to the study of the evolution of several anharmonic oscillator systems under various decoherence conditions, although some other models will be explored for practice and to compare to the anharmonic case. Note that for systems with anharmonic effect, we will take the interaction picture and a mean field approximation as described in the previous section in order to make computation and analysis more manageable. Also note that although much of the procedure in the previous section would likely work for a relativistic model, this research will not include relativistic extensions of the mentioned models since the models that we are looking at are not relativistic.

1.5 Significance of the Research

After studying and publishing these results, the scientific community will better know how to interpret and control the evolution of anharmonic oscillators under decoherence. In particular, since anharmonic systems lead to cat states which are approximately qubit states, this should hopefully somewhere down the line help experimentalists and engineers further their goal to create a quantum computer. In these models we are developing, we can compare how long it takes for decoherence and dissipation to affect the system where relevant. In studying the list of systems, which have varying complexity and degrees of freedom, we may address the question of how many degrees of freedom are really necessary to model a system with decoherence. This study will also help in furthering understanding and techniques to achieve quantum control in systems. During and after this project, a Mathematica program which automates many of the steps listed in the Methodology

and Procedures section has been available to assist REU students and undergraduate/graduate students for BYU quantum physics research.

1.6 Dissertation Summary

In Chapter 2 we establish Lie algebraic methods for analyzing dynamic quantum systems. We address some rules for coherent states and number states and discuss decoherence and partial tracing. Chapters 3-5 are copies of papers published or currently in the submission process. In Chapter 3 we look into a method to control a generalized time dependent Caldirola-Kanai system using temporally compact fluctuation repetition. This paper was published [24]. In Chapter 4 we look at an optomechanical system which contains implicit anharmonic effects in the Lie algebra while maintaining the second order term in the laser-mirror coupling. The decoherence effects lead to rotational smearing in phase space while the squeeze factor causes rotational smearing after a squeezing effect. In Chapter 5 we also address the dynamic evolution and decoherence of an anharmonic oscillator with infinite coupling using the Born-Markov master equation. The system is compared to the Born-Markov master equation for the harmonic oscillator, the regular anharmonic oscillator, and the dynamic double anharmonic oscillator. In Chapter 6 we summarize the results.

Chapter 2

Lie Algebraic Methods for Analyzing Quantum Dynamics

Throughout this dissertation, there is a focus on using Lie algebraic properties to solve and analyze quantum systems. Thus, we use concepts such as the Wei-Norman procedure, the Heisenberg and interaction pictures, unitarity conditions, and faithful Lie algebraic representations often. For the most part, most of these concepts will be taken for granted and unexplained in subsequent chapters. Thus, this chapter explains these Lie algebraic methods.

2.1 Lie Algebra

A Lie algebra is a vector space that also has a binary operation of Lie brackets that respects bilinearity, altenativity, the Jacobi identity, and anticommutivity. For an associative algebra, we can create a Lie algebra by allowing the Lie brackets to be the commutator defined as $[A,B] = AB - BA$. Since we mainly are dealing with linear operators, this is the type of Lie algebra that we work with throughout the dissertation.

2.2 Wei-Norman and the Adjoint Representation

The Wei-Norman factorization method [25] is a general procedure to solve first order linear differential equations $y'(t) = A(t)y(t)$, where A(t) is equal to a time dependent weighted sum of time independent operators that form a finite Lie algebra basis. The solution using this method $y(t)$ is given as a product of a finite number of operator exponentials. When A(t) and y(t) are associated with the Hamiltonian and time evolution operator respectively, this method can find the time evolution operator for a Schrödinger equation.

Allow the Schrödinger equation to have the form $i\hbar\dot{U} = HU$, with a time dependent Hamiltonian of the form $H/\hbar = \sum_{i=1}^{n} A_i b_i$, with $\{A_i\}_{i=1}^{n}$ a time independent set of operators closed under commutation, and b_i a set of time dependent scalars and U the time evolution operator. Then, the implementation of the Wei-Norman method is as follows.

1. We assume the Ansatz of time evolution operator to be of the form

$$U(t) = e^{g_1 A_1} e^{g_2 A_2} \dots e^{g_n A_n} \tag{2.1}$$

with g_n undetermined coefficients.

2. We reorganize the Schrödinger equation to the form

$$\frac{dU}{dt} U^{-1} = -iH/\hbar \tag{2.2}$$

3. Using the chain rule, we find

$$\frac{dU}{dt} U^{-1} = \sum_{i=1}^{n} e^{g_1 A_1} e^{g_2 A_2} \dots e^{g_i A_i} A_i g_i'(t) e^{-A_i g_i} \dots e^{-A_2 g_2} e^{-A_1 g_1} \tag{2.3}$$

Then, using the formula $e^B A e^{-B} = e^{B\times} A$ with the notation $e^{B\times} A \equiv A + \frac{[B,A]}{1!} + \frac{[B,[B,A]]}{2!} + \dots$, we have

$$\frac{dU}{dt} U^{-1} = \sum_{i=1}^{n} \left(\prod_{j \le i} e^{g_j A_j \times} \right) A_i g_i'(t) = \sum_{j=1}^{n} c_j A_j, \tag{2.4}$$

where c_i is the coefficient of A_i.

4. Finally, we match linearly independent coefficients and solve the set of linear differential equations which are obtained by the equation $-ib_j = c_j$. Upon solving these differential equations for the time dependent coefficients g_i, we then have a well defined time evolution operator that satisfies the Schrödinger equation.

Much of the process associated in the Wei-Norman method can be simplified by use of the adjoint representation. The adjoint representation of an operator B is a matrix representing the commutator action of operator B. We define the matrix cells of the adjoint representation B as $\text{adj}(B)_{ij}$ given by the equation

$$[B, A_i] = \sum_j \text{adj}(B)_{ij} A_j, \tag{2.5}$$

where the set A_i are basis elements of the Lie algebra containing B and all other operators to which we apply this representation.

We note that this representation is not necessarily faithful (linearly independent elements in the basis may not be linearly independent in the representation), but it does preserve commutation relations.

For the Wei-Norman factorization method, we use the commutation action properties of the adjoint representation. Returning the form of $\frac{dU}{dt}U^{-1}$, and assuming the ansatz in Eq. (2.3) we can

rewrite the equation as

$$\frac{dU}{dt}U^{-1} = \sum_{i=1}^{n} \begin{pmatrix} A_1 & A_2 & \dots & A_i \end{pmatrix} \left(e^{g_1 \mathrm{adj}(A_1)} e^{g_2 \mathrm{adj}(A_2)} \dots e^{g_i \mathrm{adj}(A_i)} \right) \begin{pmatrix} \delta_{i1} & 0 & \dots & 0 \\ 0 & \delta_{i2} & \dots & 0 \\ 0 & 0 & \ddots & \vdots \\ 0 & 0 & \dots & \delta_{in} \end{pmatrix} \begin{pmatrix} g_1'(t) \\ g_2'(t) \\ \vdots \\ g_n'(t) \end{pmatrix}$$

$$= \begin{pmatrix} A_1 & A_2 & \dots & A_i \end{pmatrix} [\text{g-Matrix}]^{-1} \begin{pmatrix} g_1'(t) \\ g_2'(t) \\ \vdots \\ g_n'(t) \end{pmatrix} \tag{2.6}$$

where

$$[\text{g-Matrix}]^{-1} = \sum_{i=1}^{n} \left(e^{g_1 \mathrm{adj}(A_1)} e^{g_2 \mathrm{adj}(A_2)} \dots e^{g_i \mathrm{adj}(A_i)} \right) \begin{pmatrix} \delta_{i1} & 0 & \dots & 0 \\ 0 & \delta_{i2} & \dots & 0 \\ 0 & 0 & \ddots & \vdots \\ 0 & 0 & \dots & \delta_{in} \end{pmatrix} \tag{2.7}$$

or more compactly,

$$[\text{g-Matrix}]^{-1}_{j,k} = \left(\prod_{i \le k} e^{g_i \mathrm{adj}(A_i)} \right)_{j,k}. \tag{2.8}$$

Applying (2.6) to (2.2) with $H/\hbar = \sum_{i=1}^{n} A_i b_i$, we find

$$\begin{pmatrix} A_1 & A_2 & \dots & A_n \end{pmatrix} [\text{g-Matrix}]^{-1} \begin{pmatrix} g_1'(t) \\ g_2'(t) \\ \vdots \\ g_n'(t) \end{pmatrix} = -i \begin{pmatrix} A_1 & A_2 & \dots & A_n \end{pmatrix} \begin{pmatrix} b_1(t) \\ b_2(t) \\ \vdots \\ b_n(t) \end{pmatrix}.$$

Or, removing the linearly independent operators A_i, we get

$$i[\text{g-Matrix}]^{-1}\begin{pmatrix} g_1'(t) \\ g_2'(t) \\ \vdots \\ g_n'(t) \end{pmatrix} = \begin{pmatrix} b_1(t) \\ b_2(t) \\ \vdots \\ b_n(t) \end{pmatrix}. \tag{2.9}$$

Note that Eq. (2.9) is interesting from a control theory perspective in that Eq. (2.9) suggests given a set of $g_i(t)$ values for our time evolution operator, the time dependent parameters for the Hamiltonian $b_i(t)$ are fully determined. Thus, given a time evolution operator with determined coefficients $g_i(t)$, we can find the Hamiltonian $b_i(t)$ required to fulfill the particular time evolution operator path.

After a little more rearranging we find a more simplified form of the differential equation

$$i\begin{pmatrix} g_1'(t) \\ g_2'(t) \\ \vdots \\ g_n'(t) \end{pmatrix} = [\text{g-Matrix}]\begin{pmatrix} b_1(t) \\ b_2(t) \\ \vdots \\ b_n(t) \end{pmatrix}, \tag{2.10}$$

where, given a Lie algebra basis $\{A_i\}_{i=1}^n$, the b_i are given by the Hamiltonian $H = \hbar\sum_{i=1}^n A_i b_i$, g-Matrix is given by Eq. (5.4), and the coefficients g_i are for the time evolution operator of the form $U(t) = e^{g_1 A_1} e^{g_2 A_2} \dots e^{g_n A_n}$.

It is interesting to note that g-Matrix is based solely on the structure of the Lie algebra and the order in which the ansatz basis is listed since Eq. (2.6) contains no direct reference to the Hamiltonian. Another property we notice is at time $t = 0$, g-Matrix is the identity matrix which confirms $ig_i' = b_i$ at $t = 0$.

As a side note to the reader, thus far I have not found a general equation for the g-Matrix directly. This is unfortunate since anecdotally, I have found that the g-Matrix is typically simpler than its inverse. I sense calculations would become more straightforward and we would gain more insights into the dynamics of these Lie algebraic first order differential equations if a more direct method of

calculating the g-Matrix were discovered, but for now, we find g-Matrix by taking the inverse of Eq. (5.4).

To give an example of the Wei-Norman process we apply procedure to the driven harmonic oscillator. This consists of a harmonic oscillator with a time dependent force applied. The driven harmonic oscillator has a Hamiltonian $H = \frac{p^2}{2m} + \frac{\omega^2}{2}mx^2 + f(t)x$ where x and p are the position and momentum operators. Allowing the dimensionless variable replacements $P = \frac{p}{\sqrt{\omega m\hbar}}$, $X = \sqrt{\frac{\omega m}{\hbar}}$, and $F(t) = \frac{1}{\omega\hbar}\sqrt{\frac{\hbar}{2\omega m}}f(t)$ the Hamiltonian simplifies to $H = \frac{\hbar\omega}{2}\left(P^2 + X^2\right) + \hbar\omega\sqrt{2}F(t)X$. Furthermore, we make the substitutions to the rising and lowering operators $a = \frac{X+iP}{\sqrt{2}}$, $a^\dagger = \frac{X-iP}{\sqrt{2}}$, and $a^\dagger a = \hat{n}$ making the Hamiltonian become

$$H = \hbar\omega\left(\hat{n} + \frac{\mathrm{I}}{2} + F(t)\left(a + a^\dagger\right)\right) \tag{2.11}$$

where I is the identity operator.

Because the basis set $\{a^\dagger, a, \hat{n}, \mathrm{I}\}$ forms a Lie algebra with $[a, a^\dagger] = \mathrm{I}$, $[\hat{n}, a^\dagger] = a^\dagger$, $[\hat{n}, a] = -a$ with I commuting with everything, we identify $A_1 = a^\dagger$, $A_2 = a$, $A_3 = \hat{n}$, and $A_4 = \mathrm{I}$; and set the ansatz for the time evolution operator

$$U = e^{g_1 a^\dagger} e^{g_2 a} e^{g_3 \hat{n}} e^{g_4 \mathrm{I}}. \tag{2.12}$$

For this dissertation, the procedure for finding the g-Matrix is usually done with an algebraic manipulation program such as Mathematica, but for this particular case, we will show the steps in finding the g-Matrix. For future cases, we forgo this procedure, assuming it trivial. Using Eq. (2.5),

we find the adjoint representation

$$\begin{aligned}\mathrm{adj}(a^\dagger) &= \begin{pmatrix} 0 & 0 & -1 & 0 \\ 0 & 0 & 0 & 0 \\ 0 & 0 & 0 & 0 \\ 0 & -1 & 0 & 0 \end{pmatrix} \quad ,\mathrm{adj}(a) = \begin{pmatrix} 0 & 0 & 0 & 0 \\ 0 & 0 & 1 & 0 \\ 0 & 0 & 0 & 0 \\ 1 & 0 & 0 & 0 \end{pmatrix} \\ \mathrm{adj}(\hat{n}) &= \begin{pmatrix} 1 & 0 & 0 & 0 \\ 0 & -1 & 0 & 0 \\ 0 & 0 & 0 & 0 \\ 0 & 0 & 0 & 0 \end{pmatrix} \quad ,\mathrm{adj}(\mathrm{I}) = \begin{pmatrix} 0 & 0 & 0 & 0 \\ 0 & 0 & 0 & 0 \\ 0 & 0 & 0 & 0 \\ 0 & 0 & 0 & 0 \end{pmatrix}\end{aligned} . \tag{2.13}$$

Using Eq. (5.4), we find

$$[\text{g-Matrix}]^{-1} = \left(\prod_{i \leq k} e^{g_i \mathrm{adj}(A_i)} \right)_{j,k} = \begin{pmatrix} 1 & 0 & -g_1 & 0 \\ 0 & 1 & g_2 & 0 \\ 0 & 0 & 1 & 0 \\ 0 & -g_1 & -g_1 g_2 & 1 \end{pmatrix} \tag{2.14}$$

Concluding, we take the inverse of Eq. (2.14) to obtain the g-Matrix

$$\text{g-Matrix} = \begin{pmatrix} 1 & 0 & g_1 & 0 \\ 0 & 1 & -g_2 & 0 \\ 0 & 0 & 1 & 0 \\ 0 & g_1 & 0 & 1 \end{pmatrix} \tag{2.15}$$

From the Hamiltonian in Eq. (2.11) we identify $b_1 = \omega F(t)$, $b_2 = \omega F(t)$, $b_3 = \omega$, and $b_4 = \omega/2$. Thus, according to Eq. (5.3)

$$i \begin{pmatrix} g_1' \\ g_2' \\ g_3' \\ g_4' \end{pmatrix} = \begin{pmatrix} 1 & 0 & g_1 & 0 \\ 0 & 1 & -g_2 & 0 \\ 0 & 0 & 1 & 0 \\ 0 & g_1 & 0 & 1 \end{pmatrix} \begin{pmatrix} \omega F(t) \\ \omega F(t) \\ \omega \\ \omega/2 \end{pmatrix} . \tag{2.16}$$

Solving for the g_i's using the set of first order differential equations in Eq. (2.16), we find

$$\begin{aligned} g_1 &= -i\omega e^{-it\omega}\int_0^t e^{i\tau\omega}F(\tau)d\tau \\ g_2 &= -i\omega e^{it\omega}\int_0^t e^{-i\tau\omega}F(\tau)d\tau \\ g_3 &= -i\omega t \\ g_4 &= -\frac{i\omega t}{2} - i\omega\int_0^t F(\tau)g_1(\tau)d\tau \end{aligned} \quad . \tag{2.17}$$

With these coefficients solved for, we have now obtained the general dynamics of the time evolution operator of a time-dependent forced harmonic oscillator.

2.3 Heisenberg Representation and Interaction Picture

The Heisenberg representation is a well used concept in quantum mechanics that can be assisted using Lie algebraic techniques. Often it is necessary to calculate the Heisenberg representation of a given operator. The notation for the Heisenberg representation of an operator p is typically given as an operator as a specified function of time $p(t)$, and is defined given a time evolution operator U as $p(t) = U^\dagger pU$. The Heisenberg representation has many uses including a convenient step for calculating the expectation value of an operator $\langle p\rangle$. This is done using the relationship

$$\langle p\rangle = \langle\psi(t)|\,p\,|\psi(t)\rangle = \langle\psi_0|U^\dagger pU\,|\psi_0\rangle = \langle\psi_0|\,p(t)\,|\psi_0\rangle\,. \tag{2.18}$$

When the time evolution operator is of the form $U = e^{g_1A_1}e^{g_2A_2}\ldots e^{g_nA_n}$ where, as in the previous section, the set $\{A_i\}$ forms a Lie algebra, we can often calculate the Heisenberg representation of an operator p using the adjoint representation provided that the time evolution operator is unitary ($U^\dagger = U^{-1}$). If p is a member of the Lie algebra with $p = \sum_{i=1}^n d_iA_i$, where d_i's are scalars, the

Heisenberg representation of p can be written as

$$\begin{aligned} p(t) &= U^\dagger p U = U^{-1} p U = \sum_{i=0}^{n} U^{-1} A_i U \times d_i \\ &= (A_1, A_2, \ldots, A_n) e^{g_1 \mathrm{adj}(A_1)} e^{g_2 \mathrm{adj}(A_2)} \ldots e^{g_n \mathrm{adj}(A_n)} \begin{pmatrix} d_1 \\ d_2 \\ \vdots \\ d_n \end{pmatrix} \end{aligned} \tag{2.19}$$

Should one run into a situation where an operator $p(B_1, B_2, \ldots, B_n)$ is a function of a set of elements in the Lie algebra $\{B_i\}$, but p itself is not in the Lie algebra, we can still use this method by noting,

$$\begin{aligned} p(t) &= U^\dagger p(B_1, B_2 \ldots B_n) U = p(U^{-1} B_1 U, U^{-1} B_2 U \ldots U^{-1} B_n U) \\ &= p(B_1(t), B_2(t) \ldots B_n(t)). \end{aligned} \tag{2.20}$$

Thus, after calculating the Heisenberg representation for the basis elements, it is simple to calculate p by replacing the operator elements that are in the Lie algebra with their respective Heisenberg representation.

As an example of this technique, we find the Heisenberg representations for the dimensionless position $X = \frac{a+a^\dagger}{\sqrt{2}}$ and position squared $X^2 = \hat{n} + \frac{\mathrm{I}}{2} + \frac{a^2 + a^{\dagger 2}}{2}$ for a time evolution operator of the form $U = e^{g_1 a^\dagger} e^{g_2 a} e^{g_3 \hat{n}} e^{g_4 \mathrm{I}}$. This is the time evolution operator of the driven harmonic oscillator given in Section 2.2. From Eq. (2.19), we calculate the Heisenberg representation of X to be $X(t) = \frac{e^{g_3} a + e^{-g_3} a^\dagger + (g_1 - g_2)\mathrm{I}}{\sqrt{2}}$. Although X^2 is not a member of the Lie algebra associated with Eq. (2.11), X is a member. Thus, we can still calculate the Heisenberg representation using Eq. (2.20) by noting $(X^2)(t) = (X(t))^2$.

Another concept often used in quantum dynamics is the interaction picture. The interaction picture is a method of splitting a time evolution operator, U, with a Schrödinger equation $i\frac{dU}{dt} = (H_0 + \Delta H) U$, into two parts by allowing $U = U_0 U_\mathrm{I}$, where $i\frac{dU_\mathrm{I}}{dt} = H_\mathrm{I} U_\mathrm{I}$, $i\frac{dU_0}{dt} = H_0 U_0$, and $H_\mathrm{I} =$

$U_0(\Delta H)U_0^\dagger$. Assuming $U_0 = e^{g_1 A_1} e^{g_2 A_2} \cdots e^{g_n A_n}$ where the set of A_i forms a Lie algebra, we can often calculate H_I by finding $U_0 p_i U_0^\dagger$ for the operators within ΔH. This is effectively taking the reverse-Heisenberg, *RevHeis* of the elements p_i. Using a similar method to our calculation for the Heisenberg, but in reverse, we find

$$\begin{aligned} RevHeis(p) &= U_0 p U_0^\dagger = UpU^{-1} = \sum_{i=0}^{n} d_i U A_i U^{-1} \\ &= (A_1, A_2, \ldots, A_n) e^{-g_n \mathrm{adj}(A_n)} \ldots e^{-g_2 \mathrm{adj}(A_2)} e^{-g_1 \mathrm{adj}(A_1)} \begin{pmatrix} d_1 \\ d_2 \\ \vdots \\ d_n \end{pmatrix}. \end{aligned} \tag{2.21}$$

Once again, the reverse Heisenberg can be further generalized to operators $p(B_1, B_2 \ldots B_n)$ where p is a function of operators B_i which are part of the Lie algebra, but p is not part of the Lie algebra by the property:

$$\begin{aligned} RevHeis(p) &= U p(B_1, B_2 \ldots B_n) U^\dagger = p(UB_1U^{-1}, UB_2U^{-1} \ldots UB_nU^{-1}) \\ &= p(RevHeis(B_1), RevHeis(B_2) \ldots RevHeis(B_n)) \end{aligned} \tag{2.22}$$

Thus, for the cases where the time evolution operator is of the form in Eq. (2.1), operators and Hamiltonians that are functions of operators within the associated Lie algebra can easily be calculated using the adjoint representation. For this dissertation, this is usually done using a computer program.

2.4 Faithful Representation of Time Evolution Operator and Unitarity Conditions

In the past few sections, we have discussed the usefulness of the adjoint representation of a Lie algebra for calculating the time evolution operator using the Wei-Norman method, as well as for

working with the Heisenberg and interaction pictures. We will now discuss the uses of faithful representations in quantum dynamics for time evolution operators of the form Eq. (2.1). We note that at times, the adjoint representation is faithful when it is semi-simple; that is when the set of all elements that commute with everything (which is called the center) is limited to 0. Otherwise, as our experience has shown, the techniques described in this section will give incomplete information when using the adjoint representation. Also observe that in making these transformations, we are sacrificing information on how the operators interact with bras and kets, while gaining insight into relationships between the operator exponential coefficients. This sacrifice is easily recovered as more often than not, one can find a relationship to return to the usual operator space after performing the matrix calculations in the faithful representation.

A faithful representation of a Lie algebra A is a mapping from A to a set of matrices that preserve the commutation relations and is injective. With such a mapping, it is easy to limit the basis of the matrix set, making the mapping bijective.

Noting from the Baker-Campbell-Hausdorff formula:

$$e^X e^Y = e^{X+Y+\frac{1}{2}[X,Y]+\frac{1}{12}[X,[X,Y]]-\frac{1}{12}[Y,[X,Y]]+\ldots}, \tag{2.23}$$

we see that combining and reordering linear exponential operators is determined through the commutation rules of those operators. This leads to the following useful theorem.

Theorem 2.4.1. *Allow $e^{A_1}e^{A_2}\ldots e^{A_n} = e^{B_1}e^{B_2}\ldots e^{B_m}$ where A_i and B_i are linear operators and allow R to be a Lie algebra representation that encompasses a Lie algebra containing $\{A_i\}$ and $\{B_i\}$. Then, $e^{R(A_1)}e^{R(A_2)}\ldots e^{R(A_n)} = e^{R(B_1)}e^{R(B_2)}\ldots e^{R(B_m)}$.*

Proof. Allow

$$e^{A_1}e^{A_2}\ldots e^{A_n} = e^{B_1}e^{B_2}\ldots e^{B_m} \tag{2.24}$$

where there is a faithful representation R that encompasses a Lie algebra containing $\{A_i\}$ and $\{B_i\}$. Then, by the Baker-Campbell-Hausdorff formula Eq. (2.23), we know that B_j is a function of

commutation relation combinations of the set $\{A_i\}$. Call this function $f_j(A_1, A_2, \ldots, A_n) \equiv f_j(\{A_i\})$.

Then, $B_j = f_j(\{A_i\})$. Applying our representation, we note $R(B_j) = R(f_j(\{A_i\})) = f_j(\{R(A_i)\})$ since R is a representation and preserves commutation. Furthermore, using the Baker-Campbell-Hausdorff formula again, we can assert that:

$$e^{R(A_1)}e^{R(A_2)}\ldots e^{R(A_n)} = e^{f_1(\{R(A_i)\})}e^{f_2(\{R(A_i)\})}\ldots e^{f_j(\{R(A_i)\})} \tag{2.25}$$

since the same commutation combinations governed by the Baker-Campbell-Hausdorff formula for Eq. (2.24) would be required for their representations since R preserves the commutation relations. Since we have already established that $R(B_j) = f_j(\{R(A_i)\})$,

$$e^{R(A_1)}e^{R(A_2)}\ldots e^{R(A_n)} = e^{R(B_1)}e^{R(B_2)}\ldots e^{R(B_m)}. \tag{2.26}$$

□

Thus, when replacing the exponential terms by their representation, we do not change the validity of the equation. This is true even when the representation is not faithful.

If we assume the form of the time evolution operator to be $U(t) = e^{g_1 A_1}e^{g_2 A_2}\ldots e^{g_n A_n}$ and allow the representation R to be faithful, it is unlikely that any of the $\{g_i\}$ terms fully disappear from the matrix $R(U(t)) = e^{g_1 R(A_1)}e^{g_2 R(A_2)}\ldots e^{g_n R(A_n)}$. Thus, after examining the cells, one can usually find a method to convert from $R(U(t))$ to $U(t)$ using the relationships between the cells and the $\{g_i\}$ coefficients.

For an example, we look again to the driven harmonic oscillator. Previously, we gave the adjoint representation in Eq. (2.13). You may have noticed that the adjoint representation mapped the

identity I to zero, making that representation not faithful. Here we give a faithful representation

$$\begin{aligned} R(a^\dagger) &= \begin{pmatrix} 0 & 0 & -1 & 0 \\ 0 & 0 & 0 & 0 \\ 0 & 0 & 0 & 0 \\ 0 & 0 & 0 & 0 \end{pmatrix} \quad , R(a) = \begin{pmatrix} 0 & 0 & 0 & 1 \\ 0 & 0 & 0 & 0 \\ 0 & 1 & 0 & 0 \\ 0 & 0 & 0 & 0 \end{pmatrix} \\ R(\hat{n}) &= \begin{pmatrix} 0 & 0 & 0 & 0 \\ 0 & 0 & 0 & 0 \\ 0 & 0 & -1 & 0 \\ 0 & 0 & 0 & 1 \end{pmatrix} \quad , R(\mathrm{I}) = \begin{pmatrix} 0 & 1 & 0 & 0 \\ 0 & 0 & 0 & 0 \\ 0 & 0 & 0 & 0 \\ 0 & 0 & 0 & 0 \end{pmatrix} \end{aligned} . \tag{2.27}$$

Using these to calculate $R(U(t))$ where $R(U(t)) = e^{g_1 R(a^\dagger)} e^{g_2 R(a)} e^{g_3 R(\hat{n})} e^{g_4 R(\mathrm{I})}$, we find the explicit form of the time evolution operator under this representation

$$R(U(t)) = \begin{pmatrix} 1 & -g_1 g_2 + g_4 & -e^{-g_3} g_1 & e^{g_3} g_2 \\ 0 & 1 & 0 & 0 \\ 0 & g_2 & e^{-g_3} & 0 \\ 0 & 0 & 0 & e^{g_3} \end{pmatrix} . \tag{2.28}$$

Now, we can find a relationship between the g_i functions and the $R(U(t))_{j,k}$ matrix cells by looking at the cells in the matrix $R(U(t))$ and using simple algebraic manipulation

$$\begin{aligned} g_1 &= -R(U(t))_{1,3} R(U(t))_{4,4}, \\ g_2 &= R(U(t))_{3,2}, \\ e^{g_3} &= R(U(t))_{4,4}, \\ g_4 &= -R(U(t))_{1,3} R(U(t))_{1,4} + R(U(t))_{1,2}. \end{aligned} \tag{2.29}$$

With these relations, we can map from our representation back to the time evolution operator $U(t)$.

We now find a composition rule of time evolution operators for this system. Allow $U_h =$

$e^{h_1 a^\dagger} e^{h_2 a} e^{h_3 \hat{n}} e^{h_4 \mathrm{I}}$, and $U_k = e^{k_1 a^\dagger} e^{k_2 a} e^{k_3 \hat{n}} e^{k_4 \mathrm{I}}$. Then, using our representation, we find

$$R(U_h U_k) = \begin{pmatrix} 1 & h_4 - k_1 k_2 - h_1(h_2 + e^{-h_3} k_2) + k_4 & e^{-k_3}\left(-e^{-h_3} h_1 - k_1\right) & e^{k_3}\left(e^{h_3} h_2 + k_2\right) \\ 0 & 1 & 0 & 0 \\ 0 & h_2 + e^{-h_3} k_2 & e^{-h_3 k_3} & 0 \\ 0 & 0 & 0 & e^{h_3 + k_3} \end{pmatrix}. \tag{2.30}$$

Applying the relation in Eq. (2.29), we find the time evolution operator composition rules are:

$$\left(h_1, h_2, e^{h_3}, h_4\right)\left(k_1, k_2, e^{k_3}, k_4\right) = \left(h_1 + e^{h_3} k_1, h_2 + e^{-h_3} k_2, e^{h_3 + k_3}, e^{h_3} h_2 k_1 + h_4 + k_4\right). \tag{2.31}$$

Faithful representations can be used to find conditions of unitarity. It is often simpler to analyze systems when we apply conditions of unitarity to our calculations. A time evolution operator is unitary when its conjugate transpose equals its inverse, i.e. $U^{-1} = U^\dagger$. This is always the case for the time evolution operator when the Hamiltonian is Hermitian. Finding the unitarity conditions is easily done by taking a representation and applying it to the equation $U^{-1} = U^\dagger$, or $U = U^{\dagger -1}$. Assuming again that the time evolution operator is of the form $U = e^{g_1 A_1} e^{g_2 A_2} \dots e^{g_n A_n}$, and assuming the Lie algebra's faithful representation of R, the unitarity condition matrix equation takes the more explicit form

$$e^{g_n{}^* R\left(A_n{}^\dagger\right)} \dots e^{g_2{}^* R\left(A_2{}^\dagger\right)} e^{g_1{}^* R\left(A_1{}^\dagger\right)} = e^{-g_n R(A_n)} \dots e^{-g_2 R(A_2)} e^{-g_1 R(A_1)}, \tag{2.32}$$

corresponding to the equation $U^{-1} = U^\dagger$, or, equivalently, the unitarity conditions can be given by

$$R(U) = e^{-g_1{}^* R(A_1{}^\dagger)} e^{-g_2^* R(A_2{}^\dagger)} \dots e^{-g_n^* R(A_n{}^\dagger)} \tag{2.33}$$

corresponding to the equation $U = U^{\dagger -1}$. Note that this typically eliminates half of the degrees of freedom in the time evolution operator, simplifying calculation and enlightening us on the limitations of the time evolution operator.

Applying this to the example of the driven harmonic oscillator, using Eq. (2.27) as our representation, and using Eq. (2.33), we calculate that

$$R(U(t)) = R(U^{\dagger -1}) = \begin{pmatrix} 1 & -{g_4}^* & e^{{g_3}^*}{g_2}^* & -e^{-{g_3}^*}{g_1}^* \\ 0 & 1 & 0 & 0 \\ 0 & -{g_1}^* & e^{{g_3}^*} & 0 \\ 0 & 0 & 0 & e^{-g_3 *} \end{pmatrix}. \tag{2.34}$$

Applying Eq. (2.29), we obtain the unitarity conditions

$$g_1 = -{g_2}^*, g_2 = -{g_1}^*, e^{g_3} = e^{-{g_3}^*}, g_4 = {g_1}^*{g_2}^* - {g_4}^*, \tag{2.35}$$

which, simplified, are the unitarity conditions

$$g_2 = -{g_1}^*, \Re(g_3) = 0, \Re(g_4) = -\frac{|g_1|^2}{2}. \tag{2.36}$$

Note that as expected, the unitarity conditions have eliminated 4 independent variables, leaving the time evolution of the system to depend only on the functions g_1, $\Im(g_3)$, and $\Im(g_4)$.

It is also worth noting that the g-Matrix in Eq. (5.3) for a time evolution operator U is only dependent on the commutation table for the Lie algebra, the order that those operator exponentials are multiplied in U, and the linear independence of the operators. Since all these properties are preserved in $R(U)$, it is necessary that $R(U)$ satisfies the same Schrödinger equation, replacing the Hamiltonian H with $R(H)$ and with the same g-Matrix. Note that the representation $R(H)$ may not necessarily be Hermitian. In those cases, the representation $R(U)$ will not be unitary.

Finding a faithful representation for a given Lie algebra can be quite a complicated and lengthy process, but an algorithm for finding a faithful representation is given in [19]. The algorithm involves splitting the Lie algebra into its Levi subalgebra part (which is semi-simple) and its solvable radical part with the solvable radical split into its elementary sequences. Then it involves some specific assignments for the nilpotent part, some methods of extending the representations for each solvable

step in the elementary sequence (via choosing elements beyond the Lie algebra and gauging their actions on the added elements) until the representation is faithful for the solvable radical part, then doing a direct product with the respective adjoint representations for each element, which is faithful for the Levi subalgebra part. After creating a Mathematica program to fulfill the algorithm and find faithful representations, the process becomes automatic. Thus, for the future, we omit the details of such calculations.

2.5 Rules for Coherent States, Number States, Husimi and Wigner Functions

When dealing with time evolution operators, especially those given in this dissertation, we typically deal with some combinations of operators in exponentials. In order to obtain the dynamics of a specific state evolving in time, it is necessary to apply these states to such exponentials. In this section, we give the rules for applying exponentials of operators to coherent and number states. Such rules are used throughout this research. Furthermore, we give a small summary of the properties and uses of Husimi and Wigner functions which are necessary to visualize the evolution of quantum systems. We also address treatments of decoherence and introduce the Born-Markov Master equation which assists in modeling systems with infinite couplings.

2.5.1 Number States and Coherent States

Number states are the eigenvalues of the number operator $\hat{n} = a^\dagger a$ and are associated with the Hamiltonian of the simple harmonic oscillator $H = \hat{n} + \frac{1}{2}$. Number states are orthonormal and

complete. Some properties of the number state are

$$\begin{aligned} a\,|n\rangle &= |n-1\rangle\,\sqrt{n} \\ a^{\dagger}\,|n\rangle &= |n+1\rangle\,\sqrt{n+1} \\ \hat{n}\,|n\rangle &= |n+1\rangle\,n \\ e^{\gamma\hat{n}}\,|n\rangle &= |n\rangle\,e^{\gamma n} \\ e^{\gamma a^{m}}\,|n\rangle &= \sum_{j=0}^{n} |n-mj\rangle\,\frac{\gamma^{j}}{j!}\sqrt{\frac{n!}{(n-mj)!}}. \end{aligned} \tag{2.37}$$

Coherent states are eigenvalues of the lowering operator a. They are also the states of minimal uncertainty with spreads in dimensionless position and canonical momentum equal to each other. The coherent state $|\alpha\rangle$ written in a number state basis is

$$|\alpha\rangle = e^{-\frac{|\alpha|^2}{2}} \sum_{n=0}^{\infty} \frac{\alpha^{n}}{\sqrt{n!}}\,|n\rangle\,. \tag{2.38}$$

These states are overcomplete and follow the property

$$\int |\alpha\rangle\,\langle\alpha|\,\frac{d\alpha^{2}}{\pi} = \mathrm{I} \tag{2.39}$$

where I is the identity operator.

Some useful properties for the coherent states are

$$\begin{aligned} a\,|\alpha\rangle &= |\alpha\rangle\,\alpha \\ e^{\gamma a}\,|\alpha\rangle &= |\alpha\rangle\,e^{\gamma\alpha} \\ e^{\gamma\hat{n}}\,|\alpha\rangle &= |\alpha e^{\gamma}\rangle\,e^{\frac{1}{2}\left(|\alpha e^{\gamma}|^2-|\alpha|^2\right)} \\ e^{\gamma a^{\dagger}}\,|\alpha\rangle &= |\alpha+\gamma\rangle\,e^{\frac{|\gamma|^2}{2}+\Re(\gamma\alpha^{*})} \\ \langle\beta|\alpha\rangle &= e^{-\frac{1}{2}\left(|\alpha|^2+|\beta|^2-2\alpha\beta^{*}\right)} \\ \langle\beta|\,e^{\gamma\hat{n}^2}\,|\alpha\rangle &= e^{-\frac{1}{2}\left(|\alpha|^2+|\beta|^2\right)} \sum_{j=0}^{\infty} \frac{\left(\alpha\beta^{*}\right)^{j}}{j!} e^{\gamma j^2}. \end{aligned} \tag{2.40}$$

2.5.2 Husimi Function

The Husimi function $Q(z)$ is the normalized projection of a coherent state $|z\rangle$ on an evolved state. It is given by

$$Q(z) = \frac{1}{\pi} \langle z| \rho |z\rangle . \tag{2.41}$$

Looking at this equation, we see that $Q(z)$ gives a transition probability distribution of measuring the coherent state $|z\rangle$. Because of the nature of coherent states, $z = \langle z| \frac{a+a^\dagger + a - a^\dagger}{2} |z\rangle = \sqrt{2}\langle x\rangle + i\sqrt{2}\langle p\rangle$ where $\langle x\rangle = \langle \frac{a+a^\dagger}{\sqrt{2}}\rangle$ and $\langle p\rangle = \langle \frac{a-a^\dagger}{i\sqrt{2}}\rangle$ are the average position and momentum for the coherent state $|z\rangle$. Thus, $Q(z)$ gives a plot of the projected coherent state $|z\rangle$ with respect to the average positions and momentums of $|z\rangle$.

2.5.3 Wigner Function

The Wigner function is the quantum equivalent to a phase diagram distribution, and has the properties

$$\begin{aligned} \int_{-\infty}^{\infty} W(X,P)dP &= \langle X| \rho |X\rangle \\ \int_{-\infty}^{\infty} W(X,P)dX &= \langle P| \rho |P\rangle \end{aligned} \tag{2.42}$$

for a given density matrix ρ. The Wigner function is related to the Husimi function via an inverted Gaussian filter:

$$W(X,P) = \int Q(z) \left(\frac{1}{\pi} e^{2\left|z - \frac{X+iP}{\sqrt{2}}\right|^2} \right) dz^2. \tag{2.43}$$

This is easily calculated when Q(z) is a Gaussian using the Gaussian complex integral property:

$$\int e^{A|z|^2 + Bz^2 + Cz^{*2} + Dz + Ez^* + F} dz^2 = \frac{e^{\frac{CD^2 + A^2F - 4BCF - ADE + BE^2}{A^2 - 4BC}} \pi}{\sqrt{A^2 - 4BC}}. \tag{2.44}$$

2.5.4 Decoherence and Partial Tracing

Quantum decoherence is the loss of quantum coherence in a system. When a quantum system is coherent, the state of the system can be described by a wave function or sum of wave functions

$\sum c_i |i\rangle$. Quantum decoherence occurs when information is lost due to classical uncertainty. When this occurs, the state of the system is described by a mixed state which is a sum of pure state density matrices $\sum p_i |i\rangle \langle i|$ where p_i are the classical probability weights for the state $|i\rangle$ due to classical uncertainty. Often, decoherence effects are caused by open systems.

Closed systems are when all is known about a quantum system. In closed systems, we assume that its Hamiltonian is Hermitian, all variables in the system are known, and that the initial state for evolution is also known. An open system is one where the system we are analyzing is linked to another system called the environment within which, we are ignorant of the wave function. This adds classical uncertainty to the situation, causing quantum decoherence and the need to describe the system in terms of a density matrix.

Oftentimes, decoherence can be modeled by allowing the Hamiltonian to be in the form $H = H_S + H_E + H_{SE}$ where H_S is the Hamiltonian for the system, H_E is the Hamiltonian for the environment, and H_{SE} is the part of the Hamiltonian coupling the two. After solving for the evolution of the system for a density matrix operator ρ one can filter out information of the state in the environment via partial tracing. One can take the partial trace via infinite sums of number state projections associated with the environment via the equation

$$\rho_s = \sum_n^{\infty} \langle n| \rho |n\rangle. \tag{2.45}$$

where $|n\rangle$ are number states associated with the environment. One can also take the partial trace through an integration of coherent state projections associated with the environment through the equation

$$\rho_s = \int \langle \beta| \rho |\beta\rangle \frac{d\beta^2}{\pi}. \tag{2.46}$$

where $|\beta\rangle$ are coherent states associated with the environment.

Chapter 3

Quantum Manipulation Through Finite Fluctuations for a Generalized Parametric Oscillator Using a Lie Algebra Representation

3.1 Abstract

In this paper, we focus on the effects of temporally compact fluctuations on the parameters $m(t)$ (mass), $\omega(t)$ (frequency), and $\gamma(t)$ (spatial dilation coefficient), for the generalized Caldirola-Kanai Hamiltonian. We propose an algorithm such that given control over the timing of repeated compact fluctuations, one can produce any time-evolution associated with complete parameter control of the generalized Caldirola-Kanai Hamiltonian. Computational simplicity is achieved in this endeavor using a faithful representation of the Hamiltonian's associated Lie algebra. Further simplification occurs as a result of using unitarity conditions for the time-evolution operator. We apply our analysis

to the effects of Dirac delta fluctuations in mass and frequency, both separately and simultaneously. We also numerically demonstrate control of the generalized Caldirola-Kanai system for the case of timed Gaussian fluctuations in the mass term. Furthermore, we use the faithful Lie algebra representation to show that any unitary evolution of this generalized Caldirola-Kanai system is given by the squeeze operator multiplied with a phase factor. We also show that the classical evolution of a probabilistic Gaussian phase space distribution and the evolution of the Wigner function of a coherent state in the quantum Caldirola-Kanai system are identical.

3.2 Introduction

Quantum control is the ability to manipulate variables in the Hamiltonian in order to achieve desired quantum states [26]. It applies in fields such as molecular dynamics [26–29], quantum gate and operations [30–32], and assessments of system controllability [33]. Here, we treat the issue of time-evolutionary control for a system with time-dependent mass, frequency, and spatial dilation coefficient for a parametric harmonic oscillator. The goal of this paper is to set up a method to control the time-evolution operator for the generalized Caldirola-Kanai system using well timed, but arbitrary finite pulses in these parameters. These pulses can be of any shape so far as they are repeatable.

The harmonic oscillator model is applicable to many situations and can approximate any system near a point of equilibrium up to first order in a Taylor series approximation [34]. Such harmonic oscillator systems include molecular vibrations [9], photons, and field modes in a cavity [10]. Harmonic oscillator models become more useful when time-dependence is included in their parameters. Examples of time-dependent oscillators include the parametric oscillator, in which the frequency is time-dependent $\omega(t)$, and the generalized Caldirola-Kanai system, in which the mass is time-dependent $m(t)$. The dynamics of parametric oscillators [35–38] and Caldirola-

Kanai [12–14, 39] have been studied for many cases and have confirmed the resulting squeezing effects that appear in these systems [11]. Such systems are applicable in optics [10] since variations in mass and frequency can be interpreted as variations in permittivity and permeability of space for a single mode cavity.

In this paper, we will deal with the harmonic oscillator with variations in frequency $\omega(t)$ and mass $m(t)$, as well as a spatial dilation coefficient $\gamma(t)$. The effect of this additional dilation term has been studied for the case in which $\gamma(t)$ preserves the structure of the Caldirola-Kanai oscillator in position space [40]. Here we deal with the general compact $\gamma(t)$ case. A more general review using the xp space propagator is given in [41]. Some numerical analysis of the Caldirola-Kanai system was done using fractional derivatives in [42, 43]. A semi-classical interpretation of a Wei-Norman factorization for the generalized Caldirola-Kanai system is given in [44]. The explicit form of the generalized Caldirola-Kanai Hamiltonian, $H_{\mathrm{GCK}}(t)$, is given as

$$H_{\mathrm{GCK}} = \frac{1}{2m(t)}p^2 + \frac{1}{2}m(t)\omega(t)^2x^2 + \omega_0\gamma(t)(xp+px). \tag{3.1}$$

A further generalization of this Hamiltonian is given by adding a $g\frac{1}{x^2}$ term and has also been studied [45, 46] with $g(t)m(t) = constant$.

In this paper, we focus on the effects of temporally compact fluctuations of the parameters $m(t)$, $\omega(t)$, and $\gamma(t)$ on the time-evolution operator. We give an algorithm with which, given control over the timing to repeat a given temporally compact fluctuation, one can produce any evolution associated with general control over the parameters in the Hamiltonian in Eq. (3.1). In particular, any squeezed state with nonzero expectation value for position and momentum can evolve to any other squeeze state of nonzero position and momentum through these temporally compact fluctuations in the given parameters.

Several papers have addressed methods of quantum control systems similar to this [47–55]. Most of these use matrices associated with solving a differential equation for a function in the propagator. Uniquely here, we directly start with a faithful representation of a Lie algebra associated with the

time-evolution operator to perform the dynamic calculations and Lie group multiplications. This gives a direct connection to describe time-evolution operator variations given dynamic variables. Furthermore, all the calculations are done in terms of g_i coefficients of the time-evolution operator $U(t)$ taking into account the unitarity conditions, which will be shown as

$$U(t) = e^{g_1 \frac{a^{\dagger 2}}{2}} e^{\frac{g_1^*}{-1+|g_1|^2} \frac{a^2}{2}} e^{\left(\ln\left[1-|g_1|^2\right]+i\gamma_3\right)\frac{1}{2}\left(a^\dagger a+\frac{1}{2}\right)}. \tag{3.2}$$

This expression gives a different perspective to the propagator and often leads to simpler equations. It also gives more dynamic flexibility than assigning specific Hamiltonian time-dependencies. Thus, by using the faithful Lie algebra representation, we develop a general analysis for general parameter variations in the Hamiltonian to control the time-evolution operator which can apply to any initial ket. After this general analysis concludes in Section 3.8, we apply our results to two specific pulse variations in Sections 3.9 and 3.10.

As far as the authors have seen, the time-evolution operator has yet to be manipulated in this direct way using Lie algebra faithful representations. Furthermore, such an analysis can be obtained for any system with a time-dependent Hamiltonian composed of a Lie algebra basis using the techniques given in this paper. An alternative method for analyzing this problem is through Lewis-Riesenfeld invariants [36–38, 48, 56], though the method is more focused on the evolution of the eigenvalue basis for the Lewis-Riesenfeld invariants, and less directly focused on the time-evolution operator.

This paper is organized as follows. In Section 3.3 we give a description of the classical dynamics for the Caldirola-Kanai Hamiltonian. In Section 3.4 we re-express the quantum Hamiltonian in terms of raising and lowering operators. In Section 3.5 we introduce a representation for the time-evolution operator, find the conditions for unitarity, and prove that any unitary evolution is given by a squeeze operator with a phase factor. In Section 3.6 we discuss the effects of the time-evolution on an initial coherent state. In Section 3.7 we discuss the connection between classical evolution of a probabilistic phase space distribution and quantum evolution of the Wigner function. In Section

3.8 we find ways to fully control the system using temporally compact fluctuations combined with waiting periods. In Section 3.9 we analytically explore the effects of Dirac delta fluctuations in mass and frequency. In Section 3.10 we numerically demonstrate control of this system using Gaussian fluctuations which are approximately temporally compact.

3.3 Classical Caldirola-Kanai Dynamics

We start by exploring the dynamics of the Caldirola-Kanai Hamiltonian in the classical, i.e., non-quantum case. Early on, the classical Caldirola-Kanai Hamiltonian was used to model the motion of damped harmonic oscillators [57]. The form of the classical Hamiltonian is

$$H_{\text{cl}} = \frac{1}{2m_0} p^2 e^{-\int_0^t \xi(t')dt'} + \frac{1}{2} m_0 \omega^2 x^2 e^{\int_0^t \xi(t')dt'}, \tag{3.3}$$

where x and p are the position and canonical momentum respectively, and traditionally $\xi(t')$ is constant [57]. Using Hamilton's equations leads to $\dot{x} = \frac{p}{m(t)}$, $\dot{p} = -\omega^2 x m(t)$ where $m(t) = m_0 e^{\xi(t)}$.

Decoupling, we obtain the equation of motion for the damped harmonic oscillator:

$$0 = \ddot{x} + 2\omega_0 \xi(t)\dot{x} + \omega^2 x. \tag{3.4}$$

Thus, $\xi(t)$ can be interpreted as a time-dependent oscillator decay term.

Allowing $\xi(t)$ to be constant, and assuming the mass to be m_0, we see in the (x, v) phase diagram where $v = \dot{x}$ is the velocity, given in Fig. (3.1), an energy decay consistent with a typical damped harmonic oscillator.

Alternatively, we could allow ξ to be time-dependent, and reinterpret this Hamiltonian as an oscillator with a time-dependent mass:

$$H_{\text{cl}} = \frac{1}{2m(t)} p^2 + \frac{1}{2} m(t) \omega^2 x^2. \tag{3.5}$$

As was done earlier, we allow $m(t) = m_0 e^{\xi_0 t}$, but the resulting (x, p) phase diagram where p is the momentum, under this new interpretation is much different. The contour plot with initial

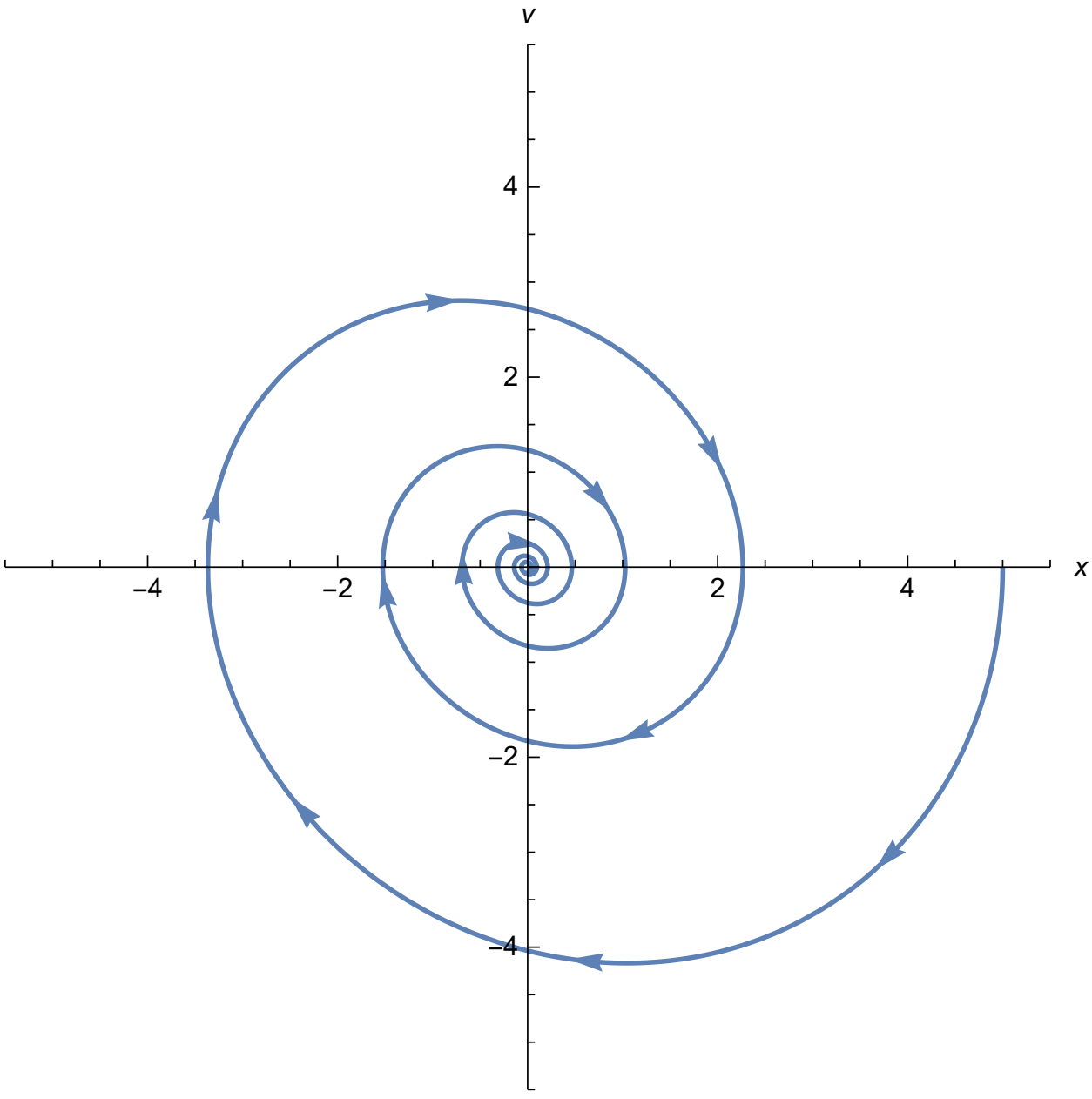

Figure 3.1 Phase diagram (x, v) of a single trajectory of a damped oscillator

conditions of a Gaussian probability distribution in phase space evolves, using Hamilton's equations, as given in Fig. (3.2). Note that the distribution in Fig. (3.2) shows a classical "squeezing" in the phase distribution in that the distribution, is forming into the shape of an ellipse, a feature that is similar to the quantum case shown later.

In this paper, we focus on temporary changes, i.e., temporally compact variations in the Hamiltonian. One could, for example, allow a mass to have the temporal Gaussian variation about $t = t_0 : m(t) = m_0\left(1 + Ce^{-\varepsilon(t-t_0)^2}\right)$. Fig. (3.3) gives a series of contour plots in phase space describing the evolution of an initial Gaussian probability distribution with this mass variation.

Note that this classical analysis approximately mirrors what happens with the quantum case as shown later. As we see, the spread of the system is affected by variations in the mass term. Further experimentation shows that the magnitude of C has an effect on which direction the distribution spreads and that similar effects happen when C is negative. We also see that such variation effects are not reversed by simply returning the mass to its initial value.

3.4 Dynamic Generalized Quantum Caldirola-Kanai

We now consider a more general Caldirola-Kanai quantum Hamiltonian. To increase generality, for the sake of more flexibility, we allow the frequency to be time-dependent. Since our analysis involves Lie algebra manipulation, we also add a direct squeezing control term $(xp + px)$ with no added complication to the Lie algebra of this analysis, allowing the Hamiltonian to extend to all Hermitian operators spanned by the Lie algebra basis $\left\{p^2, x^2, (xp + px)\right\}$. Thus, the Hamiltonian becomes

$$H_{\mathrm{GCK}} = \frac{1}{2m(t)}p^2 + \frac{1}{2}m(t)\omega(t)^2x^2 + \omega_0\gamma(t)(xp + px). \tag{3.6}$$

Eq. (3.6) is a generalized Hermitian Hamiltonian preserving the Lie algebraic structure of the

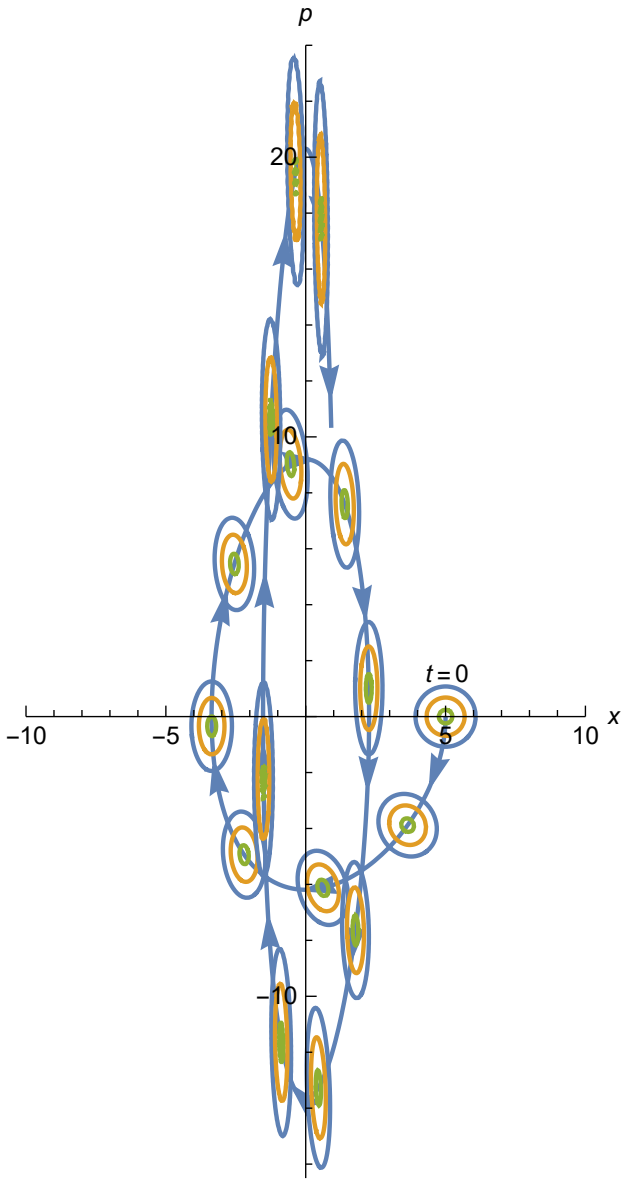

Figure 3.2 Evolving phase diagram (x, p) of oscillator with an initial Gaussian distribution in phase space and exponentially increasing mass with time. The distribution performs classical "squeezing".

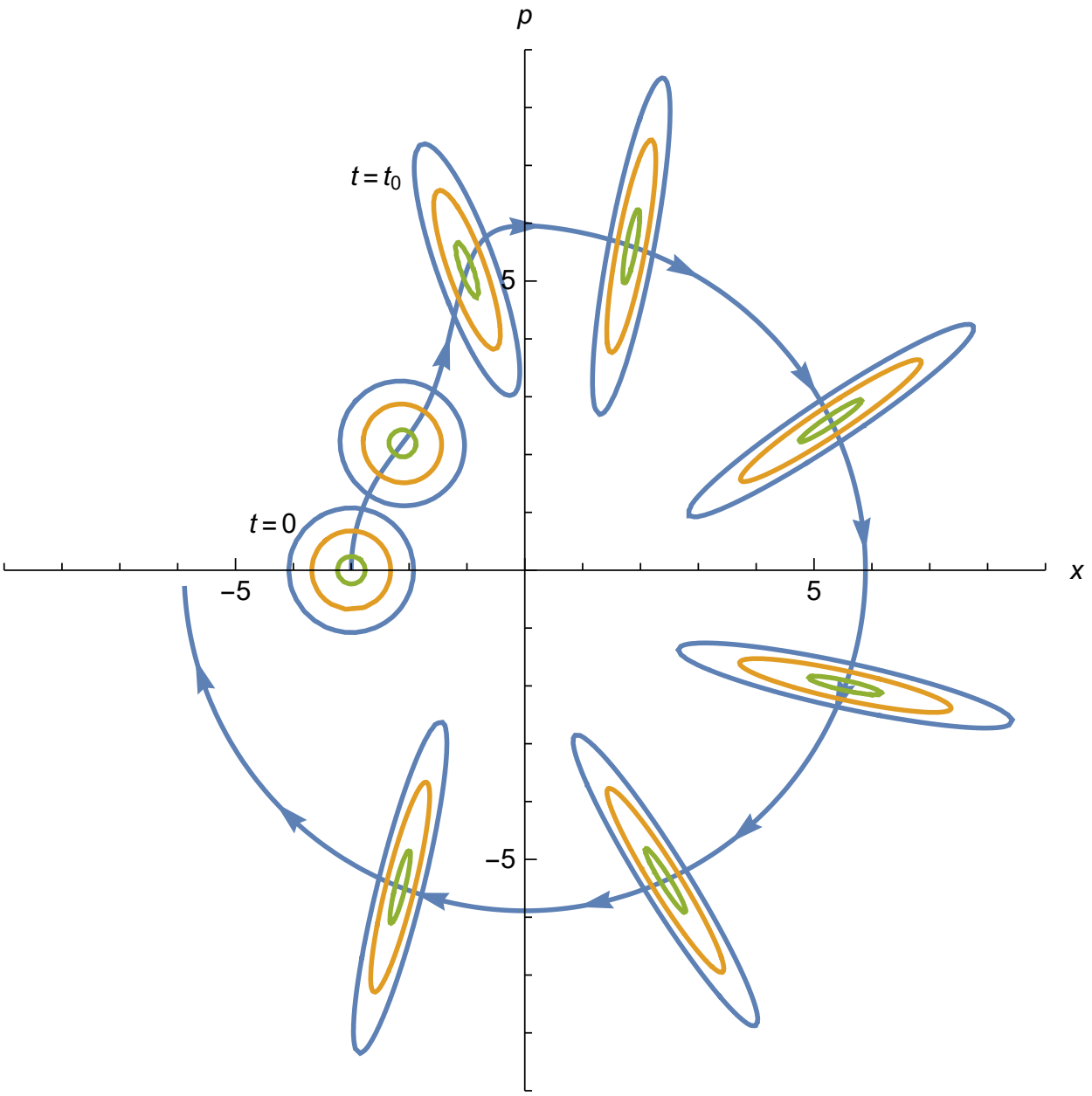

Figure 3.3 Evolving phase diagram (x, p) of an oscillator with an initial Gaussian distribution in phase space starting centered at $(x, p) = (-3, 0)$ and a Gaussian mass variation centered at a time t_0, where t_0 corresponds to the distribution centered at $(x, p) \approx (-1, 5)$.

original Caldirola-Kanai Hamiltonian. For convenience of analysis later, we will set $m(0) = m_0$, $\omega(0) = \omega_0$, and allow for a $x - p$ commutation preserving substitution such that $\gamma(0) = 0$. The Caldirola-Kanai system has been well studied in the x^2 and p^2 operator basis with Lie Algebra basis $\{\frac{x^2}{2\hbar}, \frac{p^2}{2\hbar}, \frac{1}{2} + i\frac{xp}{\hbar}\}$. However, for our convenience and simpler solutions, we convert this Hamiltonian to a basis of raising and lowering operators:

$$a = \frac{X + iP}{\sqrt{2}}, a^\dagger = \frac{X - iP}{\sqrt{2}}, \tag{3.7}$$

where $X = \sqrt{\frac{m_0\omega_0}{\hbar}}x$ and $P = \frac{p}{\sqrt{\omega_0 m_0 \hbar}}$ are dimensionless variables for position and momentum. Defining $M(t) = \frac{m(t)}{m_0}$ and $\Omega(t) = \frac{\omega(t)}{\omega_0}$ and introducing the variables

$$A(t) = \omega_0 \frac{-1 + M(t)^2\Omega(t)^2}{2M(t)} + i\omega_0\gamma(t) \tag{3.8}$$

and

$$B(t) = \omega_0 \frac{1 + M(t)^2\Omega(t)^2}{2M(t)}, \tag{3.9}$$

we reduce the Hamiltonian to the form

$$H_{\text{GCK}} = \hbar\left(A(t)\frac{a^{\dagger 2}}{2} + A(t)^*\frac{a^2}{2} + B(t)\frac{1}{2}\left(a^\dagger a + \frac{1}{2}\right)\right), \tag{3.10}$$

where the associated Lie algebra is $su(1,1)$ with generator basis $\{\frac{a^{\dagger 2}}{2}, \frac{a^2}{2}, \frac{1}{2}\left(a^\dagger a + \frac{1}{2}\right)\}$ and the commutation relations

$$\begin{aligned}
\left[\frac{a^{\dagger 2}}{2}, \frac{a^2}{2}\right] &= -2\left(\frac{1}{2}\left(a^\dagger a + \frac{1}{2}\right)\right), \\
\left[\frac{a^{\dagger 2}}{2}, \frac{1}{2}\left(a^\dagger a + \frac{1}{2}\right)\right] &= -\frac{a^{\dagger 2}}{2}, \\
\left[\frac{a^2}{2}, \frac{1}{2}\left(a^\dagger a + \frac{1}{2}\right)\right] &= \frac{a^2}{2}.
\end{aligned} \tag{3.11}$$

We note that at $t = 0$, this Hamiltonian reduces to the time-independent simple harmonic oscillator.

3.5 Structure of the Time-Evolution Operator

In order to solve the Schrödinger equation, we assume the evolution operator U can be factorized as a product of exponentials of all the generators of the associated Lie algebra [25]

$$U = e^{g_1 \frac{a^{\dagger 2}}{2}} e^{g_2 \frac{a^2}{2}} e^{g_3 \frac{1}{2}(a^\dagger a + \frac{1}{2})}, \tag{3.12}$$

where the time-dependent complex coefficients $g_1(t)$, $g_2(t)$, and $g_3(t)$ are time-dependent regular functions to be determined.

Substituting this form of the evolution operator into its own evolution equation

$$i\hbar \frac{\partial U}{\partial t} U^{-1} = H, \tag{3.13}$$

and using the property [21, p. 39]

$$e^F G e^{-F} = G + \frac{[F,G]}{1!} + \frac{[F,[F,G]]}{2!} + \ldots, \tag{3.14}$$

and matching linearly independent operator coefficients, we obtain the following set of nonlinear ordinary differential equations (ODEs):

$$\left.\begin{aligned} i\dot{g}_1 &= A(t) + B(t) g_1 + A(t)^* g_1^2 \\ i\dot{g}_2 &= A(t)^* - B(t) g_2 - 2A(t) g_1 g_2 \\ i\dot{g}_3 &= B(t) + 2A(t)^* g_1 \end{aligned}\right\}. \tag{3.15}$$

With these nonlinear ODEs, we can solve for the time-evolution of this system. Note the lack of analytic solution to these differential equations for general $A(t)$ and $B(t)$ means the dynamics need to be solved numerically for most cases. Nonetheless, we can gain more insight by studying the system's Lie algebraic structure. In order to simplify algebraic calculations, we will use the following faithful representation of the Lie algebra, which is similar to the set of Pauli matrices, to

fulfill the commutation relations in Eq. (3.11):

$$\begin{aligned} R\left(\frac{a^{\dagger 2}}{2}\right) &= \begin{pmatrix} 0 & i \\ 0 & 0 \end{pmatrix} \\ R\left(\frac{a^2}{2}\right) &= \begin{pmatrix} 0 & 0 \\ i & 0 \end{pmatrix} \\ R\left(\frac{1}{2}\left(a^\dagger a+\frac{1}{2}\right)\right) &= \frac{1}{2}\begin{pmatrix} 1 & 0 \\ 0 & -1 \end{pmatrix}. \end{aligned} \tag{3.16}$$

As a consequence of the Baker-Campbell-Hausdorff theorem [58], which is

$$e^A e^B = e^{A+B+\frac{1}{2}[A,B]+\frac{1}{12}[A,[A,B]]-\frac{1}{12}[B,[A,B]]+\ldots}, \tag{3.17}$$

equalities of products of exponentials of operators are preserved under a faithful representation since such exponential combinations only rely on the commutation relations of the operators. Thus, applying the representation Eq. (3.16) to the unitarity equation $U^{-1} = U^\dagger$, and matching matrix elements, we obtain the following conditions for unitarity:

$$\left.\begin{aligned} g_2 &= \frac{{g_1}^*}{-1+|g_1|^2} \\ \Re\left(g_3\right) &= \ln\left(1-|g_1|^2\right) \end{aligned}\right\}, \tag{3.18}$$

where $\Re\left(g_3\right)$ is the real part of g_3, thereby reducing the independent variables from six to three. We note that, although the classical Caldirola-Kanai system is dissipative, we still maintain unitarity in the time-evolution operator for the quantum case since the Hamiltonian is Hermitian.

Looking at Eq. (3.18), we see this system is completely determined by the coefficients g_1 and $\gamma_3 \equiv \Im\left(g_3\right)$, where $\Im\left(g_3\right)$ is the imaginary part of g_3. With this in mind, the time-evolution operator can be rewritten as

$$U = e^{g_1 \frac{a^{\dagger 2}}{2}} e^{\frac{{g_1}^*}{-1+|g_1|^2}\frac{a^2}{2}} e^{\left(\ln\left[1-|g_1|^2\right]+i\gamma_3\right)\frac{1}{2}\left(a^\dagger a+\frac{1}{2}\right)}. \tag{3.19}$$

Note that because of the structure of the time-evolution operator, the effect of the coefficient γ_3 is indistinguishable from $\gamma_3(mod\ 4\pi)$. Thus, throughout this paper, we will often portray a time-evolution as a function of g_1 and $e^{i\frac{\gamma_3}{2}}$.

We now examine the representation for U under the unitarity conditions given in Eq. (3.19). Applying the representation Eq. (3.16) to Eq. (3.19), we find

$$R(U) = \frac{1}{\sqrt{1-|g_1|^2}} \begin{pmatrix} e^{i\frac{\gamma_3}{2}} & ig_1 e^{-i\frac{\gamma_3}{2}} \\ -ig_1^* e^{i\frac{\gamma_3}{2}} & e^{-i\frac{\gamma_3}{2}} \end{pmatrix}. \tag{3.20}$$

By looking at $R(U)$ in Eq. (3.20), we make the following observations:

$$\left.\begin{aligned} e^{i\frac{\gamma_3}{2}} &= \frac{R(U)_{1,1}}{\left|R(U)_{1,1}\right|} \\ g_1 &= -i\frac{R(U)_{1,2}}{R(U)_{2,2}} \end{aligned}\right\}. \tag{3.21}$$

Using these relations, we can map from a representation back to a time-evolution operator written in the convenient form given in Eq. (3.19).

In order to differentiate between different time-evolution operators, we will label them and their exponential coefficients. Given a time-evolution operator $U_{(k)}$, we will denote $U_{(k)}$'s exponential coefficients when in the form Eq. (3.19) by $h_i^{(k)}$ rather than g_i. More explicitly and for reference, given a time-evolution operator in representation form $R(U_k)$, we can convert back to operator form using the equations

$$U_{(k)} = e^{h_1^{(k)}\frac{a^{\dagger 2}}{2}} e^{\frac{h_1^{(k)*}}{-1+\left|h_1^{(k)}\right|^2}\frac{a^2}{2}} e^{\left(\ln\left[1-\left|h_1^{(k)}\right|^2\right]+i\gamma_3^{(k)}\right)\frac{1}{2}\left(a^\dagger a+\frac{1}{2}\right)} \tag{3.22}$$

with

$$e^{i\frac{\gamma_3^{(k)}}{2}} = \frac{R\left(U_{(k)}\right)_{1,1}}{\left|R\left(U_{(k)}\right)_{1,1}\right|},\ \ h_1^{(k)} = -i\frac{R\left(U_{(k)}\right)_{1,2}}{R\left(U_{(k)}\right)_{2,2}}. \tag{3.23}$$

For a generic time-evolution U, we will still denote the exponential coefficients by g_i.

To demonstrate the process of converting between the faithful representation and the operator form, consider the squeeze operator $S(\xi) = e^{\frac{1}{2}\left(\xi^* a^{\dagger 2} - \xi a^2\right)} \equiv U_S$. We wish to put it into the convenient form in Eq. (3.22). Using the representation depicted in Eq. (3.16), $S(\xi)$ corresponds to:

$$R(S(\xi)) = \begin{pmatrix} \cosh(|\xi|) & ie^{-i\arg(\xi)}\sinh(|\xi|) \\ -ie^{i\arg(\xi)}\sinh(|\xi|) & \cosh(|\xi|) \end{pmatrix}. \tag{3.24}$$

Since $S(\xi)$ is unitary, we can use relation Eq. (3.23) to identify $h_1^{(S)} = e^{i\arg(\xi)}\tanh(|\xi|)$ and effectively $\Im\left(h_0^{(S)}\right) = 0$. Thus, applying this to Eq. (3.22), we find

$$S(\xi) = e^{h_1^{(S)}\frac{a^{\dagger 2}}{2}} e^{\frac{h_1^{(S)*}}{-1+\left|h_1^{(S)}\right|^2}\frac{a^2}{2}} e^{\left(\ln\left[1-\left|h_1^{(S)}\right|^2\right]\right)\frac{1}{2}\left(a^\dagger a+\frac{1}{2}\right)}. \tag{3.25}$$

If we allow $h_1^{(S)} = g_1$, $S(\xi)$ is the general time-evolution operator U given in Eq. (3.19) barring the phase factor $e^{i\gamma_3\frac{1}{2}\left(a^\dagger a+\frac{1}{2}\right)}$. Thus, in general, the time-evolution operator for this generalized Caldirola-Kanai system can also be written in the form

$$U = S(\xi)\, e^{i\gamma_3\frac{1}{2}\left(a^\dagger a+\frac{1}{2}\right)}, \tag{3.26}$$

where $\xi = \tanh^{-1}(|g_1|)e^{i\arg(g_1)}$, which is consistent with the literature. This product can be interpreted as a phase space rotation followed by a squeezing operation.

3.6 Evolution from Coherent to Squeezed States

We now apply the time-evolution operator to a coherent state. An initial coherent state can be expressed as the displacement operator (with respect to the initial system), acting on the ground state

$$|\alpha_i\rangle = e^{\alpha_i a^\dagger - \alpha_i^* a}|0\rangle = D(\alpha_i)|0\rangle, \tag{3.27}$$

where $D(\alpha_0) \equiv e^{\alpha_0 a^\dagger - \alpha_0^* a}$ is the displacement operator. Applying the time-evolution operator to the coherent state, and using the property

$$e^A B e^{-A} = B + \frac{[A,B]}{1!} + \frac{[A,[A,B]]}{2!} + \ldots, \tag{3.28}$$

again, we find the evolved coherent state to be

$$\begin{aligned} U\,|\alpha_i\rangle &= UD(\alpha_i)\,|0\rangle \\ &= \left(UD(\alpha_i)U^{-1}\right)U\,|0\rangle \\ &= D(\beta)U\,|0\rangle, \end{aligned} \tag{3.29}$$

where $\beta = \frac{e^{\frac{1}{2}i\gamma_3}\alpha_i + e^{-\frac{1}{2}i\gamma_3}\alpha_i^* g_1}{\sqrt{1-|g_1|^2}}$.

Thus, substituting Eq. (3.26) into Eq. (3.29), we obtain the following:

$$\begin{aligned} U\,|\alpha_i\rangle &= D(\beta)U\,|0\rangle \\ &= D(\beta)S(\xi)\,e^{i\gamma_3\frac{1}{2}\left(a^\dagger a+\frac{1}{2}\right)}\,|0\rangle \\ &= D(\beta)\;S(\xi)\,|0\rangle\,e^{i\frac{\gamma_3}{4}} \\ &= |\beta,\xi\rangle\,e^{i\frac{\gamma_3}{4}} \end{aligned} \tag{3.30}$$

where

$$\xi = \tanh^{-1}(|g_1|)e^{i\arg(g_1)} \tag{3.31}$$

and

$$\beta = \frac{e^{\frac{1}{2}i\gamma_3}\alpha_i + e^{-\frac{1}{2}i\gamma_3}\alpha_i^* g_1}{\sqrt{1-|g_1|^2}}, \tag{3.32}$$

and where the squeezed state $|\beta,\xi\rangle \equiv D(\beta)S(\xi)\,|0\rangle$ is referred to in the literature as an intelligent state. Thus, all evolutions of coherent states subject to the generalized Caldirola-Kanai Hamiltonian lead to a squeezed state with a phase factor $e^{i\frac{\gamma_3}{4}}$.

The squeezed state has been well studied [10]; here we give some of its properties in terms of g_1 and $\gamma_3 = \Im(g_3)$. The variances for X and P are

$$\sigma_X^2 = \frac{1}{2}\frac{1+|g_1|^2+2\Re(g_1)}{1-|g_1|^2}, \tag{3.33}$$

$$\sigma_P^2 = \frac{1}{2}\frac{1+|g_1|^2-2\Re(g_1)}{1-|g_1|^2}. \tag{3.34}$$

The expectation values for X and P are

$$\begin{aligned}\langle X\rangle + i\langle P\rangle &= \sqrt{2}\left(\frac{e^{\frac{1}{2}i\gamma_3}\alpha_i + e^{-\frac{1}{2}i\gamma_3}\alpha_i^* g_1}{\sqrt{1-|g_1|^2}}\right) \\ &= \sqrt{2}\beta.\end{aligned} \tag{3.35}$$

Since the squeezed state rotates when evolving in simple harmonic dynamics, it is convenient to show the variances in X-P with the rotated coordinates following the direction of maximal spread. Thus, allowing the rotating variables $X_{\theta_+} = X\cos\theta_+ - P\sin\theta_+$ and $X_{\theta_-} = X\cos\theta_- - P\sin\theta_-$, where X_{θ_+} is the coordinate in the direction of maximal spread and X_{θ_-} is the coordinate in the direction of minimal spread, the rotated spreads are

$$\sigma^2_{X_{\theta_\pm}} = -\frac{1}{2} + \frac{1}{1\mp|g_1|}, \tag{3.36}$$

$$\theta_\pm = \tan^{-1}\left(\frac{\Re(g_1)\pm|g_1|}{\Im(g_1)}\right) + n\pi, \tag{3.37}$$

where $\theta_\pm$ refers to the angle of maximal/minimal variance from the X axis and n is an integer. It is worth noting that $\sigma^2_{X_{\theta_{\max}}}\sigma^2_{X_{\theta_{\min}}} = \frac{1}{4}$, thus confirming again that this system preserves minimal uncertainty.

3.7 Classical Phase space and the Wigner Function

We now compare classical and quantum evolutions of this system. To do this, we find the Husimi and Wigner functions. With respect to the coherent states, the Husimi function is given by

$$\begin{aligned}Q(z) &= \frac{1}{\pi}|\langle z \mid U \mid \alpha_i\rangle|^2 \\ &= \frac{1}{\pi}\sqrt{1-|g_1|^2}e^{-(1-|g_1|)\Re(\mu(z))^2-(1+|g_1|)\Im(\mu(z))^2},\end{aligned} \tag{3.38}$$

with $\mu(z) = (z-\beta)e^{-\frac{i\arg(g_1)}{2}}$, and β given in Eq. (3.32). We now calculate the Wigner function to be

$$\begin{aligned} W(\tilde{X},\tilde{P}) &= \frac{1}{\pi}\iint \langle\beta_1|U|\alpha_i\rangle \left\langle \alpha_i|U^\dagger|\beta_2\right\rangle e^{-\frac{|\beta_1|^2+|\beta_2|^2+4|z|^2}{2}+2(z^*\beta_1+z\beta_2{}^*)-\beta_1\beta_2{}^*}\frac{d\beta_1^2}{\pi}\frac{d\beta_2^2}{\pi} \\ &= \frac{1}{\pi}e^{-\left(\frac{\Re(\mu(z))}{\sigma_{X_{\theta_+}}}\right)^2-\left(\frac{\Im(\mu(z))}{\sigma_{X_{\theta_-}}}\right)^2}, \end{aligned} \tag{3.39}$$

where $\mu(z)$ is defined by Eq. (3.38), $\sigma^2_{X_{\theta_\pm}}$ is defined in Eq. (3.36), and $z = \frac{\tilde{X}+i\tilde{P}}{\sqrt{2}}$. Note that the form of the Wigner function is a displaced, rotated, and squeezed Gaussian with respect to that of the initial coherent state.

Looking at the classical case and the quantum case of a single Gaussian mass fluctuation ($m(t) = m_0\left(1+Ce^{-\varepsilon(t-t_0)^2}\right)$), we can compare the evolution of a phase diagram with an initially Gaussian probability in Fig. (3.4) and, using Eq. (3.39), the Wigner function with an initial coherent state in Fig. (3.5). Comparing the two evolutions, we find that the resulting plots are *identical*. This is a general feature for all cases we have considered.

3.8 Discrete Dynamic Control

In this Section, we establish a method to control the time evolution via finite fluctuations. From the unitarity conditions, we found that any possible time-evolution is determined by the three parameters $\Im(g_3) = \gamma_3$, $\arg(g_1)$, and $|g_1|$. Thus, here we demonstrate that given any repeatable compact fluctuations in the system that lead to a nonzero $|g_1|$, any time-evolution can be achieved via repetitions of this compact fluctuation and waiting periods. We will then study the effect of these time-evolutions on squeezing, and the possibility of reversing a time-evolution.

The evolution of a waiting period is given by the time independent Hamiltonian $H_0 = \frac{1}{2m_0}p^2 + \frac{1}{2}m_0{\omega_0}^2x^2$. This evolution is easily solved using the differential equations in Eq. (3.15), which yields the exponential coefficients for the simple harmonic time evolution operator U_0 to be $h_1^{(0)} = 0$

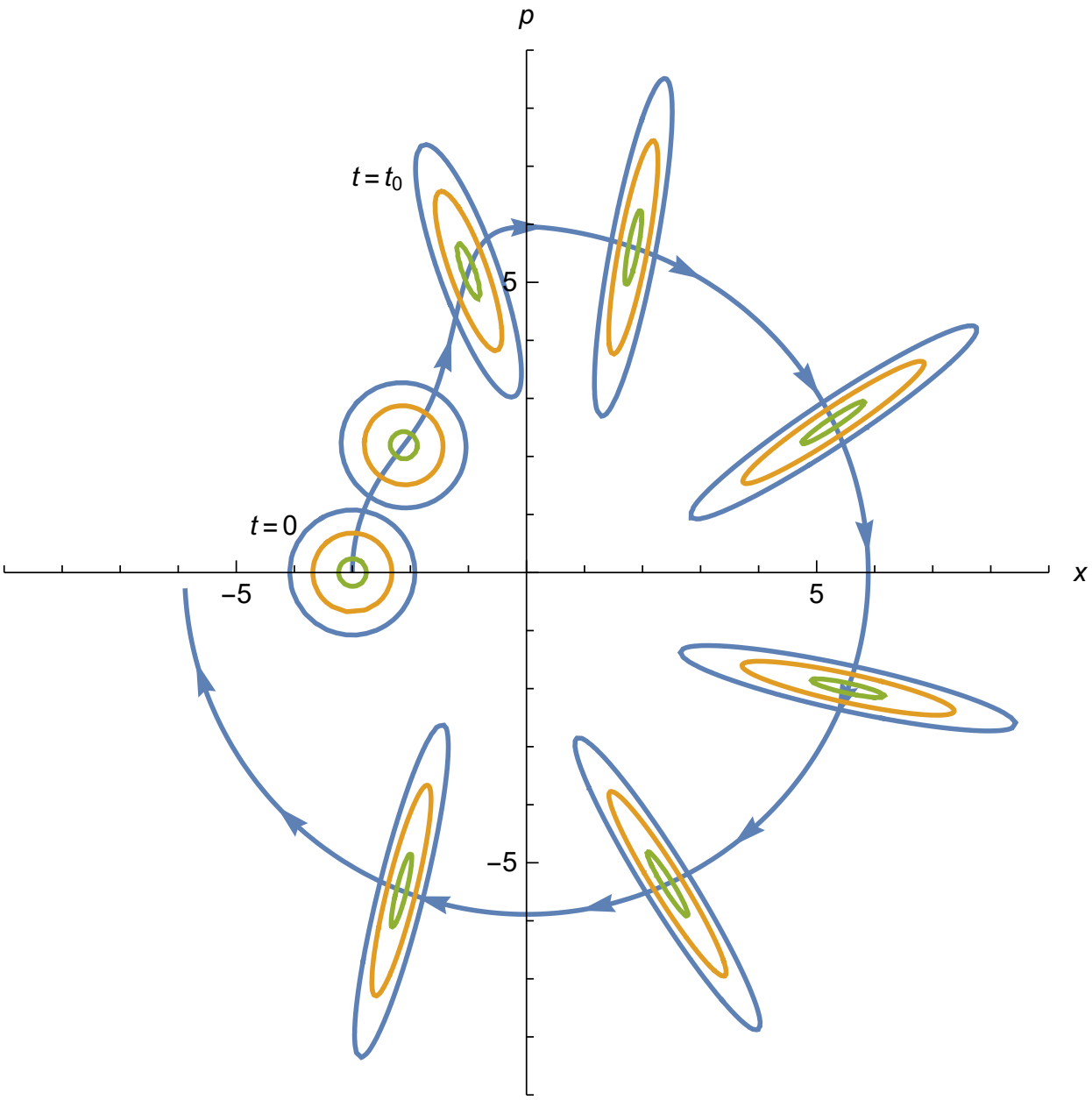

Figure 3.4 Classical Gaussian Phase Distribution Contour Plot evolving with a Gaussian mass fluctuation

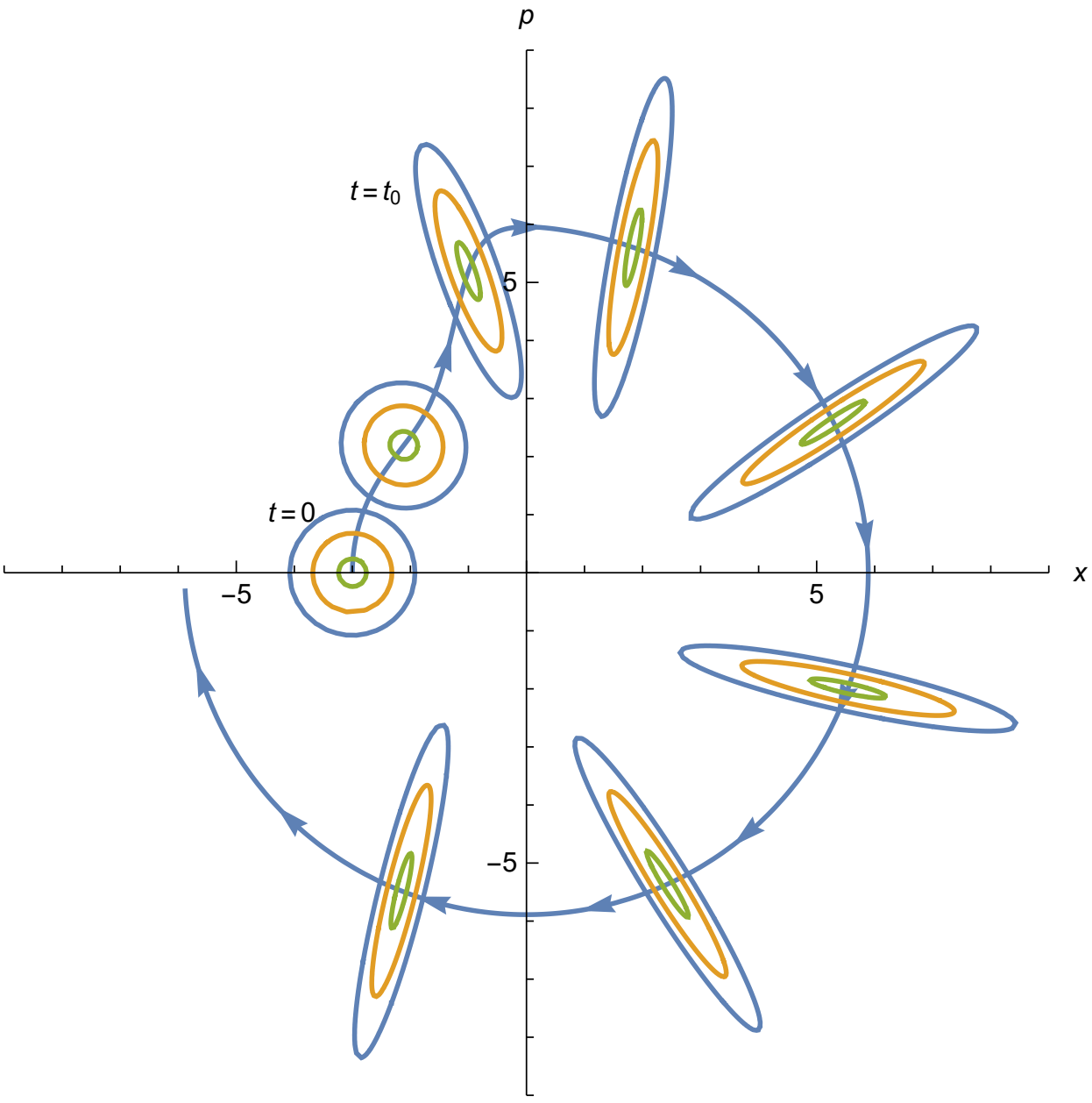

Figure 3.5 Wigner function of a Coherent State Contour Plot evolving with a Gaussian mass fluctuation.

and $h_3^{(0)} = -2it\omega_0$. Thus,

$$R\left(U_0\left(t\right)\right) = \begin{pmatrix} e^{-it\omega_0} & 0 \\ 0 & e^{it\omega_0} \end{pmatrix}. \tag{3.40}$$

We now find a way to control the phase factor coefficients γ_3 and $\arg\left(g_1\right)$ using waiting periods. Selecting $U_{\phi_1,\phi_2} \equiv U_0\left(\frac{\phi_1+2\pi m}{2\omega_0}\right) U U_0\left(\frac{\phi_2-\phi_1+2\pi n}{2\omega_0}\right)$, with U from Eq (3.19), then calculating $R\left(U_{\phi_1,\phi_2}\right)$, and using relations Eq. (3.23), we find the resulting coefficients to be $h_1^{(\phi_1,\phi_2)} = e^{-i\phi_1} g_1$ and $e^{i\frac{\gamma_3^{(\phi_1,\phi_2)}}{2}} = e^{i\frac{1}{2}(\gamma_3 - i\phi_2)}$. Thus,

$$U_0\left(\frac{\phi_1+2\pi m}{2\omega_0}\right) U\left(g_1, e^{i\frac{\gamma_3}{2}}\right) U_0\left(\frac{\phi_2-\phi_1+2\pi n}{2\omega_0}\right) = U\left(e^{-i\phi_1} g_1, e^{i\frac{1}{2}(\gamma_3-\phi_2)}\right). \tag{3.41}$$

By simply waiting before and after the fluctuation, we can control the phase factor coefficients γ_3 and $\arg\left(g_1\right)$ for the time-evolution operator.

Having established a method for controlling the phases for the time-evolution operator, we focus on controlling the parameter $|g_1|$. We do this via repetitions. Allow U_n to be the n times repeated evolution of U. Then $U_n = U^n$. Calculating $R\left(U_n\right) = R\left(U\right)^n$ and once again applying relation Eq. (3.23), we identify the exponential coefficients to be of the form

$$h_1^{(n)} = \frac{g_1}{|g_1|} \frac{e^{-i\frac{\gamma_3}{2}} \sinh\left(n\Phi\right)}{\cosh\left(n\Phi - i\Theta\right)}, \tag{3.42}$$

and

$$e^{i\frac{\gamma_3^{(n)}}{2}} = \frac{\cosh\left(n\Phi + i\Theta\right)}{\left|\cosh\left(n\Phi + i\Theta\right)\right|}, \tag{3.43}$$

with

$$\begin{aligned} \Phi &= \cosh^{-1}\left(\frac{\Re\left(e^{i\frac{\gamma_3}{2}}\right)}{\sqrt{1-|g_1|^2}}\right), \\ \Theta &= \sin^{-1}\left(\frac{\Im\left(e^{i\frac{\gamma_3}{2}}\right)}{|g_1|}\right). \end{aligned} \tag{3.44}$$

Thus,

$$U^n\left(g_1, e^{i\frac{\gamma_3}{2}}\right) = U\left(\frac{g_1}{|g_1|}\frac{e^{-i\frac{\gamma_3}{2}}\sinh(n\Phi)}{\cosh(n\Phi - i\Theta)}, \frac{\cosh(n\Phi + i\Theta)}{|\cosh(n\Phi + i\Theta)|}\right), \tag{3.45}$$

with Φ and Θ given in Eq. (3.44).

Since we are interested in controlling the term $|g_1|$, we take the magnitude of $h_1^{(n)}$ and find

$$\left|h_1^{(n)}\right| = \left|\frac{\sinh(n\Phi)}{\sqrt{\cosh^2(n\Phi) - \sin^2(\Theta)}}\right|. \tag{3.46}$$

Adjusting the parameter γ_3 using Eq. (3.41) and n, we can cause $\left|h_1^{(n)}\right|$ to become any number between 0 and 1 if the evolution term $|g_1|$ from a single pulse variation is nonzero. Thus by using waiting periods and repetitions of a given temporally compact pulse fluctuation with $|g_1| \neq 0$, we can completely control the time-evolution operator of the system.

We now examine the possibility of inverting a time-evolution. We first guess the form of the inverse to be $U^{-1} = U_0(\Delta t_1) U U_0(\Delta t_2)$, with Δt_1 and Δt_2 undetermined. Allowing for $U_D = U_0(\Delta t_1) U U_0(\Delta t_2) U$, with eventual intention of setting $U_D = I$, then calculating $R(U_D)$ and using relation Eq. (3.23) to find $h_1^{(D)}$and $e^{i\frac{\gamma_3^{(D)}}{2}}$, as before, then forcing the conditions $h_1^{(D)} = 0$ and $e^{i\frac{\gamma_3^{(D)}}{2}} = 1$ to make U_D the identity, we find

$$\begin{aligned} \Delta t_1 &= \frac{\gamma_3 + (1+2m)\pi}{2\omega_0}, \\ \Delta t_2 &= \frac{\gamma_3 + (1+2n)\pi}{2\omega_0}, \end{aligned} \tag{3.47}$$

with n and m integers of opposite parity. Thus,

$$U^{-1} = U_0(\Delta t_1) U U_0(\Delta t_2), \tag{3.48}$$

with Δt_1 and Δt_2 given in Eq. (3.47). Thus one can cancel a time-evolution by waiting, repeating that evolution, then waiting again. Related work on time reversal is given in [49, 50].

We now consider the evolution of repeating fluctuations timed for maximal squeezing. As shown in Eq. (3.36), the maximal squeeze of a coherent state is solely determined by $|g_1|$. From Eq. (3.46),

we see that if Φ is real, in the limit as $n \to \infty$, $\left|h_1^{(n)}\right| \to 1$, which implies by Eq. (3.36) that the squeeze approaches infinity. In order to maximize the squeeze per repetition, we could phase shift the initial time-evolution U using Eq. (3.41) such that $e^{i\frac{\gamma_3}{2}} = \pm 1$, which is achieved by spacing the time between pulses $\frac{\gamma_3}{2\omega_0}$ apart. By doing so, $|g_1| \to \tanh[n\Phi] = \frac{Q^n-1}{Q^n+1}$ with $Q = \frac{|g_1|+1}{|g_1|-1}$. Applying this to Eq. (3.36) and Eq. (3.37), we find under these conditions, applied to an initial coherent state:

$$\sigma^2_{X_{\theta_\pm}} = \frac{Q^{\pm n}}{2}, \tag{3.49}$$

$$\theta_\pm = \tan^{-1}\left(-\frac{\Re\left(e^{-i\arg(g_1)}\right) \pm 1}{\Im\left(e^{-i\arg(g_1)}\right)}\right), \tag{3.50}$$

with $Q = \frac{|g_1|+1}{|g_1|-1}$. Thus, under optimized squeezing conditions, repeated evolutions cause exponential squeezing to occur. Also, should g_1 be near to real, the angle of squeezing will focus in the P direction. Should g_1 be near imaginary, the angle of squeezing will be close to the 45° between X and P axis. Similar claims of exponential squeezing are given in [47, 52].

3.9 Delta Fluctuations

We now examine the extreme case of Dirac delta fluctuations in the mass and frequency terms. We allow

$$\begin{aligned} M(t) &= 1 + \Delta M \frac{\theta(t)\,\theta(\Delta t - t)}{\omega_0 \Delta t}, \\ \Omega(t) &= 1 + \Delta\Omega \frac{\theta(t)\,\theta(\Delta t - t)}{\omega_0 \Delta t}, \end{aligned} \tag{3.51}$$

noting that

$$\lim_{\Delta t \to 0} \frac{\theta(t)\,\theta(\Delta t - t)}{\Delta t} = \delta(t), \tag{3.52}$$

where θ is the Heaviside function. Then, after solving for the exponential coefficients g_i using Eq. (3.15) and taking the limits as $\Delta t \to 0$, we find the effects of $M(t) = 1 + \Delta M \frac{\delta(t)}{\omega_0}$ and $\Omega(t) =$

Table 3.1 Dirac Delta Fluctuations Characterization

Case	ΔM	$\Delta\Omega$	g_1	$e^{i\frac{\gamma_3}{2}}$
1	$\neq 0$	$\neq 0$	-1	$-i\frac{\Delta M\Delta\Omega}{\lvert\Delta M\Delta\Omega\rvert}$
2	$\neq 0$	$=0$	$\frac{\Delta M}{2i-\Delta M}$	$\frac{2-i\Delta M}{\lvert 2-i\Delta M\rvert}$
3	$=0$	$\neq 0$	$\frac{\Delta\Omega}{2i-\Delta\Omega}$	$\frac{2-i\Delta\Omega}{\lvert 2-i\Delta\Omega\rvert}$

$1+\Delta\Omega\frac{\delta(t)}{\omega_0}$. Three cases are shown in Table 3.1.

From Eq. (3.36) and Eq. (3.37), we see that Case 1 suggests an infinite squeezing in the 0° direction. Cases 2 and 3 suggest more moderate squeezing.

By spacing the time between pulses to be $\frac{\gamma_3}{2\omega_0}$ apart, in case 2, we optimize the squeezing per pulse. The variance effects on an initial coherent state would increase/decrease exponentially in the maximal/minimal directions in the X-P plane according to $\sigma^2_{X_{\theta_\pm}} = \frac{Q^{\pm n}}{2}$, with

$$Q = \frac{\sqrt{4+\Delta M^2}+|\Delta M|}{\sqrt{4+\Delta M^2}-|\Delta M|} \tag{3.53}$$

given by Eq. (3.49). Related work on Dirac delta fluctuations that does not use the Lie algebra representations is given in [53–55].

3.10 Gaussian Fluctuations

We now perform a similar analysis for a series of Gaussian mass term pulses

$$M(t) = 1 + C\sqrt{\frac{\varepsilon}{\pi}}\sum_k e^{-\varepsilon(t-t_k)^2}, \tag{3.54}$$

which could be associated with variations in the permittivity of a cavity.

Since the differential equations with this mass variation are significantly more complicated, we solve them numerically allowing $C = 5$, $\omega_0 = 1/2$, and $\varepsilon = 10$. To find the evolution of the system,

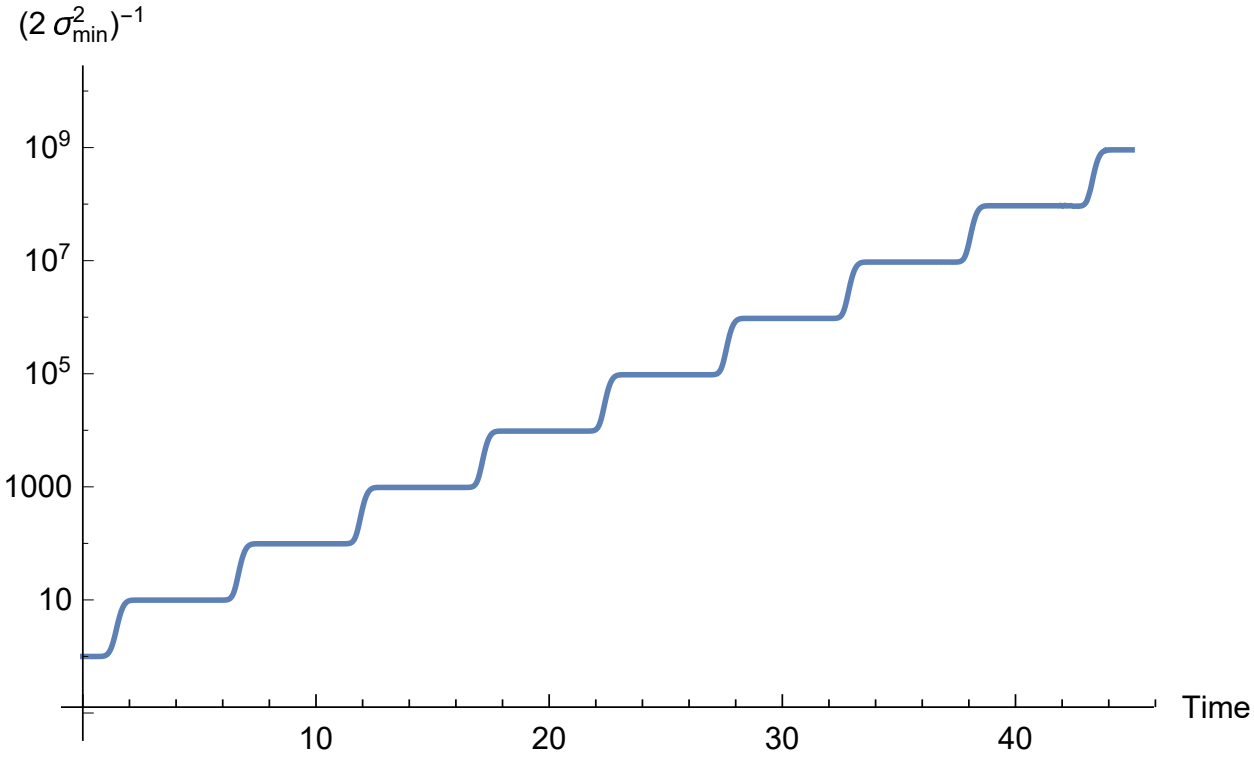

Figure 3.6 Squeeze of coherent state under effect of timed Gaussian pulses for exponential growth

we study the effect of one pulse of width $2t_0$ where $t_0 = 1.5$. By using Eq. (3.15), the evolution is given by:

$$\begin{aligned} 2i\dot{g}_1 &= \omega_0 \left(-M(t)^{-1}(1-g_1)^2 + M(t)(1+g_1)^2 \right) \\ i\dot{g}_3 &= \omega_0 \left(M(t)^{-1}(1-g_1) + M(t)(1+g_1) \right), \end{aligned} \tag{3.55}$$

with $M(t) = 1 + C\sqrt{\frac{\varepsilon}{\pi}} e^{-\varepsilon(t-t_0)^2}$ and initial conditions $g_1(0) = 0$ and $g_3(0) = 0$. Numerically, we find $g_1(2t_0) \approx -0.734 + i0.359$, and $\gamma_3(2t_0) \approx -4.051$.

The rest time interval between pulses that maximizes the squeeze is given by $\Delta t_{\max} = \frac{1}{\omega_0}\frac{\gamma_3(t_0)}{2} \approx 2.23$. Since each pulse takes $2t_0$ time, the maximizing period is $\Delta T_{\max} = \Delta t_{\max} + 2t_0 = 5.23$. Allowing the function to be $M(t) = 1 + C\sqrt{\frac{\varepsilon}{\pi}} \sum_{k=0} e^{\varepsilon(t-t_0-kT_{\max})^2}$, we find that the spread and squeeze grow exponentially as shown in Fig. (3.6). This squeezing is consistent with the general analysis that

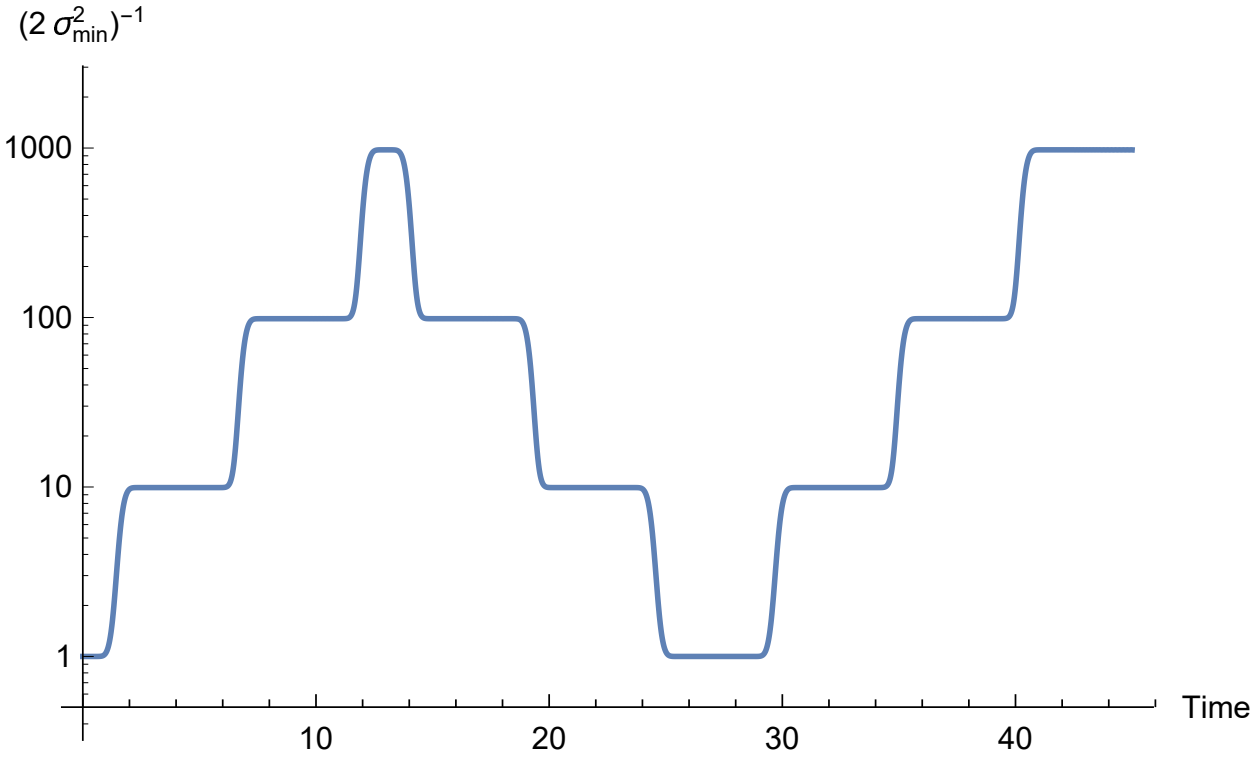

Figure 3.7 Squeeze of coherent state under effect of timed Gaussian pulses for reversible squeezing

$\sigma^2_{X_{\theta_\pm}} = \frac{Q^{\pm n}}{2}$ with $Q = \frac{|g_1|+1}{|g_1|-1} = 9.919$ where n is the number of repetitions.

Noting from Eq. (3.48) that $U^{-1} = U_0\left(\frac{\gamma_3-\pi}{2\omega_0}\right)UU_0\left(\frac{\gamma_3-\pi}{2\omega_0}\right)$ and allowing $\Delta T_{min} = \frac{\gamma_3-\pi}{2\omega_0} + 2t_0$, we could cause the system to squeeze, return to a coherent state, then squeeze again by judiciously timing the Gaussian pulse fluctuations in the mass term:

$$M(t) = 1 + C\sqrt{\frac{\varepsilon}{\pi}}\sum_{k=1} e^{-\varepsilon\left(t-\sum_{i=1}^{k}\Delta t_i\right)^2} \quad , \quad \Delta t_i = \begin{cases} t_0 & i = 1 \\ \Delta T_{\text{min}} & i = 4 \\ \Delta T_{\text{max}} & i \neq 1,4 \end{cases} . \tag{3.56}$$

This evolution containing two squeezing events is depicted in Fig. (3.7).

To further illustrate the evolution of this particular system, we allow the initial coherent state to arbitrarily be $\left|\frac{.2\left(\sqrt{2}+i\right)}{\sqrt{3}}\right\rangle$ and provide the Husimi plot in Fig. (3.8). Taking the angle of minimal

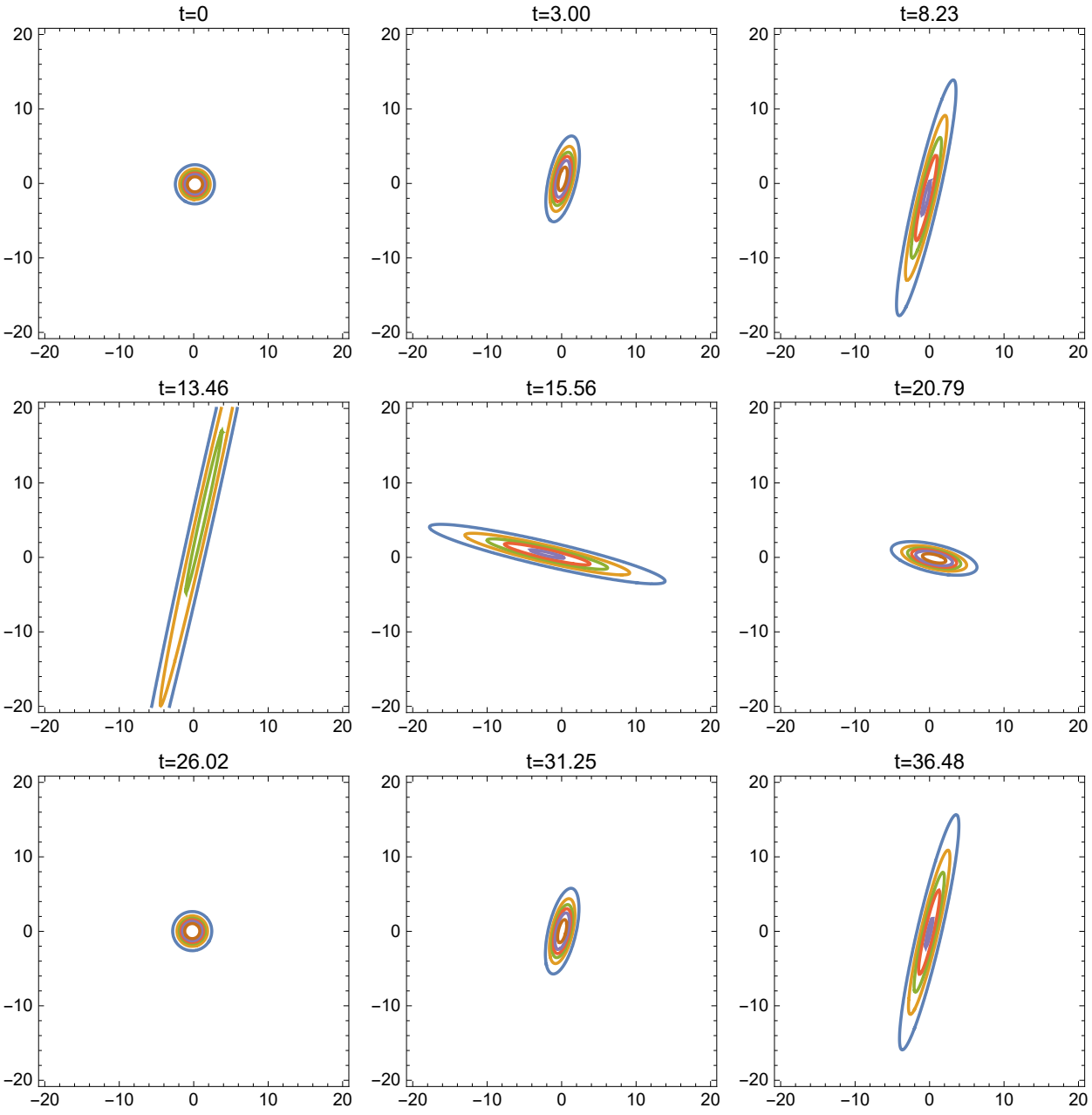

Figure 3.8 Frames of the Husimi function for the evolution of a coherent state subject to a series of Gaussian pulse variations given in Eq. (3.56) and illustrated in Fig. (3.7) demonstrating quantum control. Each frame represents the Husimi function after a Gaussian pulse. More precisely, $t_0 = 1.5$ after the center of Gaussian pulse variation.

and maximal spread at time $2t_0$ using Eq. (3.50), we calculate

$$\begin{aligned}\theta_{\pm} &= \tan^{-1}\left(-\frac{\Re\left(e^{-i\arg(g_1(2t_0))}\right)\pm 1}{\Im\left(e^{-i\arg(g_1(2t_0))}\right)}\right) \\ &= 31.97^\circ \mp 45^\circ,\end{aligned} \tag{3.57}$$

which is consistent with $t = 3.00$ on Fig. 3.8. Note that the timing chosen for maximal and minimal squeezing are set up such that the directions of spreads in Fig. 3.8 are pointing in the $\theta = 31.97^\circ \mp 45^\circ$ directions.

3.11 Conclusion

In this paper, we have analyzed the quantum Caldirola-Kanai system in terms of the raising and lowering operators. We found a representation for the time-evolution operator Eq. (3.16) and used this to find conditions for unitarity Eq. (3.18). We showed that any unitary evolution of the generalized Caldirola-Kanai system is given by the squeeze operator with a phase factor using the Lie algebraic representation and unitarity conditions. We discussed the time-evolution on an initial coherent state, and a connection between the classical evolution of a probabilistic phase space distribution and the quantum evolution of the Wigner function. We then found ways to fully control the system using temporally compact fluctuations combined with waiting periods. We analytically explored the effects of Dirac delta fluctuations in mass and frequency. We then numerically demonstrated the effectiveness in controlling this system for the case of Gaussian fluctuations in the mass term.

Note that the methods described here are similar to some of those implemented for the "shortcuts to adiabaticity" [59] in that we use matrices to set up time-evolution operators to transport a quantum state from one to another using finite variations in the parameters. However, the further generalization involving the Lagrangian density [60] to approximately apply to systems that are

unharmonic is incompatible with the methods using faithful representations. The work here can, however, apply to any system with a Hamiltonian composed of time-independent operators forming a Lie algebra, and can be further extended to systems where a mean field approximation can be used with an interaction picture as in [61].

Chapter 4

Photon Creation, Decoherence, and Squeezing in a Second Order Optomechanical System

4.1 Abstract

Optomechanical systems consist of a coupling between a mirror and a laser, and present a possible way to create cat states. Cat states can function as qubits, essential for quantum computers. But this mirror-laser coupling leads to decoherence effects, which muddle such desired dynamics and requires correction. Furthermore, maintaining the second order coupling terms, which are usually ignored, adds important effects, such as photon creation and squeezing. Here we analyze an optomechanical system with second order coupling using a mean field approximation, the Wei-Norman method, partial tracing, and Husimi plots. We show that the effects of decoherence lead to a rotational smearing of the Husimi function, demonstrating a loss of harmonic oscillator phase information for the laser for first order coupling. We then study and show that second order

laser-mirror coupling causes photon creation via a dynamic Casimir effect and effectively adds a squeeze term to the density matrix of the laser. We also show that the added squeeze term causes decoherence effects to have the same rotational smearing after the squeeze effects in the Husimi function.

4.2 Introduction

4.2.1 Optomechanical Systems and Schrödinger Cat States

Optomechanical systems typically involve a Fabry-Pérot cavity with one of its mirrors endowed with the ability to move. Radiation pressure on the mirror and momentum transfer creates a mirror-laser coupling [62]. With this coupling, we attempt to use the mirror to control and/or gauge the laser [63, 64]. For this paper, we will assume the mirror to move in such a way as to mimic the motion and response of a harmonic oscillator [65–68]. It has been shown that such an optomechanical system can create Schrödinger cat states [65].

Schrödinger cat states, often referred to as simply cat states, appear as a superposition of two equally weighted coherent states with opposing eigennumbers [10]. When measuring for one of these coherent states, the probability of getting a false positive for its opposing twin is very low. Because of this, the two coherent states for the cat state are approximately orthogonal, making Schrödinger cat states usable as qubits. These qubits are possible building blocks for quantum computers which represent the future of physics simulation [1],cryptography, and optimization problems, [4] as well as computational feats such as Shor's factorization algorithm [2] and Grover's algorithm [3]. The typical method utilized to creating these cat states is through a Kerr medium, i.e. a medium that presents a nonlinear response to electromagnetic fields, often modeled by adding a second order term with respect to the number operator [6, 7]. Optomechanical systems can mimic this Kerr-like effect from the number operator squared term that is not explicit in the Hamiltonian,

but implicit via the Lie algebraic structure of the system [65, 66, 69].

The optomechanical laser-mirror interaction leads to decoherence and in some scenarios the effects of second order coupling.

4.2.2 Decoherence

Much of the difficulty involved in creating quantum devices involves decoherence. Decoherence, model-wise, is the coupling of a quantum system to an outside, probabilistically ignored, environment [70]. Such probabilistic ignoring is achieved mathematically via partial tracing away the environment, while leaving the quantum part of the system to be studied [70]. By ignoring the environment, we lose information leading to a decrease in idempotency [71] for the density matrix. This causes the system to lose its "quantumness" in that the interference terms in the density matrix lose amplitude, leaving the diagonal terms to evolve without interaction—much like in classical mechanics. Thus, when decoherence occurs, the system becomes "more classical".

In an optomechanical system, a laser interacts with a mirror environment, causing some decoherence with the laser. It is therefore important to study the effects of decoherence in the laser for this system. In this paper, we show that decoherence creates a rotational smearing effect in the Husimi function [22], further exploring the phenomenon mentioned in [66]. For the case of an initial coherent state under first order interaction, we show that the Husimi function approaches a modified Bessel function with exponential decay and loses all phase distinction. When the effects of second order coupling are included, we show that this causes more of rotational smearing after squeezing in the Husimi function.

4.2.3 Second Order Coupling

Optomechanical system interactions typically are approximated to be linear, since the interactions in most experimental optomechanical systems tend to be weak [68]. Much exploration in maintaining

a second order coupling focuses on the second order term in the resonator [72–76]. Here we treat the case for a second order approximation of the coupling with respect to the laser. This system has been suggested in [68] and explored in [77] by using numerical diagonalization. In this paper, a mean field approximation is applied to the nonlinear coupling term in the interaction Hamiltonian. This is done in order to maintain some of the properties associated with the nonlinear coupling effects while allowing use of Wei-Norman Lie algebraic methods [25] to obtain some more analytical results. We also show and verify the addition of this coupling term causes squeezing [10] in the system which leads to photon creation via the dynamic Casimir effect [78] (the moving mirror causing photons to appear in an initially empty laser cavity).

4.2.4 Overview

In Section 2.1 we develop a model for an optomechanical system with second order coupling. In Section 2.2 we examine the evolution of the optomechanical system with linear coupling. In Section 2.3 we measure the decoherence of the system described in Section 2.2 and find the evolution limits as the decoherence approaches infinity. In 2.4 we create Husimi plots of the linearly coupled case and show, in the limiting case as the decoherence becomes large, this Husimi function tends towards a modified Bessel function for an initial coherent state. In Section 2.5 we examine the evolution of the expectation value of the number operator $\langle f(n) \rangle$ from the linear coupling. In Section 2.6 we analyze the effects of adding nonlinear coupling to the system. In Section 3.1 we conclude.

4.3 Methods

4.3.1 The Model

In this section, we develop our model for an optomechanical system with second order coupling. We begin with the Hamiltonian for the parametric oscillator representing a single mode field:

$$H_{\text{osc}} = \frac{P^2}{2m} + \frac{1}{2} m\, \Omega^2(t) X^2, \tag{4.1}$$

where P is the effective momentum, X is the effective position, m is the effective mass, and $\Omega(t)$ is the effective frequency for the laser with:

$$\Omega^2(t) = \left(\frac{\Omega_0}{1 + \frac{x(t)}{L}} \right)^2 \simeq {\Omega_0}^2 \left(1 - \frac{2x(t)}{L} \right), \tag{4.2}$$

$x(t)$ being the instantaneous displacement of the mechanical oscillator for the mirror from equilibrium, L being the length of the cavity, and $x(t) << L$. Substituting Eq. (4.2) into Eq. (4.1), and adding the energy of the mirror with ω_1 the frequency of the mirror and $b^\dagger b$ the number operator for the mirror, the Hamiltonian becomes,

$$\begin{aligned} H &= \frac{P^2}{2} + \frac{1}{2} m\, \Omega_0^2 \left(1 - \frac{2x(t)}{L} \right) X^2 + \hbar\omega_1 \left(b^\dagger b + \frac{1}{2} \right) \\ &= \hbar\Omega_0 \left(\hat{n} + \frac{1}{2} \right) + \hbar\omega_1 \left(b^\dagger b + \frac{1}{2} \right) - \frac{m\Omega_0^2 x(t)}{L} X^2 \end{aligned} \tag{4.3}$$

Quantizing the position of our mechanical oscillator, we allow $x(t) = \sqrt{\frac{\hbar}{2M\omega_1}}(b + b^\dagger)$ where $b^\dagger$ and b are standard rising and lowering operators and M and ω_1 are the mass and frequency for the mechanical oscillator. We also define $a = \sqrt{\frac{\Omega_0 m}{2\hbar}} X + i\sqrt{\frac{1}{2\Omega_0 \hbar m}} P$ with a and $a^\dagger$ standard mode rising and lowering operators. We also define $\hat{n} = a^\dagger a$ to be the standard number operator with respect to a. Making these substitutions into Eq. (4.3) and shifting the energy origin by setting the relevant $1/2$ terms to zero, we obtain

$$\begin{aligned} H =& \hbar(\Omega_0 \hat{n} + \omega_1 b^\dagger b - B\hat{n}(b + b^\dagger) \\ & - \frac{B}{2}(a^2 + {a^\dagger}^2)(b + b^\dagger)) \end{aligned} \tag{4.4}$$

with $B = \frac{\Omega_0}{L\sqrt{2M\omega_1}}$.

We now separate the Hamiltonian into terms of H_0 and V with

$$H_0 = \hbar\left(\Omega_0\hat{n} + \omega_1 b^\dagger b - B\hat{n}(b+b^\dagger)\right) \tag{4.5}$$

and

$$V = \hbar\left(-\frac{B}{2}(a^2 + a^{\dagger 2})(b+b^\dagger)\right) \tag{4.6}$$

where H_0 is the usual Hamiltonian for a linear optomechanical system [65–68]. Since the Hamiltonian H in Eq. (4.4) is not composed of operators closed under commutation, we switch to the interaction picture, allowing H_{int} to be our interaction Hamiltonian.

$$H_{\text{int}} = U_0 V {U_0}^\dagger = \frac{-B}{2}\hbar\left(a^2 W + W^\dagger a^{\dagger 2}\right) \tag{4.7}$$

Where W is determined by the equation $U_0 a^2\left(b+b^\dagger\right){U_0}^\dagger = a^2 W$ and U_0 is the time evolution operator governed by the Hamiltonian H_0 and is explored in the next Section.

4.3.2 Treatment of H_0

We begin by analyzing the properties and dynamics of H_0, the model most often used for the laser-mirror optomechanical system [65–68]. Here, we use the method given by Wei and Norman [25] to solve for the time evolution operator for H_0.

In order to solve the Schrödinger equation for H_0, we let the Ansatz for the time evolution operator be

$$U_0 = e^{g_1\hat{n}^2} e^{g_2\hat{n}} e^{g_3\hat{n}b^\dagger} e^{g_4\hat{n}b} e^{g_5 b^\dagger b} \tag{4.8}$$

allowing $\{g_i(t)\}$ to be undetermined time dependent coefficient functions.

To solve for these undetermined coefficients, we plug U_0 into the Schrödinger equation rewritten in the form

$$i\hbar\frac{\partial U_0}{\partial t}U_0^{-1} = H_0. \tag{4.9}$$

Using the property:

$$e^F G e^{-F} = G + \frac{[F,G]}{1!} + \frac{[F,[F,G]]}{2!} + \ldots, \tag{4.10}$$

and matching linearly independent operator coefficients, we obtain the following set of nonlinear ordinary differential equations:

$$\left.\begin{aligned} i\,\dot{g_1} &= B g_3 \\ i\,\dot{g_2} &= \Omega_0 \\ i\,\dot{g_3} &= B + \omega_1 g_3 \\ i\,\dot{g_4} &= B - \omega_1 g_4 \\ i\,\dot{g_5} &= \omega_1 \end{aligned}\right\}, \tag{4.11}$$

where the dots imply derivatives with respect to time.

Because the Hamiltonian is Hermitian, its respective time evolution operator is constrained to be unitary. Using Eq. (4.11) and the constraints to make the time dependent H_0 Hermitian, we solve for unitarity conditions to be

$$\left\{\Re(g_2) = 0, \Re(g_5) = 0, \Re(g_1) = -\frac{|g_3|^2}{2}, g_4 = -g_3^*\right\}, \tag{4.12}$$

where $\Re(g)$ refers to the real part of g. Solving the differential Eqs. (4.11) for the case of constant H_0 gives the time-dependent coefficient functions in terms of ω_1,B, and Ω_0:

$$\begin{aligned} g_1 &= \frac{B^2}{{\omega_1}^2}(-1 + t\omega_1 + e^{-i\omega_1 t}) \\ g_2 &= -it\Omega_0 \\ g_3 &= \frac{B}{\omega_1}\left(-1 + e^{-it\omega_1}\right) \\ g_4 &= \frac{B}{\omega_1}\left(1 - e^{it\omega_1}\right) \\ g_5 &= -it\omega_1 \end{aligned} \quad . \tag{4.13}$$

Thus, with the $\{g_i(t)\}$ solved for, we now have our time evolution operator for H_0 fully determined.

The next step is to find the evolving density matrix for the system. Since we mainly care about the evolution of the laser, we will assume the mirror is initially in a heat bath state, and take the partial trace with respect to the mirror. Thus,

$$\rho_0 = \mathrm{Tr}_{\mathrm{mirror}}\left(U_0^\dagger \frac{e^{\gamma b^\dagger b}}{1-e^\gamma}\rho_{0\mathrm{laser}}U_0\right) \tag{4.14}$$

where $\rho_{0\mathrm{laser}}$ is the initial state for the laser and $\gamma = \ln(\frac{\overline{n}}{1+\overline{n}_0})$ with $\overline{n}_0$ the expectation value of the number operator for the initial state of the mirror [10]. Taking the partial trace explicitly, the matrix elements of ρ_0 given in the number state representation are given as:

$$\begin{aligned}\langle n|\,\rho_0\,|m\rangle = {} & e^{-i\left((m^2-n^2)\Im(g_1)+(m-n)\Im(g_2)\right)} \\ & \times e^{-(m-n)^2|g_3|^2\left(\frac{1}{2}+\overline{n}_0\right)}\langle n|\,\rho_{0\mathrm{laser}}\,|m\rangle\end{aligned} \tag{4.15}$$

where $\Im(g)$ refers to the imaginary part of g and $\langle n|$ and $|m\rangle$ refer to photon number states. Throughout this paper, we will mostly assume that the initial state of the laser is a coherent state $|\alpha\rangle$. For this case, Eq. (4.15) becomes

$$\begin{aligned}\langle n|\,\rho_0\,|m\rangle = {} & e^{-i(m^2-n^2)}e^{-(m-n)^2|g_3|^2\left(\frac{1}{2}+\overline{n}_0\right)} \\ & \times e^{-|\alpha|^2}\frac{\left(\alpha e^{i\Im(g_2)}\right)^n\left(\alpha e^{i\Im(g_2)}\right)^{*m}}{\sqrt{n!m!}}\end{aligned} \tag{4.16}$$

where α is the complex eigennumber for the initial coherent state of the laser. Note that the time dependence of the system after partial tracing is now only determined by the terms $\Im(g_1)$, $\Im(g_2)$, and $|g_3|^2$.

4.3.3 Decoherence Effects of H_0

Decoherence is loosely defined as the loss of quantumness of a system. When a system is affected by decoherence, the interference terms of the density matrix become diminished making the system more classical. The partial trace of our initial density matrix, shown in Eq. (4.15), creates

decoherence for our optomechanical system. We can measure the decoherence of this system by taking the trace of ρ_0^2 and comparing it with 1, thus measuring the loss of idempotency (the property $\rho_0^2 = \rho_0$) [71] due to the loss of information from interaction with the mirror.

Taking this trace, we see:

$$\mathrm{Tr}(\rho_0^2) = \sum_{\substack{n=1 \\ m=1}}^{\infty} \frac{e^{-2|\alpha|^2+(m-n)^2|g_3|^2(1+2\overline{n}_0)}|\alpha|^{2(m+n)}}{m!n!}. \tag{4.17}$$

As far as time evolution is concerned, the term $|g_3|^2$ is the only factor that affects this measure of decoherence. This interpretation makes sense when considering Eq. (4.15): as $|g_3|^2$ becomes larger, the off-diagonal terms become less important. Taking the limit of Eq. (4.15) as $|g_3|^2$ goes to infinity gives

$$\lim_{|g_3|^2\to\infty} \rho_0 = \sum_{n=1}^{\infty} |n\rangle \langle n| \rho_{0\mathrm{laser}} |n\rangle \langle n|, \tag{4.18}$$

thus leaving the energy of the mirror and the interference terms irrelevant. Allowing $\rho_{0\mathrm{laser}}$ to again be a coherent state $|\alpha\rangle$, the trace becomes

$$Tr((\lim_{|g_3|^2\to\infty} \rho_0)^2) = e^{-2|\alpha|^2} I_0(-2|\alpha|^2) \tag{4.19}$$

where $I_0(z)$ is a modified Bessel function. Due to the $e^{-2|\alpha|^2}$ term, the decoherence effects increase quickly as $|\alpha|$ becomes larger.

4.3.4 Husimi Function for H_0

It is convenient to gain some insight into the standard optomechanical system governed by H_0 via Husimi plots associated with ρ_0. To do this, we convert Eq. (4.16) into a representation with matrix elements in the basis of a coherent state. Then, the diagonal elements of the matrix in the coherent

state basis yield the Husimi function:

$$Q(\beta) = \sum_{\substack{n=0 \\ m=0}}^{\infty} e^{-|\alpha|^2-|\beta|^2} \frac{\left(\alpha\beta^* e^{i\,\Im(g_2)}\right)^n}{n!} \frac{\left(\alpha^*\beta e^{-i\,\Im(g_2)}\right)^m}{m!} \times \left(e^{-(m-n)^2|g_3|^2\left(\frac{1}{2}+n_0\right)}\right)\left(e^{i\,\left(n^2-m^2\right)\Im(g_1)}\right). \tag{4.20}$$

In Eq. (4.20), the term $\Im\left(g_2(t)\right)$ only causes a phase shift in the initial coherent state. The decoherence term ($e^{-\frac{1}{2}(m-n)^2|g_3|^2(1+2n_0)}$) causes a rotational smearing effect . This smearing for a coherent state is shown in Fig. (4.1b). The splitting term ($e^{i\,\left(n^2-m^2\right)\Im(g_1)}$) causes the coherent state to split into cat states whenever the term ($\Im\left(g_1\right)$) is a half integer multiple of π. A plot of the Husimi function for a cat state without decoherence is given in Fig. (4.1c), and a plot of a cat state under decoherence effects is given in Fig. (4.1d).

To find the case for large decoherence effects, we take the limit as $|g_3|^2$ goes to infinity and find

$$\lim_{|g_3|^2\to\infty} Q(\beta) = e^{-|\alpha|^2-|\beta|^2} I_0(2\,|\alpha|\,|\beta|) \tag{4.21}$$

where again, $I_0(z)$ is a modified Bessel function. Thus, under large decoherence effects, the system loses all phase information resulting in a donut-shaped Husimi function.

4.3.5 Photon creation with respect to ρ_0

Looking at the Husimi plots for ρ_0 in Fig. (4.1) suggests that the evolution of this system only causes cat state splitting effects, as well as rotation in phase space and rotational smearing which suggests little change in overall energy level for the system. This suggests that the photon number should stay constant throughout any evolution governed by H_0. We can confirm this by taking the expectation value of an arbitrary function of the photon quantum number, $f(\hat{n})$:

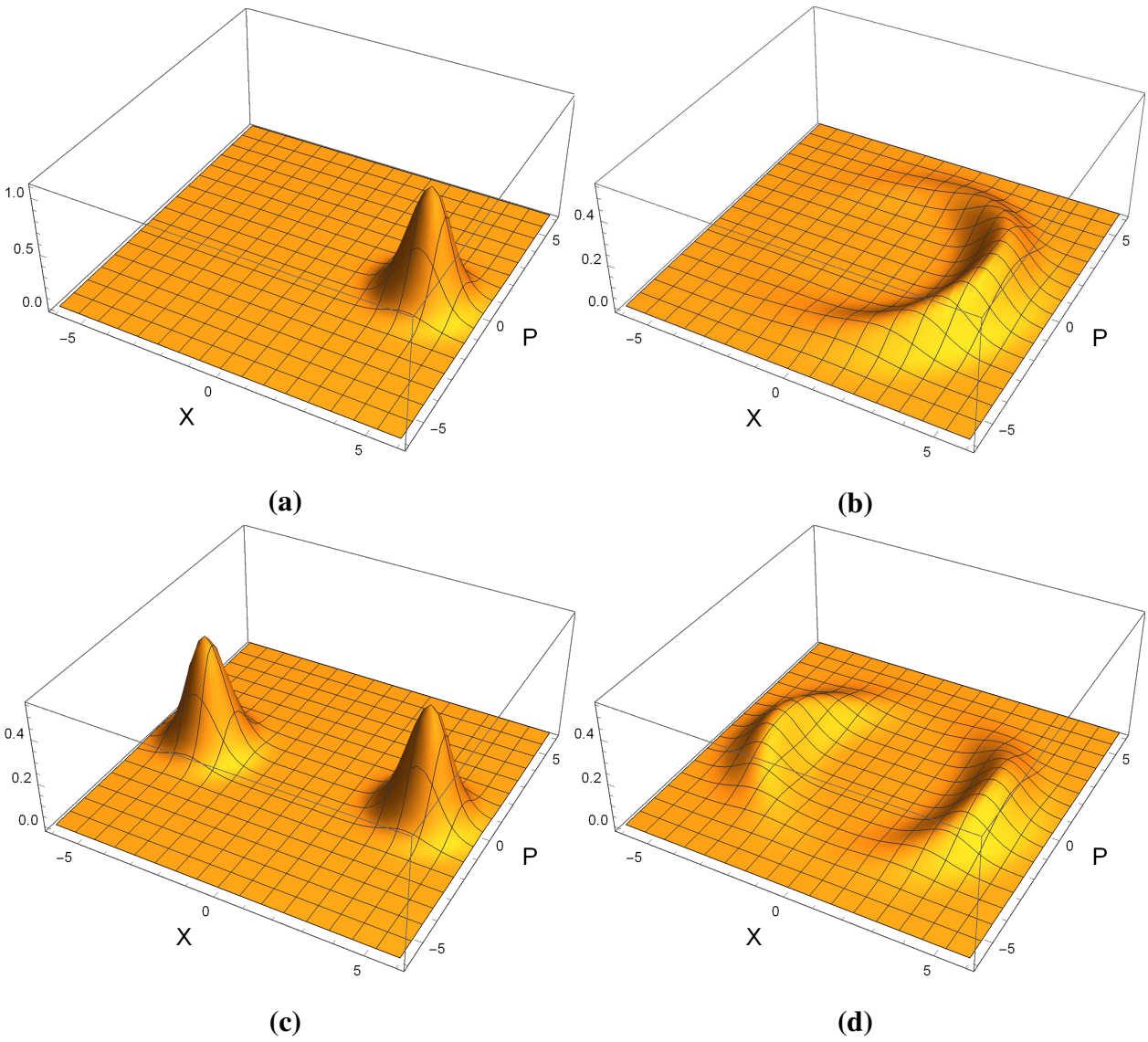

Figure 4.1 Husimi function $Q(X+iP)$ plots for attributes of decoherence and splitting into cat states. These plots show: (a) a coherent state without decoherence or splitting, (b) a coherent state with rotational smearing due to decoherence effects, (c) a coherent state split into a cat state without decoherence effects, (d) a coherent state split into a cat state with rotational smearing due to decoherence effects.

$$\begin{aligned}\langle f(\hat{n})\rangle &= \mathrm{Tr}\left(f(\hat{n})\rho_0\right)\\ &= \sum_{n=0}^{\infty} f(n)\langle n|\rho_0|n\rangle\\ &= \sum_{n=0}^{\infty} f(n)\langle n|\rho_{0\mathrm{laser}}|n\rangle\\ &= \langle f(\hat{n})\rangle_{t=0}\end{aligned} \tag{4.22}$$

where in the second to last step, we used Eq. (4.15). With this constraint, we see that no photon creation can occur for this limited system.

4.3.6 Second Order Terms Added

To add in the effects of the second order terms, we need to solve the Schrödinger equation for the interaction part of the time evolution operator U_{int}:

$$i\hbar\frac{dU_{\mathrm{int}}}{dt} = H_{\mathrm{int}}U_{\mathrm{int}} \tag{4.23}$$

where H_{int} is given in Eq. (4.7). To do this, we first solve for the operator W referred to in Eq. (4.7). Using the time evolution operator U_0 given in Eq. (4.8), applying the property Eq. (4.10), and applying the unitarity conditions given in Eq. (4.12), we find W to be

$$W = D_M(-g_2)\left(b^\dagger + b\right)e^{-2i\Im(g_1)\hat{n}+i\Im(g_1-g_2)} \tag{4.24}$$

where $D_M(-g_2)$ is the displacement operator [10] with respect to the mirror system.

Because of the time dependent and algebraically complex nature of W in H_{int}, we simplify our model invoking the mean field approximation, leading to the simplified interaction Hamiltonian:

$$H_{\mathrm{int}} = \frac{-B}{2}\hbar\left(a^2\langle W\rangle + \langle W\rangle^* a^{\dagger 2}\right) \tag{4.25}$$

Taking the time evolved expectation value of W, assuming an initial coherent state for the laser with eigenvalue α, we find:

$$\begin{aligned}\langle W\rangle = (1+\bar{n_0})\, e^{\left(e^{-2i\Im(g_1)}-1\right)|\alpha|^2+i\Im(g_1-g_2)-|g_3|^2\bar{n_0}} \\ \times\left(e^{i\Im(g_5)}g_3^*(1+\bar{n_0})-e^{-i\Im(g_5)}g_3\bar{n_0}\right).\end{aligned} \tag{4.26}$$

If we allow B to be constant, g_1, g_2, g_3, and g_5 are given by Eq. (4.13).

Solving for U_{int} in the same manner as for U_0, we find the interaction time evolution operator to be of the form:

$$U_{\text{int}} = e^{h_1\frac{a^{\dagger 2}}{2}}e^{h_2\frac{a^2}{2}}e^{h_3\frac{1}{2}\left(\frac{1}{2}+\hat{n}\right)} \tag{4.27}$$

where h_1, h_2, and h_3 are governed by the system of equations

$$\left.\begin{aligned} i\,\dot{h_1} &= -B\left(\langle W\rangle^* + \langle W\rangle {h_1}^2\right) \\ i\,\dot{h_2} &= B\langle W\rangle\left(-1+2h_1h_2\right) \\ i\,\dot{h_3} &= -2B\langle W\rangle h_1 \end{aligned}\right\} \tag{4.28}$$

Since H_{int} is Hermitian, U_{int} is unitary. The unitarity conditions associated with U_{int} (which can be found using Lie algebra representations [24] and confirmed using Eq. (4.28)) are

$$\{h_2 = -\frac{{h_1}^*}{1-|h_1|^2}, \Re(h_3) = \ln\left(1-|h_1|^2\right)\}. \tag{4.29}$$

Thus, Eq. (4.27) can be rewritten as:

$$U_{\text{int}} = e^{h_1\frac{a^{\dagger 2}}{2}}e^{-\frac{{h_1}^*}{1-|h_1|^2}\frac{a^2}{2}}e^{\left(\ln\left(1-|h_1|^2\right)+i\Im(h_3)\right)\frac{1}{2}\left(\frac{1}{2}+\hat{n}\right)} \tag{4.30}$$

which can be rewritten [24] as

$$U_{\text{int}} = S(\xi)\, e^{i\Im(h_3)\frac{1}{2}\left(\frac{1}{2}+\hat{n}\right)} \tag{4.31}$$

where $S(\xi)$ is the squeeze operator [10] and $\xi = \tanh^{-1}(|h_1|)\, e^{i\arg(h_1)}$. Thus, the effects of U_{int} on the density matrix can be interpreted as an added squeeze operator with a phase term.

The complete density matrix is given by Eq. (4.15) with

$$\rho_{0laser} = U_{int}^{\dagger} \rho_i U_{int}, \tag{4.32}$$

where ρ_i is the initial state of the laser before the squeezing effects is applied. Effectively, the evolution is the same, but with squeezing effects added to the initial state before rotational smearing. These changes can be seen in the Husimi function for ρ which is

$$\begin{aligned} Q(\beta) = \sum_{\substack{n=0 \\ m=0}}^{\infty} & \left(e^{-\left|\alpha'\right|^2 - \left|\beta'\right|^2} \frac{\left(\alpha'^{*}\beta'\right)^n}{n!} \frac{\left(\alpha'\beta'^{*}\right)^m}{m!} \right) \\ & \times \left(e^{-(n-m)^2\left(\frac{1}{2}|g_3|^2(1+2\overline{n_0})\right)} \right) \left(e^{i\left(n^2-m^2\right)\Im(g_1)} \right) \\ & \times e^{\Re(\alpha'^2)|h_1|} \left(1-|h_1|^2\right)^{\frac{3}{2}} \\ & \times \left(U\left(\frac{1-n}{2}, \frac{3}{2}, \alpha'^{*2} \frac{1-|h_1|^2}{2|h_1|}\right) \left(\frac{\alpha'^{*2}}{2|h_1|}\right)^{\frac{1-n}{2}} \right) \\ & \times \left(U\left(\frac{1-m}{2}, \frac{3}{2}, \alpha'^{2} \frac{1-|h_1|^2}{2|h_1|}\right) \left(\frac{\alpha'^{2}}{2|h_1|}\right)^{\frac{1-m}{2}} \right) \end{aligned} \tag{4.33}$$

where $\beta' = \beta e^{i\left(\Im(g_2)+\frac{1}{2}\Im(h_3)-\frac{1}{2}\arg(h_1)\right)}$, $\alpha' = \alpha e^{-i\frac{1}{2}\arg(h_1)}$, and $U(k_1,k_2,k_3)$ in this equation is the confluent hypergeometric function of the second kind. Note that the first part of this Husimi function is virtually identical to that of the Husimi function for ρ_0 given in Eq. (4.20). The effects of cat state splitting and rotational smearing are virtually the same as those in Fig. (4.1) as well, except for an added squeezing that is shown in Fig. (4.2). The squeezing is purely determined by the parameter $|h_1|$ which controls the magnitude part for the squeeze operator in Eq. (4.31).

With the added squeeze term, photon creation can occur. We show this by again taking the expectation value of $\hat{n}$ while allowing the coherent state to be the ground state $|0\rangle$. The expectation

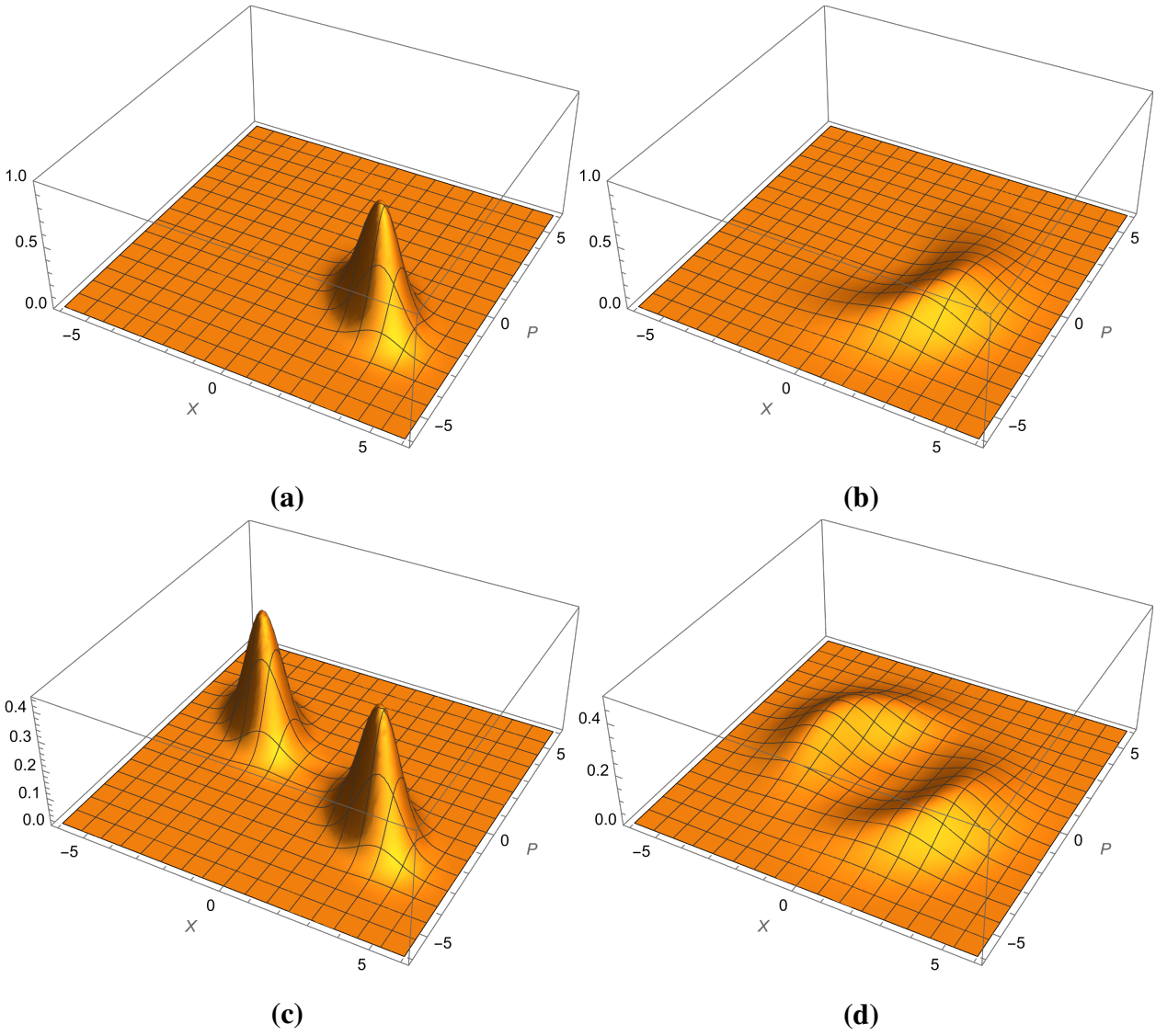

Figure 4.2 Husimi function ($Q(X+iP)$) plots for attributes of decoherence and splitting into cat states. All of these are under squeezing effects. These plots show: (a) a coherent state without decoherence or splitting, (b) a coherent state with rotational smearing due to decoherence effects, (c) a coherent state split into a cat state without decoherence effects, (d) a coherent state split into a cat state with smearing due to decoherence effects.

value is

$$\langle \hat{n} \rangle = \frac{|h_1|^2}{1 - |h_1|^2}. \tag{4.34}$$

Thus, as $|h_1|^2 \to 1$, which would indicate extreme squeezing, the photon number tends toward infinity.

4.4 Results and Conclusion

By examining Eq. (4.17) we see that decoherence is determined by $|g_3|$. Varying $|g_3|$ leads to a rotational smearing in the Husimi plots in Fig. (4.1), suggesting a loss of information with respect to the phase of the harmonic oscillator. The effect being only rotational suggests the optomechanical system without second order terms, H_0, leads to no photon creation as shown in Eq. (4.22).

The addition of the second order terms adds a squeeze operator with a phase shift as shown in Eq. (4.31). The squeeze term does cause the effects of decoherence to create rotational smearing after squeezing as shown in the Husimi functions. As a result from this squeezing, we see that there is photon creation of photons in Eq. (4.34) demonstrating the dynamic Casimir effect [78].

Chapter 5

Dynamic Evolution of an Anharmonic Oscillator with Infinite Coupling

5.1 Abstract

This paper addresses the dynamic evolution and decoherence of an anharmonic oscillator with infinite coupling using the Born-Markov master equation. This is done by using the Lie algebraic structure of the Born-Markov master equation's superoperators when applying a strategic mean field approximation to maintain dynamic flexibility. The system is compared to the Born-Markov master equation for the harmonic oscillator, the regular anharmonic oscillator, and the dynamic double anharmonic oscillator. Throughout, Husimi plots are provided to visualize the dynamic decoherence of these systems.

5.2 Introduction

We follow the dynamic evolution and decoherence of an anharmonic oscillator with infinite coupling using the Born-Markov master equation. This is achieved by using the Lie algebraic structure of

superoperators associated to the Born-Markov equation. A mean field approximation is evoked in order to simplify the problem. The system is then compared to the Born-Markov master equation for the harmonic oscillator, the regular anharmonic oscillator, and the dynamic double oscillator. Anharmonic oscillators constitute a convenient path to creating cat states [6, 7]. Among other systems, cat states can be used for quantum computing which are essential for the future of physics simulation [1] as well as for the realization of computational feats such as Shor‘s algorithm [2] and Grover‘s algorithm [3] as well as cryptography and optimization problems [4, 5].

Much work has been done on studying the dynamics of the anharmonic oscillator without extra coupling [79–81]. Adding outside coupling in general leads to decoherence. Decoherence is the loss of quantum information by ignoring the irrelevant environment [70]. The concept of decoherence, although relatively new, has been well studied for several situations such as the dynamics of systems involving the simple harmonic oscillator with decoherence which have been analytically solved [12, 13, 15]. Decoherence for more complicated systems requires some simplifying assumptions such as the Born approximation (where the environment and the system are weakly coupled) and the Markov approximation (where the effect of the environment is assumed to have no “memory”) [16]. The Born-Markov master equation is of particular note as it allows one to solve for the dynamics of the system after having already taken into account the effects of the environment [16]. The Born-Markov master equation has been well applied to the simple harmonic oscillator case, giving good simulation for decoherence in quantum dynamics [17, 18]; but the application of the Born-Markov master equation to the anharmonic oscillator is a difficult problem, as the Lie algebra does not close and has not been well studied. Some work on decoherence with anharmonic oscillators has been done, often in association with quantum computing [82–86], but little to no work has been done on the anharmonic oscillator under the Born-Markov approximation.

Thus, in this paper, we will find a Born-Markov master equation for the anharmonic oscillator with infinite couplings, solve for its dynamic evolution, and compare it to the evolution of the

infinitely coupled harmonic oscillator, the uncoupled anharmonic oscillator, and the double oscillator. We will do this by exploiting the Lie algebraic structure in the system after applying an appropriate mean field approximation.

5.2.1 Lie Algebra in Quantum Dynamics and Unitarity Conditions

To properly exploit the Lie algebra of quantum systems, we will expedite evolutionary analysis using the Wei-Norman method. Wei and Norman [25] give a convenient method for finding the time evolution operator for any time-dependent Hamiltonian composed of time independent operators that form a Lie algebra basis. For our purposes, we present this as follows. Allow a Hamiltonian H to be made up of time independent operators A_i that form a Lie algebra basis with time-dependent coefficents $b_i(t)$ such that

$$H = \hbar \sum_{i=1}^{n} A_i b_i. \tag{5.1}$$

Then, the time evolution operator for this system can be given as

$$U(t) = e^{g_1 A_1} e^{g_2 A_2} \dots e^{g_n A_n}. \tag{5.2}$$

The time-dependent $g_i(t)$ terms are determined by the set of first order differential equations

$$i \begin{pmatrix} g_1'(t) \\ g_2'(t) \\ \vdots \\ g_n'(t) \end{pmatrix} = [\text{g-Matrix}] \begin{pmatrix} b_1(t) \\ b_2(t) \\ \vdots \\ b_n(t) \end{pmatrix} \tag{5.3}$$

where g-Matrix is given by

$$[\text{g-Matrix}]^{-1}_{j,k} = \left(\prod_{i \leq k} e^{g_i \text{adj}(A_i)} \right)_{j,k}, \tag{5.4}$$

and $\text{adj}(A_i)$ is the respective adjoint representation of the A_i operator [19].

An alternative useful tool discussed in [24] is a method to use a faithful Lie algebra representation to find the conditions for unitarity for situations following Eqs. (5.1)-(5.2). This is done exploiting the matrix relationship

$$e^{g_1 R(A_1)} e^{g_2 R(A_2)} \dots e^{g_n R(A_n)} = e^{-g_1{}^* R(A_1{}^\dagger)} e^{-g_2{}^* R(A_2{}^\dagger)} \dots e^{-g_n{}^* R(A_n{}^\dagger)} \tag{5.5}$$

where R is a faithful representation for the Lie algebra referred to in Eq. (5.1). Using Eq. (5.5), one can find the conditions for unitarity for any time evolution operator of the form described in Eqs. (5.1)-(5.2) by comparing the respective matrix cells on both sides of the equation. We shall use this result in section 5.4 and section 5.5.

5.2.2 Decoherence and Partial Tracing

Quantum decoherence is the loss of quantum coherence in a system. For a coherent quantum system, the state of the system can be described by a single ket, or a superposition of kets $\sum c_i |i\rangle$. Quantum decoherence occurs when information is lost due to classical uncertainty. When this occurs, the state of the system is described by a mixed state and the system is best described using a sum of pure state density matrices $\sum p_i |i\rangle \langle i|$ where p_i are the "classical probability weights" for the state being $|i\rangle$ due to classical uncertainty. Often, decoherence effects are caused by open systems.

For a closed system, all quantum information is contained in the system studied. In a closed systems, we assume that its Hamiltonian is Hermitian, all variables in the system are known, and that the initial state for evolution is also known. An open system is a system linked to an environment system, within which we are ignorant of the wave function. This adds classical uncertainty to the situation, causing quantum decoherence and the need to describe the system in terms of a density matrix.

Oftentimes, decoherence can be modeled by allowing the Hamiltonian to be in the form $H = H_S + H_E + H_{SE}$ where H_S is the Hamiltonian for the system, H_E is the Hamiltonian for the

environment, and H_{SE} is the part of the Hamiltonian coupling the two. After solving for the evolution of the system for a density matrix operator ρ, we can filter out irrelevant environmental information of the state via partial tracing. We can take the partial trace via infinite sums of number state projections associated with the environment via the equation

$$\rho_s = \sum_{n}^{\infty} \langle n| \rho |n\rangle. \tag{5.6}$$

where $|n\rangle$ are number states associated with the environment. We can also take the partial trace through an integration of coherent state projections associated with the environment through the equation

$$\rho_s = \int \langle \beta| \rho |\beta\rangle \frac{d\beta^2}{\pi} \tag{5.7}$$

where $|\beta\rangle$ represent coherent states associated with the environment.

5.2.3 Born-Markov Master Equation

Another common method for modeling decoherence is via master equations. With these, we make assumptions to filter out the environment before solving for reduced the density matrix. The most popular of these is the Born-Markov approximation, which leads to the Born-Markov master equation.

The Born approximation results from the assumption that the coupling between the system and environment is weak to the point that the system and environment remain in an essentially separable state at all times, and the environment does not change much with time. The Markov approximation is the assumption that the environment has no memory and the environment correlation times are near zero except when comparing with the same times [70].

Let the Hamiltonian take the general form

$$H = H_S + H_E + \sum_{\alpha} S_\alpha E_\alpha \tag{5.8}$$

where H_S is the Hamiltonian for the system, H_E is the Hamiltonian for the environment, S_α are operators associated with the system, and E_α are operators associated with the environment. The Born-Markov master equation [70], with system density matrix ρ_s, is then

$$i\hbar\frac{d}{dt}\rho_s = [H_s,\rho_s] - i\sum_\alpha [S_\alpha, B_\alpha\rho_s] + [\rho_s D_\alpha, S_\alpha] \tag{5.9}$$

with

$$\begin{aligned} B_\alpha &= \int_0^\infty d\tau \sum_\beta C_{\alpha\beta}(\tau)\,\text{Heisenberg}(S_\beta)_{H_S}(-\tau), \\ D_\alpha &= \int_0^\infty d\tau \sum_\beta C_{\beta\alpha}(-\tau)\,\text{Heisenberg}(S_\beta)_{H_S}(-\tau), \\ C_{\alpha\beta} &= \left\langle \text{Heisenberg}(E_\alpha)_{H_E} E_\beta \right\rangle_{\rho_\varepsilon} \end{aligned} \tag{5.10}$$

where $\text{Heisenberg}(A)_{H_b}$ refers to the Heisenberg representation of A with respect to the evolution governed by the Hamiltonian H_b.

In our case we will use the Wei-Norman method for finding the evolution of the Born-Markov master equation. As an example, we show this procedure firstly for an oscillator with infinite oscillator couplings.

In section 5.3, we look at the usual harmonic oscillator with the Born-Markov master equation using the superoperator Lie algebraic structure. In section 5.4, we establish the dynamics for the single anharmonic oscillator using its Lie algebraic structure and time evolution operator for reference and comparison. In section 5.5, we look at the dynamic anharmonic double oscillator using its Lie algebraic structure. In section 5.6, we use the results and techniques in previous sections to establish the dynamics of the anharmonic oscillator with infinite coupling using its Born-Markov master equation and a mean field approximation that preserves the anharmonic effects.

5.3 Harmonic Oscillator Born-Markov Master Equation

In this section, we solve for the dynamics of the Born-Markov master equation for a harmonic oscillator coupled to an infinite number of independent harmonic oscillators representing the environment. The Hamiltonian for such a system is

$$H = \hbar\left(\omega_c\hat{n} + \sum_{i=1}^{\infty}\omega_i\hat{n}_i + \left(c_i^* a a_i{}^\dagger + c_i a^\dagger a_i\right)\right) \tag{5.11}$$

where ω_c is the frequency for the oscillator of our system, ω_i are the frequencies for the oscillators in the environment, and c_i is the coupling strength between the systemic and respective environmental oscillators. Identifying for this particular system the operators $E_{i,\{1,2\}} = \{c_i^* a_i{}^\dagger, c_i a_i\}$ and $S_{i,\{1,2\}} = \{a, a^\dagger\}$, and setting the environmental density matrices to be thermal states, $\rho_E = \prod \frac{e^{\ln\left(\frac{n_i}{1+n_i}\right)\hat{n}_i}}{1+n_i}$, where $\bar{n}_i$ is the initial expectation value for $\hat{n}_i$, and using Eq. (5.9), the Born-Markov master equation is:

$$i\frac{d\rho}{dt} = [\omega_c\hat{n},\rho] - i\left(\left(\hat{n}\rho - a\rho a^\dagger\right)\eta_1 + \left(\rho\hat{n} - a\rho a^\dagger\right)\eta_1^* + \left(\rho + \rho\hat{n} - a^\dagger\rho a + \hat{n}\rho - a\rho a^\dagger\right)\eta_2\right) \tag{5.12}$$

where $\eta_1 = \sum_{i=0}^{\infty}|c_i|^2\int_0^\infty e^{it(\omega_c-\omega_i)}dt$ and $\eta_2 = \sum_{i=0}^{\infty}\bar{n}_i|c_i|^2\int_0^\infty e^{it(\omega_c-\omega_i)} + e^{-it(\omega_c-\omega_i)}dt$. This is consistent with the literature [87]. Using the identity $\int_0^\infty e^{\pm i(\Omega)}d\tau = \pi\delta(\Omega) \pm i\mathscr{P}\frac{1}{\Omega}$ where $\mathscr{P}$ is the Cauchy principal part, we find

$$\begin{aligned}
\eta_1 &= \sum_{i=0}^{\infty}|c_i|^2\left(\pi\delta(\omega_c-\omega_i) + i\mathscr{P}\frac{1}{\omega_c-\omega_i}dt\right)\\
&= \int_{i=0}^{\infty}|c(\omega_i)|^2\left(\pi\delta\left(\omega_c-\omega_i\right) + i\mathscr{P}\frac{1}{(\omega_c-\omega_i)}\right)g(\omega_i)d\omega_i\\
&= \pi|c(\omega_c)|^2 g(\omega_c) + i\mathscr{P}\int_{i=0}^{\infty}\frac{|c(\omega_i)|^2}{\omega_c-\omega_i}g(\omega_i)d\omega_i\\
&= \frac{\gamma}{2} + i\Delta\omega
\end{aligned} \tag{5.13}$$

where we have assumed the ω_i operators are close together, where $g(\omega_i)d\omega_i$ is the number of modes in $d\omega_i$ and $\omega_i + d\omega_i$, and we define $\gamma = 2|c(\omega_c)|^2 g(\omega_c)$ and $\Delta\omega = \mathscr{P}\int_{i=0}^{\infty}\frac{c(\omega_i)^2}{\omega_c-\omega_i}g(\omega_i)d\omega_i$.

Similarly,

$$\begin{aligned}\eta_2 &= \int_0^\infty \bar{n}(\omega_i)c(\omega_i)^2 g(\omega_i) 2\pi\delta(\omega_c-\omega_i)d\omega_i \\ &= 2\pi\bar{n}(\omega_c)\left|c(\omega_c)\right|^2 g(\omega_c) \\ &= 2\bar{n}_c\gamma.\end{aligned} \tag{5.14}$$

Making these substitutions for η_1 and η_2, our master equation takes the form:

$$i\frac{d\rho}{dt} = \left((\omega_c+\Delta\omega)[\hat{n},\square] + i\gamma\left(\frac{1}{2}\square + \bar{n}_c a^\dagger \square a + (1+\bar{n}_c)a\square a^\dagger - \left(\bar{n}_c+\frac{1}{2}\right)\left\{\frac{\mathrm{I}}{2}+\hat{n},\square\right\}\right)\right)\rho \tag{5.15}$$

with the curly brackets representing the anti-commutator and the empty box $\square$ representing a place holder for an input in the superoperator after factoring out ρ.

Although Eq. (5.15) does not feature a traditional Hamiltonian, the differential equation is still in a form applicable to the Wei-Norman procedure to solve for a time evolution operator that forwards the dynamics of a given density matrix. In Eq. (5.15), we identify an associated Lie algebra superoperator basis to be $\left\{a\square a^\dagger, a^\dagger\square a, \frac{1}{2}\left\{\hat{n}+\frac{1}{2},\square\right\}, \frac{1}{2}[\hat{n},\square], \square\right\}$ with the commutation table:

$$\begin{aligned}\left[a^\dagger\square a, a\square a^\dagger\right] &= -2\left(\frac{1}{2}\left\{\hat{n}+\frac{1}{2},\square\right\}\right) \\ \left[a^\dagger\square a, \frac{1}{2}\left\{\hat{n}+\frac{1}{2},\square\right\}\right] &= -a^\dagger\square a \\ \left[a\square a^\dagger, \frac{1}{2}\left\{\hat{n}+\frac{1}{2},\square\right\}\right] &= a\square a^\dagger\end{aligned} \tag{5.16}$$

and with $\frac{1}{2}[\hat{n},\square]$ and $\square$ spanning the center of the Lie algebra.

For our Ansatz, we allow the time evolution superoperator, which propagates the density matrix forward in time, to be of the form

$$U = e^{g_1 a\square a^\dagger} e^{g_2 a^\dagger\square a} e^{g_3\left(\frac{1}{2}\left\{\hat{n}+\frac{1}{2},\square\right\}\right)} e^{g_4\frac{1}{2}[\hat{n},\square]} e^{g_5\square}. \tag{5.17}$$

Using the Wei-Norman method given in Eq. (5.3), the differential equations for the g_i functions are

$$i\begin{pmatrix} g_1' \\ g_2' \\ g_3' \\ g_4' \\ g_5' \end{pmatrix} = \begin{pmatrix} 1 & {g_1}^2 & g_1 & 0 & 0 \\ 0 & 1-2g_1g_2 & -g_2 & 0 & 0 \\ 0 & 2g_1 & 1 & 0 & 0 \\ 0 & 0 & 0 & 1 & 0 \\ 0 & 0 & 0 & 0 & 1 \end{pmatrix} \begin{pmatrix} i\gamma\bar{n}_c \\ i\gamma(1+\bar{n}_c) \\ -2i\gamma(1+2\bar{n}_c) \\ 2(\omega_c+\Delta\omega) \\ i\frac{\gamma}{2} \end{pmatrix}. \tag{5.18}$$

Note again, any unitarity conditions for the g_i's associated with this Lie algebra would not apply here since the superoperator in Eq. (5.15) is not Hermitian. However, looking at this particular differential equation, we can gather that g_1, g_2, g_3, and g_5 are real and g_4 is purely imaginary.

If we assume η_1, η_2, and ω_c to be constant, the differential equations in Eq. (5.18) yield the solutions

$$\begin{pmatrix} g_1 \\ g_2 \\ g_3 \\ g_4 \\ g_5 \end{pmatrix} = \begin{pmatrix} 1-\frac{1}{1+\bar{n}_c(1-e^{-t\gamma})} \\ (1+\bar{n}_c)\left(-1+e^{t\gamma}+2\bar{n}_c\left(-1+\cosh(t\gamma)\right)\right) \\ 2\ln\left(\frac{1}{1+\bar{n}_c(1-e^{-t\gamma})}\right)-t\gamma \\ -2it(\omega_c+\Delta\omega) \\ \frac{\gamma}{2}t \end{pmatrix}. \tag{5.19}$$

To assist with applying this time evolution superoperator U to a density matrix ρ, we state the following properties:

$$\begin{aligned} e^{\gamma\Box}\rho &= e^{\gamma}\rho \\ e^{\gamma[A,\Box]}\rho &= e^{\gamma A}\rho e^{-\gamma A} \\ e^{\gamma\{A,\Box\}}\rho &= e^{\gamma A}\rho e^{\gamma A}, \end{aligned} \tag{5.20}$$

where A is an operator and γ is a scalar. Unfortunately, in order to apply terms such as $e^{g_1 a^\dagger \Box a}$ and $e^{g_2 a \Box a^\dagger}$, it is often necessary to resort to the expansion

$$e^{\gamma A\Box B}\rho = \sum_{i=0}^{\infty}\gamma^i\frac{A^i\rho B^i}{i!}, \tag{5.21}$$

where A and B are operators.

We now apply U to an initial coherent state density matrix $\rho_0 = |\alpha\rangle\langle\alpha|$ using the following coherent state properties:

$$\begin{aligned} a|\alpha\rangle &= |\alpha\rangle\,\alpha \\ e^{\gamma a}|\alpha\rangle &= |\alpha\rangle\, e^{\gamma\alpha} \\ e^{\gamma\hat{n}}|\alpha\rangle &= |\alpha e^{\gamma}\rangle\, e^{\frac{1}{2}\left(|\alpha e^{\gamma}|^2-|\alpha|^2\right)} \\ e^{\gamma a^\dagger}|\alpha\rangle &= |\alpha+\gamma\rangle\, e^{\frac{|\gamma|^2}{2}+\Re(\gamma\alpha^*)} \\ \langle\beta|\alpha\rangle &= e^{-\frac{1}{2}\left(|\alpha|^2+|\beta|^2-2\alpha\beta^*\right)} \\ \langle\beta|e^{\gamma\hat{n}^2}|\alpha\rangle &= e^{-\frac{1}{2}\left(|\alpha|^2+|\beta|^2\right)}\sum_{j=0}^{\infty}\frac{(\alpha\beta^*)^j}{j!}e^{\gamma j^2}, \end{aligned} \tag{5.22}$$

and using Eq. (5.20)-(5.21). Furthermore, noting g_1, g_2, g_3, and g_5 are real, and g_4 is purely imaginary (from Eq. (5.18)), we find the evolved density matrix is

$$\tilde{\rho}(t) = U|\alpha\rangle\langle\alpha| = e^{\left(|\alpha|^2-|\alpha'|^2(1+g_2)\right)+g_5}\left|\frac{\alpha'}{\alpha}\right|\sum_{i=0}^{\infty}\frac{g_1^j}{j!}\,a^{\dagger j}|\alpha'\rangle\langle\alpha'|a^j, \tag{5.23}$$

with $\alpha' = \alpha e^{\frac{1}{2}(g_3+g_4)}$. Since Eq. (5.23) is not normalized, we divide it by its trace using Eq. (5.7) to obtain the normalized density matrix:

$$\begin{aligned} \rho(t) =& \frac{\tilde{\rho}(t)}{\int\langle z|\tilde{\rho}(t)|z\rangle\frac{dz^2}{\pi}} \\ =& |1-g_1|\,e^{-\frac{g_1}{1-g_1}|\alpha'|^2}\sum_{j=0}^{\infty}\frac{g_1^j}{j!}\,a^{\dagger j}|\alpha'\rangle\langle\alpha'|a^j, \end{aligned} \tag{5.24}$$

with $\alpha' = \alpha e^{\frac{1}{2}(g_3+g_4)}$. Note that after this renormalization only g_1, g_3, and g_4 are relevant.

To monitor the decoherence, we take the trace of ρ^2. Thus using the equation

$$\int e^{A|z|^2+Bz^2+Cz^{*2}+Dz+Ez^*+F}dz^2 = \frac{e^{\frac{CD^2+A^2F-4BCF-ADE+BE^2}{A^2-4BC}}\pi}{\sqrt{A^2-4BC}} \tag{5.25}$$

to integrate, we find

$$\mathrm{tr}\left(\rho(t)^2\right) = \frac{1-g_1}{1+g_1}. \tag{5.26}$$

When assuming the constant case, thus applying Eq. (5.19), the trace simplifies to

$$\mathrm{tr}\left(\rho(t)^2\right) = \frac{1}{1+2\bar{n}_c\left(1-e^{\gamma t}\right)}, \tag{5.27}$$

which is consistent with [15].

For a more graphical representation of this system, we solve for the Husimi and Wigner functions. The Husimi function is given by

$$Q(z) = \frac{1}{\pi}\langle z|\,\rho(t)\,|z\rangle = \frac{1}{\pi}(1-g_1)e^{-(1-g_1)|z-\alpha'|^2}, \tag{5.28}$$

where $|z\rangle$ is a coherent state. Since the Husimi function is in a Gaussian form, the Wigner function is easily found using Eq. (5.25); thus

$$W(X,P) = \frac{\kappa}{\pi}e^{-\kappa|X+iP-\frac{\sqrt{2}\alpha'}{1-g_1}|^2}, \tag{5.29}$$

where $\kappa = \frac{1-g_1}{1+g_1} = \mathrm{tr}\left(\rho^2\right)$. For the constant case, using Eq. (5.19), we note $\alpha' = \alpha(1-g_1)e^{-\frac{1}{2}t(\gamma+2i(\Delta\omega+\omega_0))}$, suggesting the Gaussian distribution of the Wigner function for the coherent state widens while the center of the distribution decays to the origin.

5.4 Single Anharmonic Oscillator

We consider a single anharmonic oscillator as a simple harmonic oscillator with an assumed quadratic term added given by the Hamiltonian

$$H = \hbar\omega\left(\hat{n}+\frac{1}{2}\right)+\hbar\Omega\hat{n}^2. \tag{5.30}$$

This is represents a nonlinear susceptibility [7], and is the simplest Hamiltonian that portrays the evolution of an anharmonic oscillator. This system has been well explored [6, 7], but for the purposes of comparison, we will review this system using the notation form of future Sections.

The Lie algebra associated with this Hamiltonian is described simply by the basis elements $\{\hat{n}^2, \hat{n}, \mathrm{I}\}$, all of which commute with each other. Thus, assuming the time evolution operator to be of the form

$$U = e^{g_1 \hat{n}^2} e^{g_2 \hat{n}} e^{g_3 \mathrm{I}}, \tag{5.31}$$

Eq. (5.3) yields

$$i \begin{pmatrix} g_1'(t) \\ g_2'(t) \\ g_3'(t) \end{pmatrix} = \begin{pmatrix} 1 & 0 & 0 \\ 0 & 1 & 0 \\ 0 & 0 & 1 \end{pmatrix} \begin{pmatrix} \Omega \\ \frac{\omega}{2} \\ \frac{\omega}{4} \end{pmatrix}. \tag{5.32}$$

Using a faithful representation and Eq. (5.5), we see the conditions for U to be unitary are

$$\{\Re(g_1) = 0, \Re(g_2) = 0, \Re(g_3) = 0\}, \tag{5.33}$$

which is expected from the simple Lie algebra.

We will assume the initial state is a coherent state $|\alpha\rangle$. Applying the time evolution operator to this initial state using the properties in Eq. (5.22), we find the time evolved state to be

$$U|\alpha\rangle = e^{i\Im(g_1)\hat{n}^2} |\alpha'\rangle e^{i\Im(g_3)} = e^{-\frac{|\alpha|^2}{2}} \sum_{n=0}^{\infty} e^{in^2\Im(g_1)} \frac{\alpha'^n}{\sqrt{n!}} |n\rangle e^{i\Im(g_3)} \tag{5.34}$$

where the kets $|n\rangle$ are number states and $\alpha' = \alpha e^{i\Im(g_2)}$. Some special states occur when $\Im(g_1) = 2\pi/m$ where m is an integer. In such cases, the state can be written as a finite sum of coherent states. For example, when $\Im(g_1) = \pi/2$, this becomes

$$\begin{aligned} U(\Im(g_1) \to \pi/2)|\alpha\rangle &= e^{-\frac{|\alpha|^2}{2}} e^{i\Im(g_3)} \left(\sum_{n\in\text{odd}}^{\infty} e^{in^2\pi/2} \frac{\alpha'^n}{\sqrt{n!}} |n\rangle + \sum_{n\in\text{even}}^{\infty} e^{in^2\pi/2} \frac{\alpha'^n}{\sqrt{n!}} |n\rangle \right) \\ &= e^{-\frac{|\alpha|^2}{2}} e^{i\Im(g_3)} \left(\sum_{n\in\text{odd}}^{\infty} i^n((-1)^{(n-1)/2})^n \frac{\alpha'^n}{\sqrt{n!}} |n\rangle + \sum_{n\in\text{even}}^{\infty} (-1)^n \frac{\alpha'^n}{\sqrt{n!}} |n\rangle \right) \\ &= e^{-\frac{|\alpha|^2}{2}} e^{i\Im(g_3)} \left(ie^{-\frac{|\alpha|^2}{2}} \sum_{n\in\text{odd}}^{\infty} \frac{\alpha'^n}{\sqrt{n!}} |n\rangle + e^{-\frac{|\alpha|^2}{2}} \sum_{n\in\text{even}}^{\infty} \frac{\alpha'^n}{\sqrt{n!}} |n\rangle \right). \end{aligned} \tag{5.35}$$

Noting that

$$\begin{aligned}\frac{|\alpha'\rangle - |-\alpha'\rangle}{2} &= e^{-\frac{|\alpha|^2}{2}} \sum_{n\in\text{odd}}^{\infty} \frac{\alpha'^n}{\sqrt{n!}} |n\rangle \\ \frac{|\alpha'\rangle + |-\alpha'\rangle}{2} &= e^{-\frac{|\alpha|^2}{2}} \sum_{n\in\text{even}}^{\infty} \frac{\alpha'^n}{\sqrt{n!}} |n\rangle ,\end{aligned} \tag{5.36}$$

this reduces to

$$U(\Im(g_1) \to \pi/2)\,|\alpha\rangle = e^{i\pi/4}\,|\alpha'\rangle + e^{-i\pi/4}\,|-\alpha'\rangle , \tag{5.37}$$

which turns out to be a cat state [10]. When $\Im(g_1) = 2\pi/m$ where m is an integer, similar states occur.

We can visualize this evolution using the Husimi function. Using Eq. (5.22), the Husimi function is

$$Q(z) = \frac{1}{\pi}\,\langle z|\,U\,|\alpha\rangle\,\langle\alpha|\,U^\dagger\,|z\rangle = \frac{1}{\pi} e^{-|z|^2-|\alpha'|^2} \left| \sum_{n=0} \frac{(\alpha' z^*)^n}{n!} e^{in^2\Im(g_1)} \right|^2 , \tag{5.38}$$

where $\alpha' = \alpha e^{i\Im(g_2)}$. A plot of the Husimi function is given in Fig (5.1). In these plots, we froze the motion due to the harmonic oscillator by forcing α' to be constant so we could focus on the anharmonic effects. Note the cat state at $\Im(g_1) = \frac{\pi}{2}$ as well as the formed or almost formed superpositions of coherent states when $\Im(g_1) = \frac{\pi}{8}$, $\Im(g_1) = \frac{\pi}{4}$, and $\Im(g_1) = \frac{3\pi}{8}$. Further note that at $\Im(g_1) = \frac{5\pi}{16}$ it is near equal to $\frac{\pi}{3}$ which, leads to a three-way superposition of coherent states.

5.5 Anharmonic Double Oscillator with Partial Tracing

In this Section, we develop the dynamics of the time-dependent double anharmonic oscillator using Lie algebraic techniques to add to the analysis of the anharmonic oscillator with infinite coupling in the next Section. In the first subsection we develop the double harmonic oscillator. In the second subsection, we add the anharmonic effects.

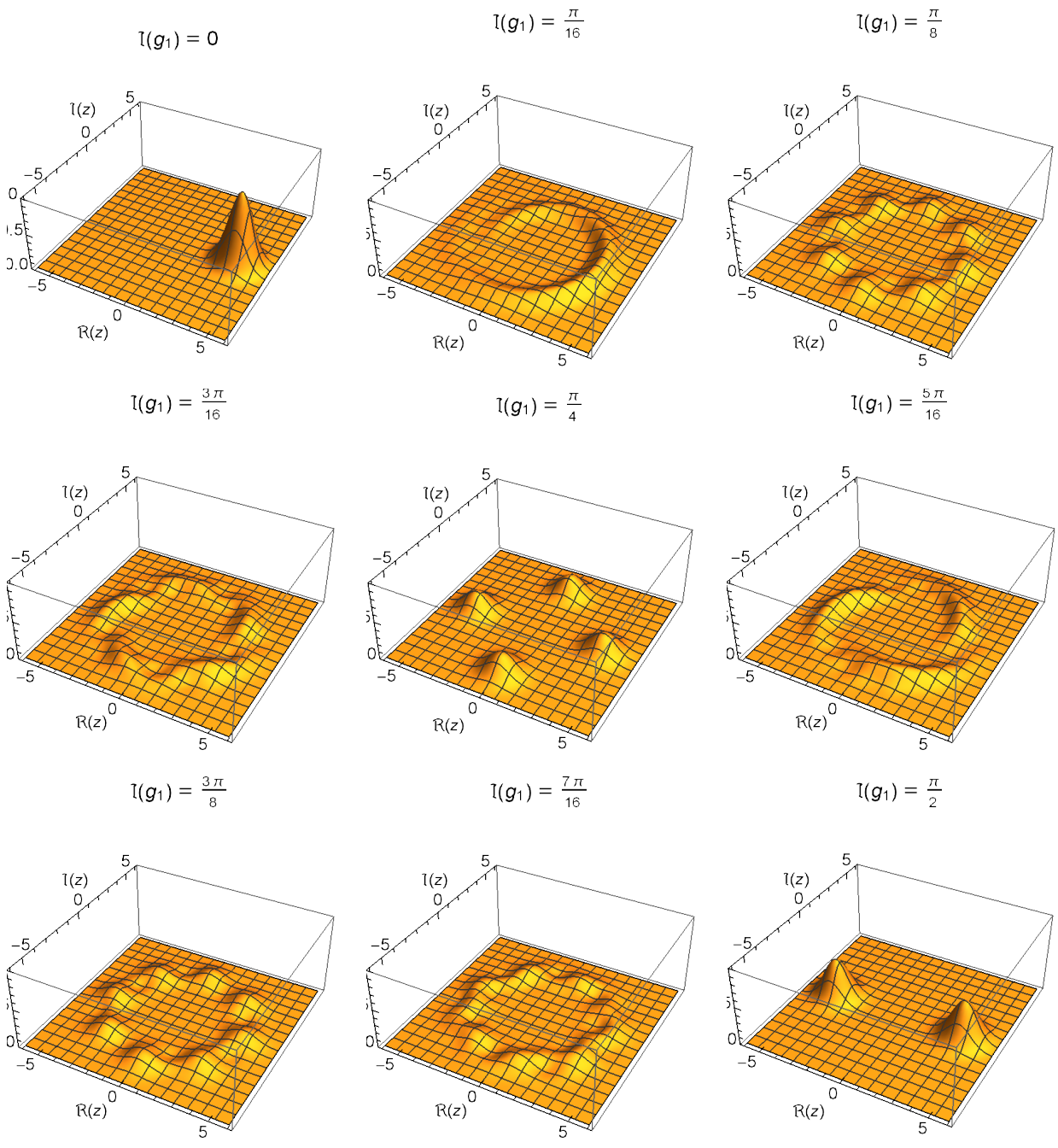

Figure 5.1 Husimi function ($\pi Q(z)$) plots evolution with rotation due to harmonic motion fixed for an initial coherent state. Note the cat state at $\Im(g_1) = \frac{\pi}{2}$ as well as the formed or almost formed superpositions of coherent states when $\Im(g_1) = \frac{\pi}{8}$, $\Im(g_1) = \frac{\pi}{4}$, and $\Im(g_1) = \frac{3\pi}{8}$.

5.5.1 Dynamics of the Double Oscillator

The general time-dependent double harmonic oscillator after taking the rotating wave approximation is [88]

$$H = \hbar\left(\omega(t)\hat{n}_1 + \Omega(t)\hat{n}_2 + g(t)^* a_1 a_2^\dagger + g(t) a_1^\dagger a_2\right), \tag{5.39}$$

where a_1 and $\hat{n}_1$ correspond to the first harmonic oscillator, while a_2 and $\hat{n}_2$ correspond to the second. The terms $\omega(t)\hat{n}_1$ and $\Omega(t)\hat{n}_2$ correspond to the different potential wells, while $g(t)^* a_1 a_2^\dagger + g(t) a_1^\dagger a_2$ is the term of interaction between the two. The basis $\left\{a_1 a_2^\dagger, a_1^\dagger a_2, \hat{n}_1, \hat{n}_2\right\}$ forms a Lie algebra with commutation relations:

$$\begin{aligned} [a_1 a_2^\dagger, a_1^\dagger a_2] = \hat{n}_2 - \hat{n}_1, \quad [a_1 a_2^\dagger, \hat{n}_1] = a_1 a_2^\dagger, \quad & [a_1 a_2^\dagger, \hat{n}_2] = -a_1 a_2^\dagger, \\ [a_1^\dagger a_2, \hat{n}_1] = -a_1^\dagger a_2, \quad & [a_1^\dagger a_2, \hat{n}_2] = a_1^\dagger a_2, \\ & [\hat{n}_1, \hat{n}_2] = 0. \end{aligned} \tag{5.40}$$

This being a Lie algebra, we can set the time evolution operator to be

$$U = e^{g_1\ a_1 a_2^\dagger} e^{g_2\ a_1^\dagger a_2} e^{g_3\ \hat{n}_1} e^{g_4\ \hat{n}_2} \tag{5.41}$$

where, using Eq. (5.3), we obtain the differential equations for the g_i coefficients:

$$i\begin{pmatrix} g_1' \\ g_2' \\ g_3' \\ g_4' \end{pmatrix} = \begin{pmatrix} 1 & -g_1^2 & -g_1 & g_1 \\ 0 & 1+2g_1 g_2 & g_2 & -g_2 \\ 0 & g_1 & 1 & 0 \\ 0 & -g_1 & 0 & 1 \end{pmatrix} \begin{pmatrix} g(t) \\ g(t)^* \\ \omega(t) \\ \Omega(t) \end{pmatrix}. \tag{5.42}$$

For the constant case, after much simplification, the coefficients can be solved for as

$$\begin{pmatrix} g_1 \\ g_2 \\ g_3 \\ g_4 \end{pmatrix} = \begin{pmatrix} -\frac{g^*}{\Omega-\omega}\frac{2}{1-i\cot\left(\frac{1}{2}t\omega'\right)} \\ g\frac{\Omega-\omega}{\omega'^2}\left(1-\cos\left(t\omega'\right)-i\sin\left(t\omega'\right)\frac{\omega'}{\Omega-\omega}\right) \\ -\ln\left(\frac{e^{\frac{1}{2}it(\omega+\Omega)}}{\cos\left(\frac{1}{2}t\omega'\right)+\frac{i\sin\left(\frac{1}{2}t\omega'\right)}{\omega'/(\Omega-\omega)}}\right) \\ \ln\left(\frac{e^{-\frac{1}{2}it(\omega+\Omega)}}{\cos\left(\frac{1}{2}t\omega'\right)+\frac{i\sin\left(\frac{1}{2}t\omega'\right)}{\omega'/(\Omega-\omega)}}\right) \end{pmatrix}, \tag{5.43}$$

with $\omega' = (\Omega - \omega)\sqrt{4\left(\frac{|g|}{\Omega-\omega}\right)^2 + 1}$. Using a faithful representation and Eq. (5.5), we see the conditions for U to be unitary are

$$\left\{ g_2 = -\frac{g_1^*}{1+|g_1|^2}, \Re(g_3) = -\frac{1}{2}\ln\left(1+|g_1|^2\right), \Re(g_4) = \frac{1}{2}\ln\left(1+|g_1|^2\right) \right\}, \tag{5.44}$$

which is true for all time-dependent cases, and is consistent with the constant case in Eq. (5.43). Thus, the time evolution operator U is determined by g_1, $\Im(g_3)$, and $\Im(g_4)$.

We will now obtain the density matrix for this time evolution operator. We will allow the initial density matrix to be a coherent state for oscillator 1 and a heat bath for oscillator 2. Thus, we allow

$$\rho_0 = (1-e^{\gamma}) e^{\gamma\,\hat{n}_2} \left|\alpha_0\right\rangle_1 \left\langle\alpha_0\right|_1, \tag{5.45}$$

where $e^{\gamma} = \frac{\bar{n}}{1+\bar{n}}$ with $\bar{n}$ as the initial expectation value of $\hat{n}_2$.

We will put the evolved density matrix in the coherent state representation, with a partial trace over the second oscillator, placing an identity operator $I = \int \left|\beta'\right\rangle_2 \left\langle\beta'\right|_2 \frac{d\beta'^2}{\pi}$ next to ρ_0 for convenience, and applying Eq. (5.22) and Eq. (5.25). We obtain

$$\begin{aligned} \rho_1(\alpha_1,\alpha_2) = \left\langle\alpha_1\right|_1 \rho_1 \left|\alpha_2\right\rangle_1 = \int \left\langle\alpha_1\right|_1 \left\langle\beta\right|_2 U \rho_0 U^{\dagger} \left|\alpha_2\right\rangle_1 \left|\beta\right\rangle_2 \frac{d\beta^2}{\pi} = \\ \int e^{-|\alpha_0|^2 - |\beta'|^2 - |\beta|^2 + 2\Re(g_3)|\alpha_0|^2 + e^{\gamma+g_4}\beta'\beta^* + e^{g_4^*}\beta\beta'^*} (1-e^{\gamma}) \\ \left\langle\alpha_1\right|_1 e^{a_1\beta^* g_1} e^{a_1^{\dagger} e^{\gamma+g_4}\beta' g_2} \left|e^{g_3}\alpha_0\right\rangle \\ \left\langle e^{g_3}\alpha_0\right| e^{a_1 e^{g_4}{}^* \beta_3{}^* g_2{}^*} e^{a_1{}^{\dagger}\beta g_1{}^*} \left|\alpha_2\right\rangle \frac{d\beta^2}{\pi}\frac{d\beta'^2}{\pi}. \end{aligned} \tag{5.46}$$

In order to evaluate further, we apply the property $e^A e^B = e^B e^A e^{[A,B]}$ when $[A,B]$ commutes with both A and B. Furthermore, we apply the unitary conditions in Eq. (5.44) and evaluate the integrals using Eq. (5.25) to obtain

$$\rho_1(\alpha_1,\alpha_2) = \frac{e^{-\frac{|\alpha_1|^2+|\alpha_2|^2-2\alpha_1{}^*\alpha_2}{2} - \frac{\left(\alpha_0'-\alpha_2\right)\left(\alpha_0'-\alpha_1\right)^*}{N}}}{N}, \tag{5.47}$$

with $\alpha_0' = \alpha_0 \frac{e^{i\Im(g_3)}}{\sqrt{1+|g_1|^2}}$ and $N = 1 + \bar{n}\left(1 - \left(|g_1|^2+1\right)^{-1}\right)$.

If we note using Eq. (5.44) that

$$\langle \alpha_1 | \alpha_0'/N \rangle = e^{-\frac{|\alpha_1|^2}{2} - \frac{|\alpha_0/N|^2}{2} + {\alpha_1}^*(\alpha_0/N)}, \tag{5.48}$$

we can expand Eq. (5.47) into an operator form. Observe

$$\begin{aligned}
\langle \alpha_1 | \rho_1 | \alpha_2 \rangle &= \frac{e^{-\frac{|\alpha_1|^2+|\alpha_2|^2-2{\alpha_1}^*\alpha_2}{2} - \frac{\left(\alpha_0'-\alpha_2\right)\left(\alpha_0'-\alpha_1\right)^*}{N}}}{N} \\
&= \frac{1}{N} e^{-\frac{|\alpha_0'|^2}{N} + \frac{|\alpha_0'|^2}{N^2}} e^{{\alpha_1}^*\alpha_2} \langle \alpha_1 | \alpha_0'/N \rangle \langle \alpha_0'/N | \alpha_1 \rangle \\
&= \frac{1}{N} e^{-\frac{|\alpha_0'|^2}{N} + \frac{|\alpha_0'|^2}{N^2}} \sum_{j=0}^{\infty} \frac{\left(1-\frac{1}{N}\right)^j}{j!} \langle \alpha_1 | {\alpha_1}^{*j} | \alpha_0'/N \rangle \langle \alpha_0'/N | {\alpha_2}^j | \alpha 2 \rangle \\
&= \langle \alpha_1 | \left(\frac{1}{N} e^{-\frac{|\alpha_0'|^2}{N} + \frac{|\alpha_0'|^2}{N^2}} \sum_{j=0}^{\infty} \frac{\left(1-\frac{1}{N}\right)^j}{j!} a^{\dagger j} | \alpha_0'/N \rangle \langle \alpha_0'/N | a^j \right) | \alpha 2 \rangle .
\end{aligned} \tag{5.49}$$

Thus, an operator form of the density matrix for the partial traced double oscillator system is

$$\rho_1 = \frac{1}{N} e^{-\frac{|\alpha_0'|^2}{N} + \frac{|\alpha_0'|^2}{N^2}} \sum_{j=0}^{\infty} \frac{\left(1-\frac{1}{N}\right)^j}{j!} a^{\dagger j} | \alpha_0'/N \rangle \langle \alpha_0'/N | a^j. \tag{5.50}$$

Taking the trace of ρ_1^2, we can obtain a measure of the decoherence of the system. Using the coherent state representation in Eq. (5.47) along with the complex Gaussian integral formula in Eq. (5.25), we find the simple form

$$\begin{aligned}
\mathrm{tr}\left(\rho_1^2\right) &= \int \rho_1\left(\beta, \beta'\right) \rho_1\left(\beta', \beta\right) \frac{d\beta^2}{\pi} \frac{d{\beta'}^2}{\pi} \\
&= \frac{1}{|1-2N|},
\end{aligned} \tag{5.51}$$

with $N = 1 + \bar{n}\left(1 - \left(|g_1|^2 + 1\right)^{-1}\right)$. Note that this implies the decoherence of this time dependent system is only determined by the energy of the environment, $\bar{n}$, and the term $|g_1|^2$.

For confirmation of this result, we apply the constant case for g_1 into the solution using Eq. (5.43). After full simplification,

$$\mathrm{tr}\left({\rho_1}^2\right) = \frac{1}{1 + 2\bar{n}\frac{|g|^2 \sin(\omega')^2}{{\omega'}^2}}, \tag{5.52}$$

which is consistent with [15].

5.5.2 Anharmonic Effects Added

We will now look at the double oscillator with an anharmonic effect added to the first oscillator. Specifically, we will use the Hamiltonian

$$H = \hbar\left(\omega(t)\hat{n}_1 + \Omega(t)\hat{n}_2 + v(t)^* a_1 a_2^\dagger + v(t) a_1^\dagger a_2 + B\hat{n}_1^2\right), \tag{5.53}$$

which is Eq. (5.39) with the $\hbar B\hat{n}_1^2$ term added. We note that with the additional $\hat{n}_1^2$ term, the Lie algebra for this Hamiltonian does not close. We will thus change this system to the interaction picture, then take a mean field approximation to make this system's evolution more manageable while retaining the anharmonic effects [89].

Changing into the interaction picture, we split the time evolution operator as $U = U_0 U_{\text{int}}$. We set $H_0 = \hbar B\hat{n}_1^2$ making $U_0 = e^{g_0\hat{n}_1^2}$ where g_0 is purely imaginary and $g_0 = -i\int_0^t B(\tau)d\tau$. With this, our interaction Hamiltonian becomes

$$\begin{aligned} H'_{\text{int}} &= U_0^\dagger(H\hbar - H_0\hbar)U \\ &= \hbar\left(\omega(t)\hat{n}_1 + \Omega(t)\hat{n}_2 + v(t)^*\left(U_0^\dagger a_1 U_0\right)a_2^\dagger + v(t)\left(U_0^\dagger a_1^\dagger U_0\right)a_2\right) \\ &= \hbar\left(\omega(t)\hat{n}_1 + \Omega(t)\hat{n}_2 + v(t)^* e^{i\Im(g_0)(2\hat{n}_1+1)} a_1 a_2^\dagger + v(t) a_1^\dagger a_2 e^{-i\Im(g_0)(2\hat{n}_1+1)}\right), \end{aligned} \tag{5.54}$$

where we used the fact that $a_1 F(\hat{n}_1) = F(\hat{n}_1+1)a_1$ to move the a_1 and $a_1^\dagger$ terms next to the $\hat{n}_1^2$ exponentials. These exponentials of operator terms in the Hamiltonian make it so the Lie algebra for the Hamiltonian will not close, so we now take the mean field approximation with respect to the operator $e^{i\Im(g_0)(2\hat{n}_1+1)}$ by replacing the operator with its expectation value [89]. With this approximation, the Hamiltonian becomes

$$\begin{aligned} H_{\text{int}} &= \hbar\left(\omega(t)\hat{n}_1 + \Omega(t)\hat{n}_2 + v(t)^*\left\langle e^{i\Im(g_0)(2\hat{n}_1+1)}\right\rangle a_1 a_2^\dagger + v(t) a_1^\dagger a_2\left\langle e^{-i\Im(g_0)(2\hat{n}_1+1)}\right\rangle\right) \\ &= \hbar\left(\omega(t)\hat{n}_1 + \Omega(t)\hat{n}_2 + g(t)^* a_1 a_2^\dagger + g(t) a_1^\dagger a_2\right), \end{aligned} \tag{5.55}$$

with $g(t) = v(t)\left\langle e^{-i\Im(g_0)(2\hat{n}_1+1)}\right\rangle$. Thus, with the mean field approximation, the interaction Hamiltonian reduces to the case of the double harmonic oscillator given in Eq. (5.39). Thus, the interaction

time evolution operator is given by Eq. (5.39), with the g_i coefficients determined by Eq. (5.42), with unitarity conditions determined by Eq. (5.44). Furthermore, we allow the initial state for the second oscillator to be a thermal state, and the first oscillator to be a coherent state $|\alpha_0\rangle$ as in the previous section. Then, since U_0 does not interact with a trace with respect to the second oscillators system,

$$\begin{aligned}
\rho_1 &= \mathrm{tr}_2\left(U\rho_0 U^\dagger\right) \\
&= U_0\ \mathrm{tr}_2\left(U_{\mathrm{int}}\rho_0 U_{\mathrm{int}}^\dagger\right) U_0^\dagger \\
&= e^{i\Im(g_0)\hat{n}_1^2}\left(\frac{1}{N}e^{-\frac{|\alpha_0'|^2}{N}+\frac{|\alpha_0'|^2}{N^2}}\sum_{j=0}^{\infty}\frac{\left(1-\frac{1}{N}\right)^j}{j!}a^{\dagger j}\,|\alpha_0'/N\rangle\,\langle\alpha_0'/N|\,a^j\right)e^{-i\Im(g_0)\hat{n}_1^2} \\
&= \frac{1}{N}e^{-\frac{|\alpha_0'|^2}{N}+\frac{|\alpha_0'|^2}{N^2}}\sum_{j=0}^{\infty}\frac{\left(1-\frac{1}{N}\right)^j}{j!}a^{\dagger j}e^{i\Im(g_0)(\hat{n}_1+j)^2}\,|\alpha_0'/N\rangle\,\langle\alpha_0'/N|\,e^{-i\Im(g_0)(\hat{n}_1+j)^2}a^j \\
&= \frac{1}{N}e^{-\frac{|\alpha_0'|^2}{N}+\frac{|\alpha_0'|^2}{N^2}}\sum_{j=0}^{\infty}\frac{\left(1-\frac{1}{N}\right)^j}{j!}a^{\dagger j}e^{i\Im(g_0)\hat{n}_1^2}\,|\alpha_0' e^{2j\ i\Im(g_0)}/N\rangle\,\langle\alpha_0' e^{2j\ i\Im(g_0)}/N|\,e^{-i\Im(g_0)\hat{n}_1^2}a^j,
\end{aligned} \tag{5.56}$$

with $\alpha_0' = \alpha_0\frac{e^{i\Im(g_3)}}{\sqrt{1+|g_1|^2}}$ and $N = 1+\bar{n}\left(1-\left(|g_1|^2+1\right)^{-1}\right)$. This was done using Eq. (5.50), noting $F(\hat{n})a^j = a^j F(\hat{n}+j)$, and using the properties of coherent states given in Eq. (5.22).

With the density matrix given in Eq. (5.56), we can find the Husimi function. Again, using the

coherent state properties given in Eq. (5.22), we find the Husimi $Q(z)$ to be

$$\begin{aligned}
Q(z) &= \frac{1}{\pi}\langle z|\,\rho_1\,|z\rangle \\
&= \frac{1}{N\pi}e^{-\frac{|\alpha_0'|^2}{N}+\frac{|\alpha_0'|^2}{N^2}}\sum_{j=0}^{\infty}\frac{\left(1-\frac{1}{N}\right)^j}{j!}z^{*j}\,\langle z|\,e^{i\Im(g_0)\hat{n}_1^2}\,|\alpha_0' e^{2j\ i\Im(g_0)}/N\rangle\,\langle\alpha_0' e^{2j\ i\Im(g_0)}/N|\,e^{-i\Im(g_0)\hat{n}_1^2}\,|z\rangle\,z^j \\
&= \frac{1}{N\pi}e^{-\frac{|\alpha_0'|^2}{N}-|z|^2}\sum_{k=0}^{\infty}\sum_{l=0}^{\infty}\frac{e^{-i\Im(g_0)k^2}\left(\frac{z\alpha_0'^*}{N}\right)^k}{k!}\frac{e^{i\Im(g_0)l^2}\left(\frac{z^*\alpha_0'}{N}\right)^l}{l!}\sum_{j=0}^{\infty}\frac{\left(\left(1-\frac{1}{N}\right)e^{2i\Im(g_0)(l-k)}\,|z|^2\right)^j}{j!} \\
&= \frac{e^{-\left(\frac{|\alpha_0'|^2}{N}+|z|^2\right)}}{N\pi}\sum_{k=0}^{\infty}\sum_{l=0}^{\infty}e^{i\Im(g_0)(l^2-k^2)}\frac{\left(\frac{z\alpha_0'^*}{N}\right)^k\left(\frac{z^*\alpha_0'}{N}\right)^l}{k!\ l!}e^{|z|^2\left(1-\frac{1}{N}\right)e^{2i\Im(g_0)(l-k)}}.
\end{aligned} \tag{5.57}$$

Looking at Eq. (5.57), we see that as N approaches 1, the $Q(z)$ function here approaches the evolution of the single anharmonic oscillator given in Eq. (5.38). Thus, when decoherence is low, the evolution is similar to the usual anharmonic oscillator as expected. When $N \to \infty$, i.e. when decoherence is large, the terms where l and k are nonzero would fade away, leaving a wide Gaussian at the origin. Further plots are given in Figs. (5.2)-(5.4).

5.6 Born-Markov Master Equation for Anharmonic Oscillator

Here we take a look at the Born-Markov approximation for an anharmonic oscillator coupled with an infinite heat bath of environmental oscillators. The Hamiltonian for such a system is of the form

$$H = \hbar\left(\omega_c\hat{n} + \Omega\hat{n}^2 + \sum_{i=1}^{\infty}\omega_i\hat{n}_i + V_i^* a{a_i}^\dagger + V_i a^\dagger a_i\right), \tag{5.58}$$

where $\hbar\omega_c\hat{n} + \hbar\Omega\hat{n}^2$ is the Hamiltonian for the single anharmonic oscillator, and the terms with subscript i refer to the oscillators to which the anharmonic system is coupled. Assuming the environmental oscillators are in respective thermal states, and following the procedure described in

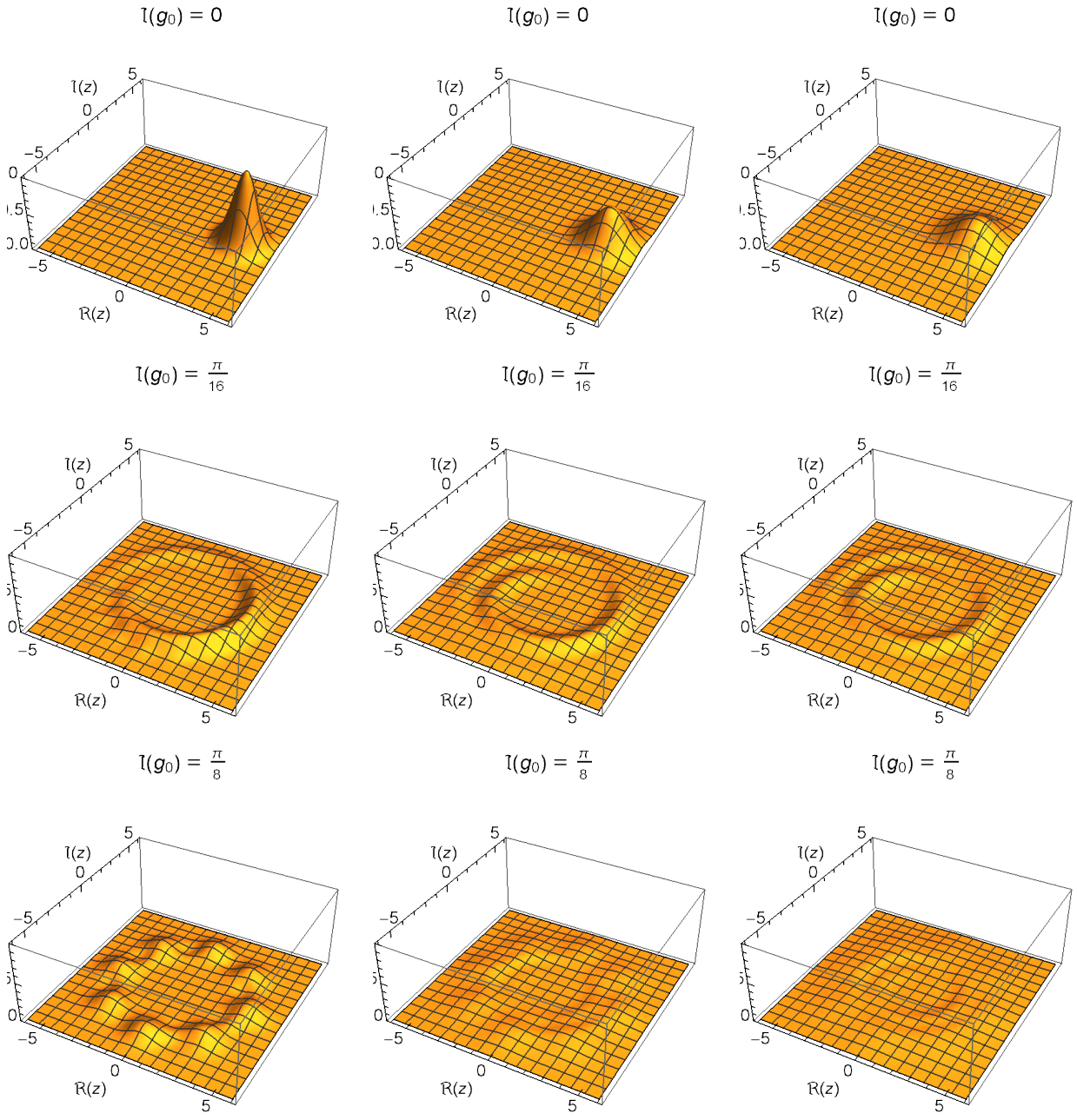

Figure 5.2 Husimi function $\pi Q(z)$ plots of the anharmonic double oscillator (given in Eq. (5.57)) of varying decoherence and times. Left column is $N = 1$; middle column is $N = 2$; right column is $N = 3$; and $\alpha_0' = 4$ throughout.

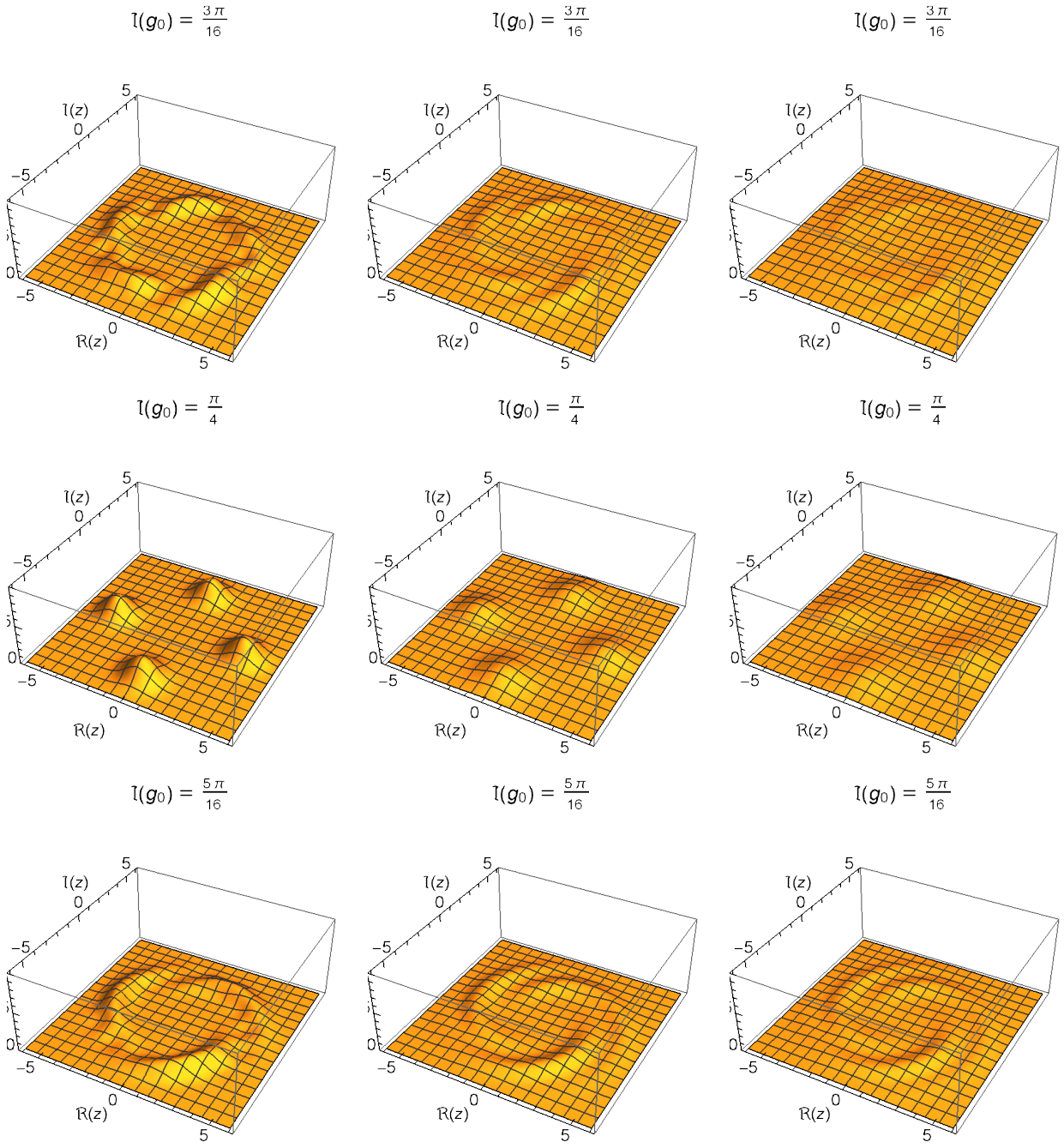

Figure 5.3 Husimi function $\pi Q(z)$ plots of the anharmonic double oscillator (given in Eq. (5.57)) of varying decoherence and times. Left column is $N = 1$; middle column is $N = 2$; right column is $N = 3$; and $\alpha_0' = 4$ throughout.

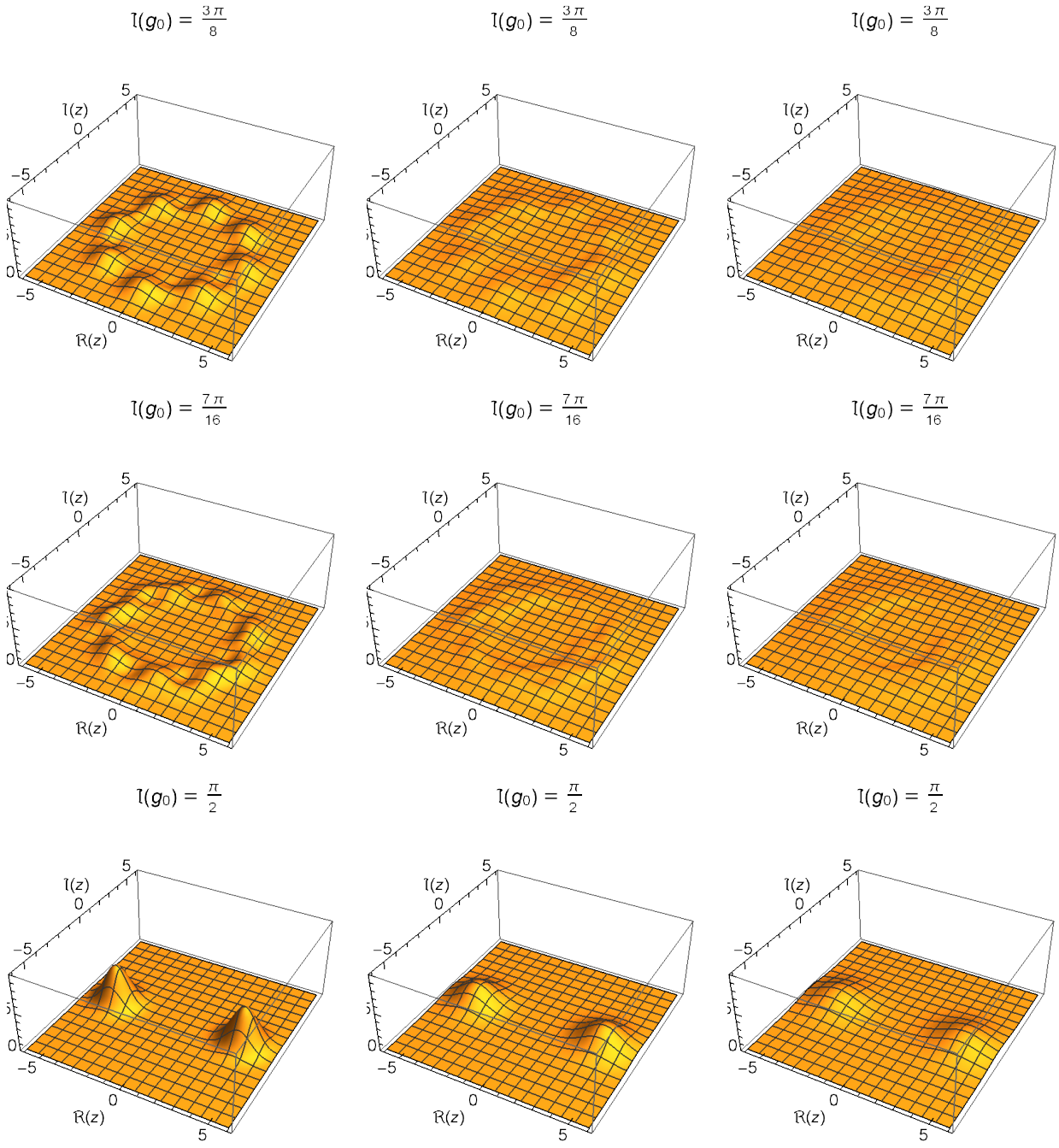

Figure 5.4 Husimi function $\pi Q(z)$ plots of the anharmonic double oscillator (given in Eq. (5.57)) of varying decoherence and times. Left column is $N = 1$; middle column is $N = 2$; right column is $N = 3$; and $\alpha_0' = 4$ throughout.

Eq. (5.9), the Born-Markov master equation for this system is

$$\begin{aligned} i\frac{d}{dt}\rho =&[\omega_0\hat{n}+\Omega\hat{n}^2,\square] \\ &-i\Big(\square\nu_1(\hat{n})\hat{n}+\hat{n}\nu_1(\hat{n})^\dagger-a\square\,\nu_1(\hat{n})a^\dagger-a\nu_1(\hat{n})^\dagger\square\,a^\dagger \\ &+\square\nu_2(\hat{n})\hat{n}+\hat{n}\nu_2(\hat{n})^\dagger\square+\square\,a\nu_2(\hat{n})^\dagger a^\dagger-a\square\,\nu_2(\hat{n})a^\dagger \\ &-a\nu_2(\hat{n})^\dagger\square\,a^\dagger+a\nu_2(\hat{n})a^\dagger\square-a^\dagger\square\,a\nu_2(\hat{n})^\dagger-\nu_2(\hat{n})a^\dagger\square\,a\Big), \end{aligned} \tag{5.59}$$

where $\nu_1(\hat{n})=\sum_{i=0}^{\infty}|V_i|^2\int_0^\infty e^{i\tau(-\omega_0+\omega_i+\Omega(1-2\hat{n}))}d\tau$ and $\nu_2(\hat{n})=\sum_{i=0}^{\infty}|V_i|^2\,\bar{n}_i\int_0^\infty e^{i\tau(-\omega_0+\omega_i+\Omega(1-2\hat{n}))}d\tau$. Note that when Ω approaches zero, Eq. (5.59) becomes the evolution of the Born-Markov approximation of the harmonic oscillator with infinite couplings in Eq. (5.12). This leads to a difficult problem. The terms $\nu_1(\hat{n})$ and $\nu_2(\hat{n})$ do not commute with the other operators, and as it stands, the Lie algebra for this system does not close. There are several directions one can go with this problem. We could take a mean field approximation of the terms $\nu_1(\hat{n})$ and $\nu_2(\hat{n})$. This would make the equation similar to the Born-Markov equation for the harmonic oscillator Eq. (5.12) with an added anharmonic term. One could go this direction, but there would be further complications since the $[\hat{n}^2,\square]$ would not form a Lie algebra with the rest of the operators in the equation. Thus it would require some sort of interaction picture for superoperators coupled with another mean field approximation.

Instead, we will return to the Hamiltonian in Eq. (5.58) and apply an interaction picture form much like in Section 5.5.2 with the anharmonic double oscillator.

Changing into the interaction picture, we split the time evolution operator such that $U=U_0U_{\text{int}}$. We set $H_0=\hbar\Omega\hat{n}^2$ making $U_0=e^{g_0\hat{n}^2}$ where g_0 is purely imaginary and $g_0=-i\int_0^t\Omega(\tau)d\tau$. With this, our interaction Hamiltonian becomes

$$\begin{aligned} H'_{\text{int}}&=U_0^\dagger(H-H_0)U_0 \\ &=\hbar\left(\omega_c\hat{n}+\omega_i\hat{n}_i+V_i^*\left(U_0^\dagger a_cU_0\right)a_i^\dagger+V_i\left(U_0^\dagger a_c^\dagger U_0\right)a_i\right) \\ &=\hbar\left(\omega_c\hat{n}+\omega_i\hat{n}_i+V_i^*e^{i\Im(g_0)(2\hat{n}+1)}aa_i^\dagger+V_ia^\dagger a_ie^{-i\Im(g_0)(2\hat{n}+1)}\right). \end{aligned} \tag{5.60}$$

To make this more manageable, we take the mean field approximation to create the new interaction Hamiltonian

$$\begin{aligned} H_{\text{int}} &= \hbar\left(\omega\hat{n}+\sum_{i=1}^{\infty}\omega_i\hat{n}_i+V_i^*\left\langle e^{i\Im(g_0)(2\hat{n}+1)}\right\rangle a_1a_i^\dagger+V_ia_1^\dagger a_i\left\langle e^{-i\Im(g_0)(2\hat{n}+1)}\right\rangle\right) \\ &= \hbar\left(\omega\hat{n}+\sum_{i=1}^{\infty}\omega_i\hat{n}_i+c_i^*(t)aa_i^\dagger+c_i(t)a^\dagger a_i\right), \end{aligned} \tag{5.61}$$

with $c_i(t)=V_i\left\langle e^{-i\Im(g_0)(2\hat{n}+1)}\right\rangle$. Again, using Eq. (5.9) with the same assumptions as above, the Born-Markov master equation for the interactive part of the density matrix is

$$i\frac{d\rho_{\text{I}}}{dt}=[\omega_c\hat{n},\rho_{\text{I}}]-i\left(\left(\hat{n}\rho_{\text{I}}-a\rho_{\text{I}}a^\dagger\right)\eta_1+\left(\rho_{\text{I}}\hat{n}-a\rho_{\text{I}}a^\dagger\right)\eta_1^*+\left(\rho_{\text{I}}+\rho_{\text{I}}\hat{n}-a^\dagger\rho_{\text{I}}a+\hat{n}\rho_{\text{I}}-a\rho_{\text{I}}a^\dagger\right)\eta_2\right), \tag{5.62}$$

with $\eta_1=\sum_{i=0}^{\infty}\int_0^{\infty}|c_i|^2e^{it(\omega_c-\omega_i)}dt$ and $\eta_2=\sum_{i=0}^{\infty}\bar{n}_i\int_0^{\infty}|c_i|^2\left(e^{it(\omega_c-\omega_i)}+e^{-it(\omega_c-\omega_i)}\right)dt$. This is the same as equation Eq. (5.12) except that $|c_i|^2$ is time-dependent. We now use the real number labels γ, $\bar{n}_c$,and $\Delta\omega$ to denote $\eta_1=\frac{\gamma}{2}+i\Delta\omega$ and $\eta_2=2\bar{n}_c\gamma$. With these labels, the Born-Markov master equation for the interaction density matrix becomes

$$i\frac{d\rho_{\text{I}}}{dt}=\left((\omega_c+\Delta\omega)[\hat{n},\square]+i\gamma\left(\frac{1}{2}\square+\bar{n}_ca^\dagger\square a+(1+\bar{n}_c)a\square a^\dagger-\left(\bar{n}_c+\frac{1}{2}\right)\left\{\frac{\text{I}}{2}+\hat{n},\square\right\}\right)\right)\rho_{\text{I}}, \tag{5.63}$$

which is the same form as Eq. (5.15). Thus, all the results of Eqs.(5.15)-(5.29) for the harmonic oscillator with infinite couplings with the Born-Markov approximation apply for the interaction density matrix ρ_{I} for this case. In particular,

$$\rho_{\text{I}}(t)=|1-g_1|\,e^{-\frac{g_1}{1-g_1}|\alpha'|^2}\sum_{j=0}^{\infty}\frac{g_1^j}{j!}\,a^{\dagger j}\,|\alpha'\rangle\langle\alpha'|\,a^j, \tag{5.64}$$

with $\alpha' = \alpha e^{\frac{1}{2}(g_3+g_4)}$ and

$$i\begin{pmatrix} g_1' \\ g_2' \\ g_3' \\ g_4' \\ g_5' \end{pmatrix} = \begin{pmatrix} 1 & {g_1}^2 & g_1 & 0 & 0 \\ 0 & 1-2g_1g_2 & -g_2 & 0 & 0 \\ 0 & 2g_1 & 1 & 0 & 0 \\ 0 & 0 & 0 & 1 & 0 \\ 0 & 0 & 0 & 0 & 1 \end{pmatrix} \begin{pmatrix} i\gamma\bar{n}_c \\ i\gamma(1+\bar{n}_c) \\ -2i\gamma(1+2\bar{n}_c) \\ 2(\omega_c+\Delta\omega) \\ i\frac{\gamma}{2} \end{pmatrix}. \tag{5.65}$$

If we take Eq. (5.64) and make the replacements $g_1 \to (1-\frac{1}{N})$ and $\alpha' \to \frac{\alpha_0'}{N}$, then the form of the interaction density matrix is the same as the interaction density matrix for the double oscillator with an anharmonic term in Eq. (5.50). Thus, Eqs. (5.47)-(5.51) apply to this interaction density matrix with the substitutions $\alpha_0' \to \alpha'/(1-g_1)$ and $N \to 1/(1-g_1)$. Since the U_0 is of the same form as well, we will copy down the evolved density matrix for the double oscillator with an anharmonic term Eq. (5.56) with the replacements $\alpha_0' \to \alpha'/(1-g_1)$ and $N \to 1/(1-g_1)$. Thus, the density matrix of the anharmonic oscillator with infinite couplings and with the mean field and the Born-Markov approximations is

$$\rho(t) = (1-g_1)e^{-g_1|\alpha'|^2}\sum_{j=0}^{\infty}\frac{(g_1)^j}{j!}a^{\dagger j}e^{i\Im(g_0)\hat{n}^2}\left|\alpha' e^{2j\ i\Im(g_0)}\right\rangle\left\langle\alpha' e^{2j\ i\Im(g_0)}\right|e^{-i\Im(g_0)\hat{n}^2}a^j, \tag{5.66}$$

with $\alpha' = \alpha e^{\frac{1}{2}(g_3+g_4)}$. Applying the same replacements to Eq. (5.57), we see the Husimi Q function takes the form

$$Q(z) = \frac{1}{\pi}(1-g_1)e^{-\left(\frac{|\alpha'|^2}{(1-g_1)}+|z|^2\right)}\sum_{k=0}^{\infty}\sum_{l=0}^{\infty}e^{i\Im(g_0)(l^2-k^2)}\frac{\left(z\alpha'^*\right)^k\left(z^*\alpha'\right)^l}{k!\ l!}e^{|z|^2 g_1 e^{2i\Im(g_0)(l-k)}}, \tag{5.67}$$

Once again, we see that as $g_1 \to 0$, the Husimi function Eq. (5.67) approaches the form of the single anharmonic oscillator in Eq. (5.38). Looking at Eq. (5.65), we see that there is a connection between g_1 and g_3 that is not apparent in Eq. (5.67). Using the constant case given in Eq. (5.19), we see $\alpha' = (1-g_1)e^{-\frac{1}{2}t(\gamma+2i(\omega_0+\Delta\omega))}$ and $g_1 = 1-\frac{1}{1+\bar{n}_c(1-e^{-t\gamma})}$. Thus, as time evolves, the Husimi function collapses to a wide Gaussian distribution centered at the origin, much like the evolution for the double anharmonic oscillator and the Born-Markov master equation for the harmonic oscillator.

5.7 Conclusion

In this paper we explore the dynamic evolution and decoherence of the anharmonic oscillator with infinite coupling using the Born-Markov master equation. This is done by exploiting the Lie algebraic structure of the Born-Markov master equation's superoperators after applying a mean field approximation. We have also analyzed the evolution of the time-dependent anharmonic double oscillator and its decoherence. We have seen that the anharmonic double oscillator and the anharmonic oscillator with the Born-Markov approximation take similar forms using the Lie algebraic structure. The difference in these are mostly hidden in the exponential g_i coefficients. We plotted the Husimi functions of these and viewed cat states with varying degrees of decoherence. We see the Husimi function for the anharmonic double oscillator collapses to a wide Gaussian distribution as the decoherence effects become large, similar to the Born-Markov master equation for the simple harmonic oscillator. Because the structure of the anharmonic oscillator with the Born-Markov master equation is Lie algebraically similar to the double anharmonic oscillator, the effects of large decoherence on the anharmonic oscillator with the Born-Markov master equation are much the same.

Chapter 6

Results Summary

We explored the effects of decoherence in various systems. These include the harmonic oscillator with infinite coupling using the Born-Markov approximation in Section 5.2.3, the anharmonic double oscillator in Chapter 5.5, the optomechanical system with second order coupling in Chapter 4.1, and the anharmonic oscillator with infinite coupling using the Born-Markov approximation in Chapter 5.6. We established that the anharmonic Born-Markov oscillator had a structure similar to the anharmonic double oscillator, and both act similar to the evolution of the single anharmonic oscillator. Looking at the density matrices and Husimi functions, we have found that the decoherence effects for the anharmonic oscillators with both Born-Markov and double oscillators cause a dissociative bulging, as expected, whereas the decoherence effects of the optomechanical system create rotational smearing with the second order coupling in the system causing rotational smearing after squeezing.

We also found the unitarity conditions for several systems which give effective time dependent restrictions for the time evolution operators. We also solved for the g-Matrix for many systems which determine the dynamics of the time evolution operators according to Eq. (5.3). The g-Matrix and unitarity conditions for the systems studied are given in Table (6.1).

Also, in Chapter 3, we made progress in quantum control. We developed a method for using faithful representations of Lie algebras associated with the Hamiltonian to control the dynamics of

the generalized Caldirola-Kanai system using timing to apply fluctuations of arbitrary shape to the Hamiltonian to control the system's time evolution. This technique could be applied to all systems with a Lie algebraic Hamiltonian. Furthermore, many of the results throughout this dissertation are written in terms of the g_i coefficients which are directly linked, via the g-Matrix, to any general time dependent Hamiltonian fulfilling the Lie algebra requirements. These are shown in Table 6.1. This allows for direct control links from the time evolution operator and density matrices to the Hamiltonian, thus dictating the time evolution of the Hamiltonian to control the quantum system's state.

Table 6.1 Wei-Norman and Unitarity Conditions Results Summary

System	Evolution operator U	g-Matrix	Unitarity Conditions
Driven Oscillator	$e^{g_1 a^\dagger} e^{g_2 a} e^{g_3 \hat{n}} e^{g_4 \mathrm{I}}$	$\begin{pmatrix} 1 & 0 & g_1 & 0 \\ 0 & 1 & -g_2 & 0 \\ 0 & 0 & 1 & 0 \\ 0 & g_1 & 0 & 1 \end{pmatrix}$	$g_2 = -{g_1}^*$ $\Re(g_3) = 0$ $\Re(g_4) = -\frac{\lvert g_1 \rvert^2}{2}$
Born-Markov Oscillator	$e^{g_1 a \Box a^\dagger} e^{g_2 a^\dagger \Box a} e^{g_3 \left(\frac{1}{2}\left\{\hat{n}+\frac{1}{2}, \Box\right\}\right)}$ $\times e^{g_4 \frac{1}{2}[\hat{n}, \Box]} e^{g_5 \Box}$	$\begin{pmatrix} 1 & {g_1}^2 & g_1 & 0 & 0 \\ 0 & 1-2g_1 g_2 & -g_2 & 0 & 0 \\ 0 & 2g_1 & 1 & 0 & 0 \\ 0 & 0 & 0 & 1 & 0 \\ 0 & 0 & 0 & 0 & 1 \end{pmatrix}$	N/A
Anharmonic Oscillator	$e^{g_1 \hat{n}^2} e^{g_2 \hat{n}} e^{g_3 \mathrm{I}}$	$\begin{pmatrix} 1 & 0 & 0 \\ 0 & 1 & 0 \\ 0 & 0 & 1 \end{pmatrix}$	$\Re(g_1) = 0$ $\Re(g_2) = 0$ $\Re(g_3) = 0$
Generalized C-K	$e^{g_1 \frac{a^{\dagger 2}}{2}} e^{g_2 \frac{a^2}{2}} e^{g_3 \frac{1}{2}(a^\dagger a + \frac{1}{2})}$	$\begin{pmatrix} 1 & {g_1}^2 & g_1 \\ 0 & 1-2g_1 g_2 & -g_2 \\ 0 & 2g_1 & 1 \end{pmatrix}$	$g_2 = -\frac{g_1^*}{1-\lvert g_1 \rvert^2}$ $\Re(g_3) = \ln\left(1-\lvert g_1 \rvert^2\right)$
Double Oscillator	$e^{g_1\ a_1 a_2^\dagger} e^{g_2\ a_1^\dagger a_2} e^{g_3\ \hat{n}_1} e^{g_4\ \hat{n}_2}$	$\begin{pmatrix} 1 & -g_1^2 & -g_1 & g_1 \\ 0 & 1+2g_1 g_2 & g_2 & -g_2 \\ 0 & g_1 & 1 & 0 \\ 0 & -g_1 & 0 & 1 \end{pmatrix}$	$g_2 = -\frac{g_1^*}{1+\lvert g_1 \rvert^2}$ $\Re(g_3) = -\frac{1}{2}\ln\left(1+\lvert g_1 \rvert^2\right)$ $\Re(g_4) = \frac{1}{2}\ln\left(1+\lvert g_1 \rvert^2\right)$
Optomechanical Oscillator	$e^{g_1 \hat{n}^2} e^{g_2 \hat{n}} e^{g_3 \hat{n} b^\dagger} e^{g_4 \hat{n} b} e^{g_5 b^\dagger b}$	$\begin{pmatrix} 1 & 0 & 0 & g_3 & 0 \\ 0 & 1 & 0 & 0 & 0 \\ 0 & 0 & 1 & 0 & g_3 \\ 0 & 0 & 0 & 1 & -g_4 \\ 0 & 0 & 0 & 0 & 1 \end{pmatrix}$	$\Re(g_2) = 0$ $\Re(g_5) = 0$ $\Re(g_1) = -\frac{\lvert g_3 \rvert^2}{2}$ $g_4 = -g_3^*$

Bibliography

[1] R. P. Feynman1982, "Simulating Physics with Computers," Int. J. Theor. Phys. **26,** 467–488 (1982).

[2] P. W. Shor, "Polynomial-Time Algorithms for Prime Factorization and Discrete Logarithms on a Quantum Computer," SIAM J.Sci.Statist.Comput **21,** 1484–1509 (1997).

[3] L. K. Grover, "A Fast Quantum Mechanical Algorithm for Database Search," In *Proceedings of the Twenty-eighth Annual ACM Symposium on Theory of Computing*, STOC '96 pp. 212–219 (ACM, New York, NY, USA, 1996).

[4] D. J. Bernstein, J. Buchmann, and E. Dahmen, *Post-Quantum Cryptography* (Springer-Verlag, Berlin Heidelberg, 2009).

[5] "D-Wave The Quantum Computing Company,", https://www.dwavesys.com/quantum-computing/applications, 2017.

[6] G. J. Milburn, "Quantum and Classical Liouville Dynamics of the Anharmonic Oscillator," Phys. Rev. A **33,** 674–685 (1986).

[7] B. Yurke and D. Stoler, "Generating Quantum Mechanical Superpositions of Macroscopically Distinguishable States via Amplitude Dispersion," Phys. Rev. Lett. **57,** 13–16 (1987).

[8] J. S. Taylor, *Classical Mechanics* (University Science Books, USA, 2005).

[9] I. N. Levine, *Molecular Spectroscopy* (Wiley & Sons, New York, NY, 1975).

[10] P. Knight and C. C. Gerry, *Introductory Quantum Optics* (Cambridge University Press, Cambridge Uk, 2004).

[11] R. W. Henry and S. C. Glotzer, Am. J. Phys. 56 (1988).

[12] S. P. Kim, A. E. Santana, and F. C. Khanna, "Decoherence of Quantum Damped Oscillators," arXiv:quant-ph/0202089 .

[13] C. M. Cheng and P. C. W. Fung, J. Phys. A: Math. Gen. **21,** 4115–4131 (1988).

[14] Ben-Aryeh, "Harmonic oscillator with time-dependent effective-mass and frequency with a possible application to 'chirped tidal' gravitational waves forces affecting interferometric detectors," arXiv:0807.4670 (2008).

[15] A. Vidiella-Barranco, "Evolution of a quantum harmonic oscillator coupled to a minimal thermal environment," Physica A **459,** 78–85 (2016).

[16] M. Schlosshauer, *Decoherence and the Quantum-To-Classical Transition* (Springer-Verlag, Berlin Heidelberg, New York, 2008).

[17] W. D. José, M. Nemes, and A. de Toledo Piza, "General aspects of decoherence and dissipation of linearly coupled oscillators," Physica A **283,** 359–368 (2000).

[18] D. Honda, H. Nakazato, and M. Yoshida, "Spectral resolution of the Liouvillian of the Lindblad master equation for a harmonic oscillator," J. Math. Phys. **51,** 072107 (2010).

[19] W. A. De Graaf, *Lie Algebras: Theory and Algorithms* (Elsevier Science B.V., The Netherlands, 2000).

[20] T. Beus (unpublished).

[21] E. Merzbacher, *Quantum Mechanics*, 3 ed. (Wiley & Sons, New York, NY, 1998), p. 363.

[22] K. Husimi, "Some Formal Properties of the Density Matrix," Phys. Math. Soc. Jpn. **22,** 264–314 (1940).

[23] E. P. Wigner, Phys. Rev. **40,** 749–759 (1932).

[24] T. Beus, J. Van Huele, and M. Berrondo, "Quantum Manipulation Through Finite Fluctuations for a Generalized Parametric Oscillator Using a Lie Algebra Representation," Phys. Scr. **96,** 075103 (2021).

[25] J. Wei and E. Norman, "Lie Algebraic Solution of Linear Differential Equations," J. Math. Phys. **4,** 575–581 (1963).

[26] M. Shapiro and P. Brumer, "Coherent control of atomic, molecular, and electronic processes," Adv. At., Mol., Opt. Phys. **42,** 287–345 (2000).

[27] R. J. Gordon and S. A. Rice, "ACTIVE CONTROL OF THE DYNAMICS OF ATOMS AND MOLECULES," Annu. Rev. Phys. Chem **42,** 601–641 (1997).

[28] H. Rabitz, "Focus on Quantum Control," Phys. Rev. Lett. **11,** 105030 (2009).

[29] M. Shapiro and P. Brumer, *Principles of the Quantum Control of Molecular Processes* (John Wiley & Sons, Inc., Hoboken, New Jersey, 2003).

[30] M. T. Carmen, L. Kurtz, and R. d. Vivie-Riedle, "Applying optimal control theory for elements of quantum computation in molecular systems," Chem. Phys. Lett **343,** 633–641 (2001).

[31] J. P. Palao and R. Kosloff, "Quantum Computing by an Optimal Control Algorithm for Unitary Transformations," Phys. Rev. Lett. **343,** 188301 (2002).

[32] H. Rabitz, M. Hsieh, and C. Rosenthal, "Landscape for optimal control of quantum-mechanical unitary transformations," Phys. Rev. A **72,** 052337 (2005).

[33] V. Ramakrishna, M. V. Salapaka, M. Dahleh, H. Rabitz, and A. Peirce, "Controllability of molecular systems," Phys. Rev. A **51,** 960–966 (1995).

[34] J. S. Taylor, *Classical Mechanics* (University Science Books, USA, 2005).

[35] K. Husimi, "Miscellanea in Elementary Quantum Mechanics, II," Prog. Theor. Phys. **9,** 381–402 (1953).

[36] H. R. Lewis, Jr. and W. Riesenfeld, "An Exact Quantum Theory of the TimeDependent Harmonic Oscillator and of a Charged Particle in a Time-Dependent Electromagnetic Field," J. Math. Phys. **10,** 1458–1473 (1969).

[37] I. Malkin, M. I. Man'ko, and D. A. Trifonov, "Coherent States and Transition Probabilities in a Time-Dependent Electromagnetic Field," Phys. Rev. D **2,** 1371–1385 (1970).

[38] V. Dodonov and V. Man'ko, "Coherent states and the resonance of a quantum damped oscillator," Phys. Rev. A **20,** 550–560 (1979).

[39] B. Baseia and A. L. De Brito, Phys. Rev. **45,** 749–759 (1992).

[40] Ş. A. Büyükaşik, J. Math. Phys. **59,** 082104 (2018).

[41] R. Cordero-Soto, E. Suazo, and S. Suslov, "Quantum integrals of motion for variable quadratic Hamiltonians," Ann. Phys. **325,** 1884–1912 (2010).

[42] A. Coronel-Escamilla, J. F. Gómez-Aguilar, D. Baleanu, T. Córdova-Fraga, R. F. Escobar-Jiménez, V. H. Olivares-Peregrino, and M. M. Al Qurashi, "Bateman-Feshbach Tikochinsky and Caldirola-Kanai Oscillators with New Fractional Differentiation," Entropy 19 (2017).

[43] D. Baleanu, J. H. Asad, I. Petras, S. Elagan, and A. Bilgen, "Fractional Euler-Lagrange Equation of Caldirola-Kanai Oscillator," Romanian Reports in Physics **64,** 1171–1177 (2012).

[44] J. Guerrero and M. Berrondo, "Semiclassical interpretation of Wei–Norman factorization for SU(1, 1) and its related integral transforms," J. Math. Phys. **61,** 082107 (2020).

[45] S. Chumakov, V. Dodonov, and V. Man'ko, "Correlation functions of the nonstationary quantum singular oscillator," J. Phys. A **19,** 3229–3239 (1986).

[46] D. Trifonov, "Exact Solutions for the General Nonstationary Oscillator with a Singular Perturbation," J. Phys. A **32,** 3649–3661 (1999).

[47] A. Dodonov, E. Dodonov, and V. Dodonov, "Photon generation from vacuum in nondegenerate cavities with regular and random periodic displacements of boundaries," Phys. Lett. A **317,** 378–388 (2003).

[48] X. Chen, A. Ruschhaupt, S. Schmidt, A. del Campo, D. Guéry-Odelin, and J. Muga, "Fast Optimal Frictionless Atom Cooling in Harmonic Traps: Shortcut to Adiabaticity," PRL **104,** 063002 (2010).

[49] B. Mielnik, "Evolution loops," J. Math. Phys. **27,** 2290–2306 (1986).

[50] D. Fernandez and B. Mielnik, "Controlling quantum motion," J. Math. Phys. **35,** 2083–2104 (1994).

[51] H. Fan and A. Wunsche, "Design of squeezing," J. Opt. B **2,** 464–469 (2000).

[52] I. Averbukh, B. Sherman, and G. Kurizki, "Enhanced squeezing by periodic frequency modulation under parametric instability conditions," Phys. Rev. A **50,** 5301–5308 (1994).

[53] V. Dodonov, O. Man'ko, and V. Man'ko, "Time-dependent oscillator with Kronig-Penney excitation," Phys. Lett. A **175,** 1–4 (1993).

[54] V. Dodonov, V. Man'ko, and D. Zhivotchenko, "Quasi-energies and chaotic behaviour of a periodically delta-kicked quantum singular oscillator," Nuovo Cim. B **108,** 1349–1363 (1993).

[55] V. Dodonov, M. Lukin, and V. Man'ko, "Squeezing for the One-Mode Electromagnetic-Field Oscillator with δ-Kicked Frequency," Nuovo Cim. B **109,** 1023–1037 (1994).

[56] C. Gerry, P. Ma, and E. Vrscay, "Phys. Rev. A," Dynamics of SU(1,1) coherent states driven by a damped harmonic oscillator **39,** 668–674 (1989).

[57] E. Kanai, "On the Quantization of the Dissipative Systems," Prog. Theor. Phys. **167,** 440 (1948).

[58] B. C. Hall, *Lie Groups, Lie Algebras, and Representations An Elementary Introduction*, 2 ed. (Springer International Publishing, Switzerland, 2015).

[59] D. Guéry-Odelin, A. Ruschhaupt, A. Kiely, E. Torrontegui, S. Martínez-Garaot, and J. G. Muga, "Shortcuts to Adiabaticity: Concepts, Methods, and Applications," Reviews of Modern Physics **91,** 045001 (2019).

[60] T.-N. Xu, J. Li, T. Busch, X. Chen, and T. Fogarty, "Effects of Coherence on Quantum Speed Limits and Shortcuts to Adiabaticity in Many-Particle System," Physical Review Research **2,** 023125 (2020).

[61] R. Román-Ancheyta, M. Berrondo, and J. Récamier, "Parametric oscillator in a Kerr medium: evolution of coherent states," J. Opt. Soc. Am. B **32,** 1651–1655 (2015).

[62] M. Aspelmeyer, T. J. Kippenberg, and F. * Marquardt, "Cavity optomechanics," Rev. Mod. Phys. **86,** 1391–1452 (2014).

[63] J. D. Teufel, T. Donner, and D. * Li, "Sideband cooling of micromechanical motion to the quantum ground state," Nature **475,** 359–363 (2011).

[64] L. F. Wei, Y.-x. Liu, and C. P. * Sun, "Probing Tiny Motions of Namomechanical Resonators: Classical or Quantum Mechanical," Phys. Rev. Lett. **97,** 237201 (2006).

[65] S. Mancini, V. I. Man'ko, and P. * Tombesi, "Ponderomotive control of quantum macroscopic coherence," Phys. Rev. A **55,** 3042–3050 (1997).

[66] S. Bose, K. Jacobs, and P. L. Knight, "Preparation of nonclassical states in cavities with a moving mirror," Phys. Rev. A **56,** 4175–4186 (1997).

[67] M. Aspelmeyer, S. Gröblacher, K. Hammerer, and N. Kiesel, "Quantum optomechanics-throwing a glance," J. Opt. Soc. Am. B **27,** A189–A197 (2010).

[68] P. D. Nation, J. Suh, and M. P. Blencowe, "Ultrastrong optomechanics incorporating the dynamical Casimir effect," Phys. Rev. A **93,** 022510 (2016).

[69] I. Ramos-Prieto, R. Román-Ancheyta, J. Récamier, M. Berrondo, and H. M. Moya-Cessa, "Ion-laser-like interaction in optomechanical systems with Kerr nonlinearities," Phys. Lett. A **408,** 127490 (2021).

[70] M. Schlosshauer, *Decoherence and the Quantum-to-Classical Transition* (Springer, Berlin Germany, 2007).

[71] S. Hassani, *Mathematical Physics*, 2 ed. (Springer International, Switzerland, 2013).

[72] G. Brawley, M. Vanner, P. Larsen, S. Schmid, A. Boisen, and W. Bowen, "Nonlinear optomechanical measurement of mechanical motion," Nat. Commun. **7,** 10988 (2016).

[73] C. Doolin, B. Hauer, P. Kim, A. MacDonald, H. Ramp, and J. Davis, "Nonlinear optomechanics in the stationary regime," Phys. Rev. A **89,** 053838 (2014).

[74] H. Xie, C.-G. Liao, X. Shang, Z.-H. Chen, and X.-M. Lin, "Optically induced phonon blockade in an optomechanical system with second-order nonlinearity," Phys. Rev. A **98,** 023819 (2018).

[75] C. Jiang, Y. Cui, and G. Chen, "Dynamics of an optomechanical system with quadratic coupling: Effect of first order correction to adiabatic elimination," Sci. Rep. **6,** 35583 (2016).

[76] S. Khorasani, "Higher-Order Interactions in Quantum Optomechanics: Analysis of Quadratic Terms," Sci. Rep. **8,** 16676 (2018).

[77] V. Macrì, A. Ridolfo, O. D. Stefano, A. F. Kockum, F. Nori, and S. Savasta, "Nonperturbative Dynamical Casimir Effect in Optomechanical Systems: Vacuum Casimir-Rabi Splittings," Phys. Rev. X **8,** 011031 (2018).

[78] S. A. Fulling and P. C. W. Davies, "Radiation from a moving mirror in two dimensional space-time: conformal anomaly," Proc. R. Soc. Lond. A. **348,** 393–414 (1976).

[79] A. Alhendi and E. Lashin, "Spectrum of one-dimensional anharmonic oscillator," Can. J. Phys. **83,** 541–550 (2005).

[80] F. Fernández and R. Tipping, "Analytical Expressions for the Energies of Anharmonic Oscillators," Can. J. Phys. **78,** 845–850 (2000).

[81] D. Isaacson, E. Isaacson, D. Marchesin, and P. J. Paes-Leme, "Numerical Analysis of the Spectral Properties of Coupled Oscillator Schrödinger Operators. II. Two-Coupled Anharmonic Oscillators," SIAM J. Numer. Anal. **19,** 126–141 (1981).

[82] J. Clarke and F. K. Wilhelm, "Superconducting quantum bits," Nature **453,** 1031–1042 (2008).

[83] G. Kirchmair *et al.*, "Observation of Quantum State Collapse and Revival Due to the Single-Photon Kerr Effect," Nature **495,** 205–209 .

[84] T. Ladd, F. Jelezko, R. Laflamme, Y. Nakamura, C. Monroe, and J. O'Brien, "Quantum Computers," Nature **464,** 54–53 (2010).

[85] K. C. McCormick, J. Keller, S. C. Burd, D. J. Wineland, A. C. Wilson, and D. Leibfried, "Quantum-Enhanced Sensing of a Single-Ion Mechanical Oscillator," Nature **572,** 86–92 (2019).

[86] S. Shankar *et al.*, "Autonomously stablized entanglement between two superconducting quantum bits," Nature **504,** 419–422 (2013).

[87] W. H. Louisell, *Quantum Statistical Properties of Radiation* (John Wiley and Sons .Inc, USA, 1990), p. 347.

[88] W. H. Louisell, *Quantum Statistical Properties of Radiation* (John Wiley and Sons .Inc, USA, 1990), p. 205.

[89] R. Ramán-Ancheyta, M. Berrondo, and J. Récamier, "Parametric oscillator in a Kerr medium: evolution of coherent states," J. Opt. Soc. Am. B **32,** 1651–1655 (2015).

Index